A second-order shape optimization algorithm for solving the exterior Bernoulli free boundary problem using a new boundary cost functional

Julius Fergy T. Rabago[1] (ORCID) · **Hideyuki Azegami**[1]

Abstract

The exterior Bernoulli problem is rephrased into a shape optimization problem using a new type of objective function called the Dirichlet-data-gap cost function which measures the L^2-distance between the Dirichlet data of two state functions. The first-order shape derivative of the cost function is explicitly determined via the chain rule approach. Using the same technique, the second-order shape derivative of the cost function at the solution of the free boundary problem is also computed. The gradient and Hessian informations are then used to formulate an efficient second-order gradient-based descent algorithm to numerically solve the minimization problem. The feasibility of the proposed method is illustrated through various numerical examples.

Keywords Bernoulli problem · Domain perturbation · Free boundary · Shape optimization · Shape derivative

1 Introduction

In this note, we are interested in the so-called *Bernoulli's free boundary problem* (FBP). The problem, which is considered as the prototype of a stationary FBP and is called in some literature as the *Alt–Caffarelli problem* (see [1]), find their origin in the description of free surfaces for ideal fluids [37]. There are, however, numerous other applications leading to similar formulations, for instance, in the context of optimal design, electro chemistry and electro statics (see [36] and also [35] for further industrial applications).

✉ Julius Fergy T. Rabago
jfrabago@gmail.com

Hideyuki Azegami
azegami@i.nagoya-u.ac.jp

1   Graduate School of Informatics, Nagoya University, A4-2 (780) Furo-cho, Chikusa-ku, Nagoya 464-8601, Japan

Bernoulli problem can be classified into two cases, namely, the *exterior* Bernoulli FBP and the *interior* Bernoulli FBP. Here, we focus our attention on the former case. In the exterior problem, a bounded and connected domain $A \subset \mathbb{R}^2$ with a *fixed boundary* $\Gamma := \partial A$ and a constant $\lambda < 0$ are known or given. The task is to find a bounded connected domain $B \subset \mathbb{R}^2$ with a *free boundary* $\Sigma := \partial B$, B contains the closure of A, and an associated state function $u := u(\Omega)$, where $\Omega = B \setminus \bar{A}$, such that the following overdetermined system of partial differential equations (PDEs) is satisfied:

$$-\Delta u = 0 \text{ in } \Omega, \quad u = 1 \text{ on } \Gamma, \quad u = 0 \quad \text{and} \quad \partial_{\mathbf{n}} u = \lambda \text{ on } \Sigma. \tag{1}$$

Here, $\partial_{\mathbf{n}} u := \nabla u \cdot \mathbf{n}$ denotes the normal derivative of u and $\mathbf{n}$ represents the outward unit normal vector to Σ.

The presence of two boundary conditions imposed on the exterior boundary Σ makes the problem difficult to solve. Nevertheless, it is known that (1) admits a classical solution for simply connected bounded domain Ω, for any given constant $\lambda < 0$. In addition, the shape solution Ω^* is unique for bounded convex domains A [36] and the free boundary Σ^* is $C^{2,\alpha}$ regular (see [47, Theorem 1.1]).

Our main intent in this work is to numerically solve (1) by performing a novel iterative second-order gradient-based optimization procedure. Our approach relies on the method known as shape optimization (see, e.g., [22, 46, 71]) which is already an established tool to solve such a free boundary problem. The main idea of the said technique is to reformulate the original problem into an optimization problem of the form

$$\min_{\Omega} J_0(\Omega, u(\Omega)) \quad \text{subject to } e(u(\Omega)) = 0, \tag{2}$$

where J_0 denotes a suitable objective functional that depends on a domain Ω as well as on a function $u(\Omega)$, which is the solution of a partial differential equation $e(u(\Omega)) = 0$ posed on Ω.

There are different ways to write (1) in the form of (2). A typical approach is to choose one of the boundary conditions on the free boundary to obtain a well-posed state equation, and then track the remaining boundary data in a least-squares sense. Such formulation has been carried-out in several previous investigations; see, for instance, [31, 32, 41, 44, 50, 65, 66]. Alternatively, one can consider an energy-gap type cost function which consists of two auxilliary states; one that is a solution of pure Dirichlet problem and one that satisfies a mixed Dirichlet–Neumann problem (see, e.g., [9–12, 33]). The objective function used in such formulation is sometimes called the Kohn-Vogelius cost functional since Kohn and Vogelius [53] were among the first who used such a functional in the context of inverse problems. Mathematically, these aforementioned formulations are given as follows:

$$\min_{\Omega} J_1(\Sigma) \equiv \min_{\Omega} \frac{1}{2} \int_{\Sigma} u_{\mathrm{N}}^2 \, d\sigma$$

Dirichlet-data-tracking approach

where the state function $u_N := u_N(\Omega)$ is the solution to the mixed Dirichlet–Neumann problem

$$-\Delta u_N = 0 \text{ in } \Omega, \quad u_N = 1 \text{ on } \Gamma, \quad \partial_\mathbf{n} u_N = \lambda \text{ on } \Sigma; \tag{3}$$

$$\min_{\Omega} J_2(\Sigma) \equiv \min_{\Omega} \frac{1}{2} \int_\Sigma \left(\frac{\partial u_D}{\partial \mathbf{n}} - \lambda \right)^2 d\sigma$$

Neumann-data-tracking approach

where the state function $u_D := u_D(\Omega)$ is the solution to the pure Dirichlet problem

$$-\Delta u_D = 0 \text{ in } \Omega, \quad u_D = 1 \text{ on } \Gamma, \quad u_D = 0 \text{ on } \Sigma; \tag{4}$$

$$\min_{\Omega} J_3(\Omega) \equiv \min_{\Omega} \frac{1}{2} \int_\Omega \left| \nabla (u_N - u_D) \right|^2 dx$$

Energy-gap type cost functional approach

where the state functions u_N and u_D satisfy systems (3) and (4), respectively.

In this study, one of our main objectives is to introduce yet another shape optimization reformulation of (1) which, to the best of our knowledge, has not been studied in any previous investigation. Similar to the cost functional J_3, we make use of a cost function consisting of two auxiliary states u_N and u_R:

$$\min_{\Omega} J(\Sigma) \equiv \min_{\Omega} \frac{1}{2} \int_\Sigma |u_N - u_R|^2 d\sigma, \tag{5}$$

where the state function u_N is the solution of (3) and $u_R := u_R(\Omega)$ satisfies, for a given strictly positive (constant) β, the following equivalent form of (1) with a Robin boundary condition:

$$-\Delta u_R = 0 \text{ in } \Omega, \quad u_R = 1 \text{ on } \Gamma, \quad \partial_\mathbf{n} u_R + \beta u_R = \lambda \text{ on } \Sigma. \tag{6}$$

Clearly, if (u, Ω) is a solution of (1), then $u_N = u_R = u$; therefore, $J(\Sigma) = 0$. Conversely, if $J(\Sigma) = 0$, then $u_N = u_R$ on Σ. Hence, the equation $\partial_\mathbf{n}(u_N - u_R) = \beta u_R = 0$ on Σ and the assumption $\beta > 0$ implies that $u_R = u_N = 0$ on Σ. Consequently, $u = u_N = u_R$ is a solution of problem (1). We remark that, in the limiting case as β goes on infinity, the PDE system (6) transforms into the pure Dirichlet problem (4) (this means that $u_R = 0$ on Σ), leading us to recover from (5) the classical Dirichlet-data-tracking formulation of the FBP (1).

We stress that the formulations presented above can also be applied to Poisson problems with overdetermined non-homogenous (sufficiently smooth) boundary conditions. Here, however, we only inspect the free boundary problem (1) in order to simplify the discussion.

Motivation Our reason for considering the new cost functional $J(\Sigma)$ stems from several previous related works. In the study carried out in [67], we have considered the cost functional J_2 with a different state constraint problem. More precisely, we replaced the state variable u_D with u_R which is the solution of the mixed Dirichlet–Robin problem (6). We found that such modification of the problem setup actually yields more regularity in the solution of the associated adjoint state problem. In fact, the adjoint state associated to the shape optimization problem "$\min_\Omega \frac{1}{2}\|\partial_\mathbf{n} u_R - \lambda\|^2_{L^2(\Sigma)}$ subject to (6)" enjoys the same degree of regularity (depending of course on the regularity of Ω) with that of u_R. Also, we observed, through various numerical examples, that this new state constraint yields faster and more stable convergence of the approximate solution to the exact solution (both in case of the exterior and interior Bernoulli FBP) than the classical setting "$\min_\Omega \frac{1}{2}\|\partial_\mathbf{n} u_D - \lambda\|^2_{L^2(\Sigma)}$ subject to (4)." On the other hand, in [68], we proposed a modification of the energy-gap cost functional approach for the exterior Bernoulli FBP (1). The optimization problem we put forward in (1) utilizes a similar functional to J_3, but, instead of (4), we took u_R as one of the state constraints. More precisely, we considered the problem "$\min_\Omega J_4(\Omega) \equiv \min_\Omega \frac{1}{2}|u_R - u_N|^2_{H^1(\Omega)}$, subject to (3) and (6)" (where $|\cdot|_{H^1(\Omega)}$ denotes the $H^1(\Omega)$-seminorm; that is, $|\cdot|_{H^1(\Omega)} := \|\nabla(\cdot)\|_{L^2(\Omega)}$) as a shape optimization reformulation of (1). We emphasize that under this formulation, and assuming appropriate conditions on the Robin coefficient β as well as on the exterior boundary Σ, we were able to express the first-order shape derivative of J_4 at Ω along a given deformation field in terms of just the state constraint u_N. This in turn allowed us to also reduce the number of PDE constraints to be solved when applying a second-order method to numerically resolve the free boundary problem (1) (see Proposition 1 and Corollary 2 in [68]). We stress that such reduction in the number of constraints in the optimization setup is certainly advantageous in terms of numerical aspects. Indeed, the numerical results presented in [68] show that the proposed modification requires less computing time per iteration to numerically solve (1) than the classical formulation "$\min_\Omega \frac{1}{2}|u_D - u_N|^2_{H^1(\Omega)}$ subject to (3) and (4)" (as expected). Meanwhile, in a related problem, Laurain and Privat [55] examined a shape optimization formulation of a Bernoulli-type problem with geometric constraints. In their work, the domain Ω, which is simply connected, is constrained to lie in the half space determined by $x_1 \geqslant 0$. The boundary of the solution domain is also forced to contain a segment of the hyperplane $\{x_1 = 0\}$ where a non-homogeneous Dirichlet condition is imposed. Then, the authors seek to find the solution of a partial differential equation satisfying a Dirichlet and a Neumann boundary condition simultaneously on the free boundary. The cost function examined by the authors in [55] has the form $J_5(\Omega) := \|u_{2,\epsilon} - u_1\|^2_{L^2(\Omega)}$, where $u_{2,\epsilon}$ satisfies a mixed Dirichlet–Robin boundary problem while u_1 is a solution of a pure Dirichlet problem. Here, $u_{2,\epsilon}$ has the property that "$u_{2,\epsilon} \to u_2$ as $\epsilon \to 0$," where u_2 is the unique (weak) solution of a mixed Dirichlet–Neumann problem. We point out here that, as opposed to the formulation minimizing J_4 whose first-order shape derivative only depends on u_N (under appropriate conditions on β and the exterior boundary Σ), the cost function J_5 actually has

a first-order shape derivative that depends on the solutions of four PDEs (two state problems and two adjoint state problems).

Besides the above statements, we mention that minimizing $J_4(\Omega)$ over the set of admissible domains $\mathcal{O}_{\text{ad}}$ (see Sect. 4) of Ω is, to some extent, equivalent to finding the optimal shape solution to the optimization problem "$\min_\Omega J(\Sigma)$ subject to (3) and (6)," and we explained it as follows. Firstly, for convenience, let us introduce the notation "$\lesssim$". This means that if $P \lesssim Q$, then we can find some constant $c > 0$ such that $P \leqslant cQ$ (obviously, $Q \gtrsim P$ is defined as $P \lesssim Q$). Then, for an open bounded domain $\Omega \subset \mathbb{R}^2$ with Lipschitz boundary (in this study, we shall in fact assume that Ω is $C^{2,1}$ regular), the inequality $\|v\|_{L^2(\partial\Omega)} \lesssim \|v\|_{H^1(\Omega)}$ holds, for all $v \in H^1(\Omega)$. We note that this bound clearly exhibits the compact embedding of $H^1(\Omega)$ in $L^2(\partial\Omega)$ (see [56, p. 159]) and it actually follows from the well-known trace theorem (see, e.g., [57, Theorem 3.3.7, p. 102], [59, Theorem 5.5, p. 95]) coupled with the compact embedding of $H^{1/2}(\partial\Omega)$ in $L^2(\partial\Omega)$ (cf. [69, Theorem, 2.5.5, p. 61]). Moreover, it is not hard to see from this result that we also have the relation $\|v\|_{L^2(\Gamma)} \lesssim \|v\|_{H^1(\Omega)}$. This inequality shows that the set $H^1_{\Gamma,0}(\Omega) = \{v \in H^1(\Omega) : v = 0 \text{ on } \Gamma\}$ is strongly closed in $H^1(\Omega)$ and, in addition, a convex set. From [19, p. 54], for instance, we know that strongly closed convex sets are also weakly closed (see also [17, Lemma 3.1.15, p. 119]). Hence, the weak convergence $v_{n_k} \rightharpoonup v$ implies that v is in fact in the same set $H^1_{\Gamma,0}(\Omega)$. Furthermore, we note that we may actually prove (following the proof of [43, Lemma 2.19, p. 62]) that $|v|_{H^1(\Omega)} = \|\nabla v\|_{L^2(\Omega)} \gtrsim \|v\|_{H^1(\Omega)}$, for all $v \in H^1_{\Gamma,0}(\Omega)$. We note that this bound in fact shows that the $H^1(\Omega)$-seminorm $|\cdot|_{H^1(\Omega)}$ is actually equivalent to the $H^1(\Omega)$-norm on $H^1_{\Gamma,0}(\Omega)$. Lastly, we mention that we can also verify, possibly by way of contradiction, that the norm

$$\|\cdot\|_{H^1_{\Gamma,0}(\Omega)} := \left(|\cdot|^2_{H^1(\Omega)} + \|\cdot\|^2_{L^2(\Sigma)} \right)^{1/2},$$

on the other hand, is equivalent to the usual Sobolev $H^1(\Omega)$-norm. Thus, by these results, taking $v = u_{\text{N}} - u_{\text{R}} \in H^1_{\Gamma,0}(\Omega)$, we can deduce the sequence of inequalities

$$\|u_{\text{N}} - u_{\text{R}}\|^2_{L^2(\Sigma)} \lesssim |u_{\text{N}} - u_{\text{R}}|^2_{H^1(\Omega)} + \|u_{\text{N}} - u_{\text{R}}\|^2_{L^2(\Omega)} \lesssim |u_{\text{N}} - u_{\text{R}}|^2_{H^1(\Omega)}.$$

It should also be recognized that the above relation is a mere consequence of the inequality $\|u_{\text{N}} - u_{\text{R}}\|^2_{L^2(\Sigma)} \lesssim \|u_{\text{N}} - u_{\text{R}}\|^2_{H^{1/2+\epsilon}(\Omega)}$ which holds true for any $\epsilon > 0$ due to the trace theorem. This observation further gives us the motivation to consider minimizing $J(\Sigma)$, subject to (3) and (6), over the set of admissible domains for Ω to numerically solve the free boundary problem (1).

The minimization problem (5) can be carried out numerically using different computational strategies [67]. Standard algorithms to minimize J utilizes some gradient information when using a first-order method and also uses the Hessian when applying second-order methods. So, in order for us to accomplish our main objective, we first need to carry out the sensitivity analysis of the cost functional $J(\Omega)$ with respect to a local perturbation of the domain Ω. Accordingly, we derive the *first-* and the *second-order shape derivative* of J through chain rule approach. This requires, beforehand, the expressions for the shape derivatives of the states u_{N} and u_{R}. Of

course, there are other ways to obtain the shape derivative of *J* such as through a technique used in [33]. However, the method employed in [33] by the authors, which was inspired by [25, 26], restricts the results to starlike domains. Another method could be to use only the *Eulerian derivatives* [22] of the states and follow [12], or apply the so-called *rearrangement method*, first used in [51], to obtain the shape derivative of *J*. We emphasize that the former approach applies not only to starlike domains but also to more general $C^{k,\alpha}$ domains. On the other hand, the rearrangement method provides a rigorous computation of the shape derivatives of cost functionals using only the Hölder continuity of the state variables, bypassing the computation of the material and shape derivatives of states (see, e.g., [10, 44, 50]). Further, this method requires less regularity of the domain than in the case when applying the classical chain rule approach. Here, we opted to apply the chain rule approach since the shape derivatives of u_{N} and u_{R} are already available in the literature (see, e.g., [11] and [72], respectively). In addition to these previously mentioned techniques, we remark that the shape gradient of *J* can also be computed using the well-known *minimax formulation* developed in [20]. Similar to the rearrangement method, this strategy in computing shape derivatives of cost functionals does not require the knowledge of the shape derivative of the states as it naturally introduces the use of adjoint states to derive the expression for the shape derivative of the cost; see, for instance, [65, 66].

The plan of the paper is as follows. In Sect. 2, we describe the weak formulations of the state equations and briefly discuss the existence, uniqueness and regularity of their solutions. In Sect. 3, we recall a few basic concepts from shape calculus and give the shape derivatives of the states. Then, we compute the first-order shape derivative of the cost *J* through chain rule approach followed by the computation of its corresponding second-order shape derivative at the solution of the free boundary problem (1). Also, we shortly discuss about the ill-posedness of the proposed shape optimization formulation by inspecting the shape Hessian form at a critical shape. Meanwhile, in Sect. 4, we examine the existence of optimal solution to the minimization problem under consideration. After that, in Sect. 5, we describe how the gradient and Hessian informations can be utilized in formulating an efficient boundary variation algorithm to numerically solve the present optimization problem. Finally, we demonstrate the feasibility of the newly proposed shape optimization approach by solving some concrete problems. Also, to illustrate the efficiency of the proposed method, we compare our numerical results with the results obtained by the classical Dirichlet-data-tracking cost functional approach. We end the paper with a brief conclusion given in Sect. 6.

2 Preliminaries

We first review an essential quality of the state solutions which is vital in guaranteeing the existence of their shape derivatives.

2.1 Weak formulation of the state equations

The respective variational formulations of the state problems (3) and (6) are stated as follows.

Find $u_{\mathrm{N}} \in H^1(\Omega)$, with $u_{\mathrm{N}} = 1$ on Γ, such that

$$\int_\Omega \nabla u_{\mathrm{N}} \cdot \nabla \varphi \, \mathrm{d}x = \int_\Sigma \lambda \varphi \, \mathrm{d}\sigma, \quad \forall \varphi \in H^1_{\Gamma,0}(\Omega); \tag{7}$$

Find $u_{\mathrm{R}} \in H^1(\Omega)$, with $u_{\mathrm{R}} = 1$ on Γ, such that

$$\int_\Omega \nabla u_{\mathrm{R}} \cdot \nabla \varphi \, \mathrm{d}x + \int_\Sigma \beta u_{\mathrm{R}} \varphi \, \mathrm{d}\sigma = \int_\Sigma \lambda \varphi \, \mathrm{d}\sigma, \quad \forall \varphi \in H^1_{\Gamma,0}(\Omega), \tag{8}$$

where $H^1_{\Gamma,0}(\Omega)$ is the space of test functions in the introduction. It is well-known that the variational equation (7) admits a unique solution in $H^1(\Omega)$, while it can easily be verified (for instance, by means of Lax-Milgram theorem) that (8) also have a unique solution in $H^1(\Omega)$ (see [39, 58]).

Remark 1 We emphasize that since $\beta > 0$, then uniqueness of weak solution $u_{\mathrm{R}} \in H^1(\Omega)$ is guaranteed for the mixed Robin-Dirichlet problem (6). Moreover, we note that we may actually consider β to be a function on Σ instead of just being a positive constant. In this case, however, we require $\beta := \beta(x)$ to be at least an L^∞ function on Σ (i.e., $\beta \in L^\infty(\Sigma)$) and be positive almost everywhere in the free boundary to ensure uniqueness of weak solution to (6) (cf., e.g, [58, Lemma 7.36.3, p. 617]). In this regard, we mention here in advance that in Section 3, we will in fact consider the mean curvature of the free boundary Σ as the function β. Evidently, $\beta = \kappa$ belongs to $L^\infty(\Sigma)$ because of Rademacher's theorem (recall that Ω, by assumption, is $C^{2,1}$ regular). Hence, the first mentioned requirement for existence of unique weak solution to (6) is satisfied, however, the condition that $\kappa(x) \geqslant 0$ on Σ only holds for convex domains. Nevertheless, this is not an issue when the domain A (whose boundary is represented by Γ) is convex because, according to [48, Theorem 2.1] (and the references therein), when A is convex, then so is the unique solution domain Ω^* to the free boundary problem (1).

2.2 Higher regularity of the state solutions

The unique solution u_{N} of the PDE system (3) actually possesses higher regularity if Ω is assumed to be at least $C^{1,1}$ regular. In fact, the solution is also in $H^2(\Omega)$ in this case, and in general, if Ω is of class $C^{k+1,1}$, where k is a non-negative integer, then u_{N} is H^{k+2} regular. This claim can easily be verified since the fixed boundary Γ and the free boundary Σ are disjoint, (see, e.g., [10, Theorem 29]). Analogously, the unique solution $u_{\mathrm{R}} \in H^1(\Omega)$ of (6) also have higher regularity depending on the degree of smoothness of Ω. More precisely, if Ω is of class $C^{k+1,1}$ (again k is a non-negative integer), then u_{R} is also an element of $H^{k+2}(\Omega)$ (see, e.g., [52, Remark 3.5]). For more details about existence and uniqueness of solutions to mixed

Robin-Dirichlet problems in $W^{s,2}$ for bounded domains in $\mathbb{R}^d$, we refer the readers to [58, Section 7.36].

3 Shape sensitivity analysis of the states and cost function

Let us consider a bounded and connected domain $U \supset \overline{\Omega}$ and a family of deformation fields

$$\Theta := \{ \mathbf{V} \in C^{2,1}(\overline{U}, \mathbb{R}^2) : \mathbf{V} = 0 \text{ on } \partial U \cup \Gamma \}. \tag{9}$$

Clearly, every $\mathbf{V} \in \Theta$ forces Γ to remain invariant after a deformation since $\mathbf{V}$ vanishes on Γ. Hence, Γ is a component of the boundary of any perturbation of Ω. In this work, every admissible perturbation of the reference domain Ω is described as follows. Given an element of Θ, we perturb Ω by means of the so-called *perturbation of the identity operator* (see, e.g., [22, Section 2.5.2, p. 147] or [10]):

$$T_t : \Omega \longmapsto \Omega_t, \quad x \longmapsto T_t(x) = x + t\mathbf{V}(x).$$

For sufficiently small t and for each $\mathbf{V} \in \Theta$, the operator T_t can be shown to be a $C^{2,1}$ diffeomorphism from Ω onto its image (cf. [71]).

With the above definition of $\Omega_t := T_t(\Omega)$, the state solutions $u_{\mathrm{N}t}$ and $u_{\mathrm{R}t}$ satisfy

$$-\Delta u_{\mathrm{N}t} = 0 \text{ in } \Omega_t, \quad u_{\mathrm{N}t} = 1 \text{ on } \Gamma_t, \quad \frac{\mathrm{d}u_{\mathrm{N}t}}{\mathrm{d}\mathbf{n}_t} = \lambda \text{ on } \Sigma_t; \tag{10}$$

$$-\Delta u_{\mathrm{R}t} = 0 \text{ in } \Omega_t, \quad u_{\mathrm{R}t} = 1 \text{ on } \Gamma_t, \quad \frac{\mathrm{d}u_{\mathrm{R}t}}{\mathrm{d}\mathbf{n}_t} + \beta u_{\mathrm{R}t} = \lambda \text{ on } \Sigma_t, \tag{11}$$

respectively, where $\mathbf{n}_t$ is the unit outward normal to Σ_t. Here, we can actually drop t in Γ_t because $\Gamma_t = \Gamma$ for all t. Note that for $t = 0$, we recover the reference domain $\Omega := \Omega_0$, with fixed boundary $\Gamma := \Gamma_0$ and free boundary $\Sigma := \Sigma_0$.

Next, let us recall some key definitions from shape calculus. We say that the function $u(\Omega)$ has a *material derivative* $\dot{u}$ and a *shape derivative* u' at zero in the direction $\mathbf{V}$ if the limits

$$\dot{u} = \lim_{t \searrow 0} \frac{u(\Omega_t) \circ T_t - u(\Omega)}{t}, \quad u' = \lim_{t \searrow 0} \frac{u(\Omega_t) - u(\Omega)}{t},$$

exist, respectively, where $(u(\Omega_t) \circ T_t)(x) = u(\Omega_t)(T_t(x))$. These expressions are related by

$$u' = \dot{u} - (\nabla u \cdot \mathbf{V}) \tag{12}$$

provided that $\nabla u \cdot \mathbf{V}$ exists in some appropriate function space [22, 71]. In general, if $\dot{u}$ and $\nabla u \cdot \mathbf{V}$ both exist in the Sobolev space $W^{m,p}(\Omega)$, then u' also exists in that space.

3.1 Shape derivative of the states

To establish the existence of the shape derivative of J, one needs to show that the material and shape derivatives of the states u_N and u_R exist and, consequently, apply the chain rule. Apparently, the shape derivatives of u_N and u_R were already obtained in [9, 72], respectively. Their existence can be guaranteed if Ω is assumed to be at least $C^{2,1}$ regular.

Lemma 1 [9] *Let Ω be a bounded $C^{2,1}$ domain. Then, $u_N \in H^3(\Omega)$ is shape differentiable with respect to the domain, and its shape derivative $u_N' \in H^1(\Omega)$ is the unique solution of the mixed Dirichlet–Neumann problem*

$$\begin{cases} -\Delta u_N' &= 0 \quad \text{in } \Omega, \\ u_N' &= 0 \quad \text{on } \Gamma, \\ \partial_{\mathbf{n}} u_N' &= \operatorname{div}_\Sigma(\mathbf{V} \cdot \mathbf{n} \nabla_\Sigma u_N) + \lambda \kappa \mathbf{V} \cdot \mathbf{n} \quad \text{on } \Sigma, \end{cases} \tag{13}$$

where κ denotes the mean curvature of Σ.

Lemma 2 [72] *Let Ω be a bounded $C^{2,1}$ domain. Then, $u_R \in H^3(\Omega)$ is shape differentiable with respect to the domain, and its shape derivative $u_R' \in H^1(\Omega)$ is the unique solution of the mixed Robin-Neumann problem*

$$\begin{cases} -\Delta u_R' &= 0 & \text{in } \Omega, \\ u_R' &= 0 & \text{on } \Gamma, \\ \partial_{\mathbf{n}} u_R' + \beta u_R' &= \operatorname{div}_\Sigma(\mathbf{V} \cdot \mathbf{n} \nabla_\Sigma u_R) + \lambda \kappa \mathbf{V} \cdot \mathbf{n} - \beta(\partial_{\mathbf{n}} u_R + \kappa u_R)\mathbf{V} \cdot \mathbf{n} & \text{on } \Sigma. \end{cases} \tag{14}$$

If $\beta = \kappa$, then for the shape derivative u_R' of the solution of (6), it holds that $u_R' \equiv 0$ when Σ is the free boundary.

3.2 First-order shape derivative of the cost function

Our objective here is to derive the shape derivative of the cost function J in the direction of a deformation field $\mathbf{V} \in \Theta$. We recall that, for a given functional $J : \Omega \to \mathbb{R}$, its directional *Eulerian derivative* at Ω in the direction $\mathbf{V}$, if it exists, is defined as the limit

$$\lim_{t \searrow 0} \frac{J(\Omega_t) - J(\Omega)}{t} =: \, \mathrm{d}J(\Omega)[\mathbf{V}].$$

In addition, if the derivative $\mathrm{d}J(\Omega)[\mathbf{V}]$ exists for all $\mathbf{V}$ and the map $\mathbf{V} \mapsto \mathrm{d}J(\Omega)[\mathbf{V}]$ is linear and continuous, then J is *shape differentiable* at Ω, and this mapping will be referred to as the *shape gradient* of J at Ω. According to the well-known *Hadamard–Zolésio structure theorem* (see, e.g., [21, Theorem 3.2 and Remark 3.1,

Corollary 1]), the shape gradient of J depends only on the normal component of $\mathbf{V}$ on the boundary of Ω when the domain is regular enough.

For our proposed cost function $J(\Sigma)$ given in (5), the shape derivative under the assumption that

$$\text{"}\beta = \kappa \text{ and } u'_R \text{ is the shape derivative of the solution of (6)} \quad\quad\text{(A)}$$
$$\text{where } \Sigma \text{ is the free boundary"}$$

is given in the following proposition.

Proposition 1 *Let Ω be of class $C^{2,1}$ and $\mathbf{V} \in \Theta$. Also, let us assume that condition (A) holds true. Then, the Dirichlet-data-gap cost functional J is shape differentiable with*

$$\mathrm{d}J_A(\Sigma)[\mathbf{V}] = \int_\Sigma \left[\left(\lambda p_N + \frac{1}{2}u_N^2\right)\kappa - \nabla_\Sigma u_N \cdot \nabla_\Sigma p_N \right]\mathbf{n} \cdot \mathbf{V}\, \mathrm{d}\sigma, \quad\quad (15)$$

where p_N denotes the adjoint state which is the unique solution to the PDE system

$$-\Delta p_N = 0 \text{ in } \Omega, \quad p_N = 0 \text{ on } \Gamma, \quad \partial_\mathbf{n} p_N = u_N \text{ on } \Sigma, \quad\quad (16)$$

κ denotes the mean curvature of Σ and the tangential gradient ∇_Σ is given by

$$\nabla_\Sigma(\cdot) = \nabla(\cdot)|_\Sigma - \partial_\mathbf{n}(\cdot)\mathbf{n}.$$

Proof We use chain rule approach coupled with the adjoint method to obtain the shape derivative of J given by (15). Let Ω be of class $C^{2,1}$ and $\mathbf{V} \in \Theta$. Since the state variables u_N and u_R are sufficiently regular, we can apply Hadamard's boundary differentiation formula (cf. [22, Theorem 4.3, p. 486] or [46, 71]):

$$\frac{\mathrm{d}}{\mathrm{d}t}\int_{\partial\Omega_t} f(t, \sigma)\, \mathrm{d}\sigma_t \bigg|_{t=0} = \int_{\partial\Omega} \frac{\partial f(0, \sigma)}{\partial t}\, \mathrm{d}\sigma$$
$$+ \int_{\partial\Omega} \left(\frac{\partial f(0, \sigma)}{\partial\mathbf{n}} + \kappa f(0, \sigma) \right)\mathbf{V} \cdot \mathbf{n}\, \mathrm{d}\sigma, \quad\quad (17)$$

where $f \in C([0, \varepsilon], W^{2,p}(U))$, $p > 1$, and $\frac{\mathrm{d}}{\mathrm{d}t}f(0)$ exists in $W^{1,p}(U)$, to obtain

$$\mathrm{d}J(\Sigma)[\mathbf{V}] = \int_\Sigma (u_N - u_R)(u'_N - u'_R)\, \mathrm{d}\sigma$$
$$+ \int_\Sigma \left[\beta u_R(u_N - u_R) + \frac{1}{2}\kappa(u_N - u_R)^2 \right]\mathbf{V} \cdot \mathbf{n}\, \mathrm{d}\sigma. \quad\quad (18)$$

Here, of course, u'_N and u'_R satisfy (13) and (14), respectively. If u'_R is the shape derivative of the solution of (6) where Σ is the free boundary and $\beta = \kappa$, then by Lemma 2, $u'_R \equiv 0$ in $\overline{\Omega}$. The expression for $\mathrm{d}J(\Sigma)[\mathbf{V}]$ given by (18) then simplifies to

$$\mathrm{d}J_A(\Sigma)[\mathbf{V}] = \int_\Sigma u_N u'_N\, \mathrm{d}\sigma + \frac{1}{2}\int_\Sigma \kappa u_N^2 \mathbf{V} \cdot \mathbf{n}\, \mathrm{d}\sigma, \quad\quad (19)$$

where we put the subscript "$\cdot_A$" to emphasize that condition (A) was imposed in the computation of the shape gradient (*see* also comment on notation below).

We stress that the representation (19) of the shape derivative J in the direction of $\mathbf{V}$ at Ω is actually not useful for practical applications, especially in the numerical realization of the minimization problem (5) because it would require the solution of (13) for each velocity field $\mathbf{V}$. This issue can be resolved using the adjoint method, particularly by introducing the adjoint system (16). Using (13) and (16), we observe, via Green's second identity, that

$$
\begin{aligned}
\int_\Sigma u'_N u_N \, d\sigma &= \int_\Sigma u'_N \partial_{\mathbf{n}} p_N \, d\sigma = \int_\Sigma p_N \partial_{\mathbf{n}} u'_N \, d\sigma \\
&= \int_\Sigma p_N \big[\mathrm{div}_\Sigma (\mathbf{V} \cdot \mathbf{n} \nabla_\Sigma u_N) + \lambda \kappa \mathbf{V} \cdot \mathbf{n} \big] \, d\sigma.
\end{aligned}
\tag{20}
$$

At this point, it is useful to recall the so-called *tangential Green's formula* (see, e.g., [22, Eq. 5.27, p. 498]): let U be a bounded domain of class $C^{1,1}$ and $\Omega \subset U$ with boundary Γ. For $\mathbf{V} \in C^{1,1}(\overline{U}, \mathbb{R}^2)$ and $f \in W^{2,p}(U)$, $p > 1$, we have

$$
\int_\Gamma (f \, \mathrm{div}_\Gamma \mathbf{V} + \nabla_\Gamma f \cdot \mathbf{V}) \, d\sigma = \int_\Gamma \kappa f \mathbf{V} \cdot \mathbf{n} \, d\sigma,
\tag{21}
$$

where κ is the mean curvature of Γ. In addition, when $\mathbf{V} \cdot \mathbf{n} = 0$, we obviously have

$$
\int_\Gamma f \, \mathrm{div}_\Gamma \mathbf{V} \, d\sigma = -\int_\Gamma \nabla_\Gamma f \cdot \mathbf{V} \, d\sigma.
$$

Now, note that $\mathbf{V} \cdot \mathbf{n} \nabla_\Sigma u_N \cdot \mathbf{n} = 0$. Hence, by the above identity, we have that

$$
\int_\Sigma p_N \mathrm{div}_\Sigma (\mathbf{V} \cdot \mathbf{n} \nabla_\Sigma u_N) \, d\sigma = -\int_\Sigma \nabla_\Sigma u_N \cdot \nabla_\Sigma p_N \mathbf{V} \cdot \mathbf{n} \, d\sigma.
\tag{22}
$$

Combining Eqs. (19), (20) and (22), we get the desired result. □

Remark 2 We recall from [50, Theorem 4.1] (with $g = \mathrm{const.} = \lambda$ and $f \equiv 0$) (see also [32, Lemma 2.1]) that the shape gradient of J_1 is given by

$$
\begin{aligned}
\mathrm{d}J_1(\Sigma)[\mathbf{V}] &= \int_\Sigma \left[\frac{\partial}{\partial \mathbf{n}} \left(\frac{1}{2} u_N^2 + \lambda p_N \right) + \left(\frac{1}{2} u_N^2 + \lambda p_N \right) \kappa - \nabla u_N \cdot \nabla p_N \right] \mathbf{n} \cdot \mathbf{V} \, d\sigma \\
&=: \int_\Sigma G_1 \mathbf{n} \cdot \mathbf{V} \, d\sigma.
\end{aligned}
$$

It seems not obvious but the kernel G given in (15) only differs by $\frac{\partial}{\partial \mathbf{n}} \left(\frac{1}{2} u_N^2 \right)$ from G_1. This can be made more clear if we apply the identity

$$
-\langle \nabla_\Sigma u_N, \nabla_\Sigma p_N \rangle = -\langle \nabla u_N, \nabla p_N \rangle + \frac{\partial u_N}{\partial \mathbf{n}} \frac{\partial p_N}{\partial \mathbf{n}} = -\langle \nabla u_N, \nabla p_N \rangle + \lambda \frac{\partial p_N}{\partial \mathbf{n}}
\tag{23}
$$

to (15). Thus, in addition, we can actually write the shape gradient of J equivalently as follows

$$dJ_A(\Sigma)[\mathbf{V}] = \int_\Sigma \left[\left(\lambda p_N + \frac{1}{2} u_N^2 \right) \kappa - \langle \nabla u_N, \nabla p_N \rangle + \lambda \frac{\partial p_N}{\partial \mathbf{n}} \right] \mathbf{n} \cdot \mathbf{V} \, d\sigma. \quad (24)$$

Notation Throughout the rest of the discussion, we shall denote the shape gradient of J in the direction of $\mathbf{V}$ at Ω obtained under condition (A) as dJ_A and its corresponding kernel by G_A; i.e.,

$$G_A := \left(\lambda p_N + \frac{1}{2} u_N^2 \right) \kappa - \langle \nabla u_N, \nabla p_N \rangle + \lambda \frac{\partial p_N}{\partial \mathbf{n}} \quad (25)$$

(cf. Proposition 1). Meanwhile, the expression dJ simply refers to the shape gradient of J obtained without imposing assumption (A). More precisely, the expression for dJ is given by equation (18):

$$dJ(\Sigma)[\mathbf{V}] = \int_\Sigma \left[ww' + \left(\beta u_R w + \frac{1}{2} \kappa w^2 \right) \mathbf{V} \cdot \mathbf{n} \right] d\sigma, \quad (26)$$

where we use the notation $w = u_N - u_R$ and $w' = u_N' - u_R'$ for simplicity.

Before going to the next subsection, let us also express $dJ(\Sigma)[\mathbf{V}]$ in another form through the adjoint method. For this purpose, let us consider two harmonic functions Ξ_N and Ξ_R that both vanish on Γ, and such that $\partial_\mathbf{n} \Xi_N = w$ and $\partial_\mathbf{n} \Xi_R + \beta \Xi_R = w$ on Σ. Then, by Green's second identity together with Eqs. (13) and (14), we have

$$\int_\Sigma ww' \, d\sigma = \int_\Sigma \left[u_N' w - u_R'(\partial_\mathbf{n} \Xi_R + \beta \Xi_R) \right] d\sigma = \int_\Sigma \left[u_N' w - \Xi_R(\partial_\mathbf{n} u_R' + \beta u_R') \right] d\sigma$$

$$= \int_\Sigma \Xi_N \operatorname{div}_\Sigma(\mathbf{V} \cdot \mathbf{n} \nabla_\Sigma u_N) \, d\sigma$$

$$- \int_\Sigma \Xi_R \left\{ \operatorname{div}_\Sigma(\mathbf{V} \cdot \mathbf{n} \nabla_\Sigma u_R) - \beta(\partial_\mathbf{n} u_R + \kappa u_R) \mathbf{V} \cdot \mathbf{n} \right\} d\sigma$$

$$=: \mathbb{J}_1 - \mathbb{J}_2.$$

Note that the integral $\int_\Sigma v \operatorname{div}_\Sigma(\mathbf{V} \cdot \mathbf{n} \nabla_\Sigma u) \, d\sigma$, for any $u, v \in H^3(\Omega)$, can be expressed as $\int_\Sigma v \operatorname{div}_\Sigma(\mathbf{V} \cdot \mathbf{n} \nabla_\Sigma u) \, d\sigma = -\int_\Sigma (\nabla_\Sigma u \cdot \nabla_\Sigma v) \mathbf{V} \cdot \mathbf{n} \, d\sigma = \int_\Sigma (\partial_\mathbf{n} u \partial_\mathbf{n} v - \nabla u \cdot \nabla v) \mathbf{V} \cdot \mathbf{n} \, d\sigma$ via (21) and because $\mathbf{V} \cdot \mathbf{n} \nabla_\Sigma u = 0$. Hence, we have

$$\mathbb{J}_1 - \mathbb{J}_2 = \int_\Sigma \left\{ \nabla_\Sigma u_R \cdot \nabla_\Sigma \Xi_R - \nabla_\Sigma u_N \cdot \nabla_\Sigma \Xi_N + \beta \Xi_R [\lambda + (\kappa - \beta) u_R] \right\} \mathbf{V} \cdot \mathbf{n} \, d\sigma$$

$$= \int_\Sigma \left[\nabla u_R \cdot \nabla \Xi_R - \nabla u_N \cdot \nabla \Xi_N + \lambda w - (\lambda - \beta u_R)(w - \beta \Xi_R) \right] \mathbf{V} \cdot \mathbf{n} \, d\sigma$$

$$+ \int_\Sigma \left\{ \beta \Xi_R [\lambda + (\kappa - \beta) u_R] \right\} \mathbf{V} \cdot \mathbf{n} \, d\sigma.$$

Inserting the above expression to (26), we arrive at the following result.

Proposition 2 *Let Ω be of class $C^{2,1}$ and $\mathbf{V} \in \Theta$. Then, J is shape differentiable with* $\mathrm{d}J(\Sigma)[\mathbf{V}] = \int_\Sigma G\mathbf{n} \cdot \mathbf{V} \,\mathrm{d}\sigma$ *where*

$$G := \nabla u_R \cdot \nabla \Xi_R - \nabla u_N \cdot \nabla \Xi_N + \lambda(u_N - u_R) - (\lambda - \beta u_R)(u_N - u_R - \beta \Xi_R)$$

$$+ \beta \Xi_R[\lambda + (\kappa - \beta)u_R] + \beta u_R(u_N - u_R) + \frac{1}{2}\kappa(u_N - u_R)^2,$$

(27)

and the quantities Ξ_N and Ξ_N are the respective solutions to the following adjoint systems

$$-\Delta \Xi_N = 0 \text{ in } \Omega, \quad \Xi_N = 0 \text{ on } \Gamma, \quad \partial_\mathbf{n} \Xi_N = u_N - u_R \text{ on } \Sigma;$$

(28)

$$-\Delta \Xi_R = 0 \text{ in } \Omega, \quad \Xi_R = 0 \text{ on } \Gamma, \quad \partial_\mathbf{n} \Xi_R + \beta \Xi_R = u_N - u_R \text{ on } \Sigma.$$

(29)

Remark 3 Again, similar to what has been pointed out in the proof of Proposition 1, we remark that the main reason for rewriting the shape gradient $\mathrm{d}J(\Sigma)[\mathbf{V}]$ given in (26) into $\mathrm{d}J(\Sigma)[\mathbf{V}] = \int_\Sigma G\mathbf{n} \cdot \mathbf{V} \,\mathrm{d}\sigma$ is to avoid the computations of solutions to the boundary value problems (13) and (14) for each velocity field $\mathbf{V}$ which are impractical to use in an iterative procedure.

As an immediate consequence of Proposition 2, we have the following optimality result.

Corollary 1 *Let the domain Ω^* be such that $u = u(\Omega^*)$ satisfies the overdetermined boundary value problem* (1); *i.e., it holds that*

$$u = u_R = u_N \quad \text{on } \overline{\Omega}^*.$$

Then, the domain Ω^* fulfils the necessary optimality condition

$$\mathrm{d}J(\Sigma^*)[\mathbf{V}] = 0 \quad \text{for all } \mathbf{V} \in \Theta.$$

In addition, of course, it also holds that $\mathrm{d}J_A(\Sigma^*)[\mathbf{V}] = 0$ for all $\mathbf{V} \in \Theta$.

Proof At the shape solution $\Omega = \Omega^*$ of the Bernoulli problem (1), $u_N = 0$ on Σ^*. Hence, $\nabla u_N = (\partial_\mathbf{n} u_N)\mathbf{n}$ on Σ and it follows that $\nabla u_N \cdot \tau = 0$ on Σ^*. Moreover, we see that $\Xi_N \equiv 0$ and $\Xi_R \equiv 0$ (and also $p_N \equiv 0$) in $\overline{\Omega}^*$. Thus, G given by (27) is zero (so is G_A given by (25)), which implies the assertion. $\square$

In the next section, we shall compute the second-order shape derivative of J at Ω in the direction of two vector fields from Θ. We first treat the case when condition (A) is imposed during the calculation of the shape derivative followed by the case when it is disregarded (*see* Sect. 3.4).

3.3 Second-order shape derivative of the cost function

Let us now compute the shape Hessian of J at Ω in the direction of two vector fields $\mathbf{V}, \mathbf{W} \in \Theta$. Due to standard regularity theory for elliptic equations, we know that the $H^3(\Omega)$ regularity of u_N provides the same regularity $H^3(\Omega)$ to p_N. Hence, for sufficiently small s, it is clear that the derivative $dJ_A(\Omega_s(\mathbf{W}))[\mathbf{V}]$ of J (under assumption (A)) at $\Omega_s(\mathbf{W}) \subset U$ is well-defined. Our next goal is to find an expression for the limit

$$\lim_{s \searrow 0} \frac{dJ_A(\Omega_s(\mathbf{W}))[\mathbf{V}] - dJ_A(\Omega)[\mathbf{V}]}{s} =: d^2 J_A(\Sigma)[\mathbf{V}, \mathbf{W}],$$

where

$$dJ_A(\Omega_s(\mathbf{W}))[\mathbf{V}] = \int_{\Sigma_s} G_{As} \mathbf{n}_s \cdot \mathbf{V} \, d\sigma_s,$$

$$G_{As} = \left(\lambda p_{Ns} + \frac{1}{2} u_{Ns}^2 \right) \kappa_s - \langle \nabla u_{Ns}, \nabla p_{Ns} \rangle + \lambda \frac{\partial p_{Ns}}{\partial \mathbf{n}_s}. \tag{30}$$

Here, $\Sigma_s := \Sigma_s(\mathbf{W})$ denotes the free boundary of the perturbed domain $\Omega_s := \Omega_s(\mathbf{W})$ obtained via the deformation field $\mathbf{W} \in \Theta$ and $u_{Ns} \in H^3(\Omega_s)$ is the unique (weak) solution of the state system (3) on $\bar{\Omega} = \bar{\Omega}_s$. On the other hand, $\kappa_s = \mathrm{div}_{\Sigma_s} \mathbf{n}_s$, and $\mathbf{n}_s$ and τ_s respectively denote the unit outward normal and unit tangent vectors on Σ_s.

Accordingly, if, for all $\mathbf{V}$ and $\mathbf{W}$ in Θ, $d^2 J(\Sigma)[\mathbf{V}, \mathbf{W}]$ exists and is bilinear and continuous with respect to $\mathbf{V}$ and $\mathbf{W}$, then J is said to be twice shape differentiable at Ω. In this case, the map $(\mathbf{V}, \mathbf{W}) \mapsto d^2 J(\Sigma)[\mathbf{V}, \mathbf{W}]$ is called the *shape Hessian* of J at Ω in the $\mathbf{V}, \mathbf{W}$ direction. For an admissible domain Ω, it can be shown that the shape Hessian has its support on $\partial\Omega$ and it is independent on the tangential component of $\mathbf{W}$ on the boundary. However, the exact expression for the shape Hessian, in general, consists of the tangential component of $\mathbf{V}$. This means, basically, that the shape Hessian is generally not symmetric (see, e.g., [22, Chapter 9, Section 6]). Even so, at the optimal shape solution Ω^* of J, it can be proved that only the normal components of $\mathbf{V}$ and $\mathbf{W}$ contributes to the shape Hessian. Here, we focus our attention on this situation since we are only interested in the expression for the shape Hessian of J at the solution Ω^* of the exterior Bernoulli free boundary problem (1).

Proposition 3 *Let Ω be of class $C^{2,1}$ and $\mathbf{V}, \mathbf{W} \in \Theta$ and β be the mean curvature of Σ. Then, the shape Hessian of J at Ω^* is given by*

$$d^2 J_A(\Sigma^*)[\mathbf{V}, \mathbf{W}] = \int_{\Sigma^*} \lambda \kappa p'_{NW} \mathbf{n} \cdot \mathbf{V} \, d\sigma, \tag{31}$$

where p'_{NW} denotes the shape derivative of the adjoint state p_N in the direction of $\mathbf{W}$ satisfying the PDE system

$$-\Delta p'_{NW} = 0 \text{ in } \Omega^*, \quad p'_{NW} = 0 \text{ on } \Gamma, \quad \partial_{\mathbf{n}} p'_{NW} = u'_{NW} + \lambda \mathbf{W} \cdot \mathbf{n} \text{ on } \Sigma^*, \quad (32)$$

where u'_{NW} denotes the shape derivative of u_N in the direction of $\mathbf{W}$.

Proof In the proof, we denote the shape derivative of φ in the direction $\mathbf{W}$ by φ' (i.e., $\varphi' = \varphi'_W$) for simplicity. Let $\mathbf{N}_s = \mathbf{N}_s(\mathbf{W})$ be a smooth extension of $\mathbf{n}_s$ (see, e.g, [22, Equation (4.37), p. 491]). Using (17) with $f(s, \sigma) = G_{As} \mathbf{n}_s \cdot \mathbf{V} = G_{As} \mathbf{N}_s \cdot \mathbf{V}$ (G_{As} is given by (30)), and $\mathbf{V}$ replaced by $\mathbf{W}$, we get

$$d^2 J_A(\Sigma)[\mathbf{V}, \mathbf{W}] = \int_\Sigma \left(G'_A \mathbf{N} + G_A \mathbf{N}' \right) \cdot \mathbf{V} \, d\sigma$$
$$+ \int_\Sigma \left\{ \frac{\partial G_A}{\partial \mathbf{n}} (\mathbf{N} \cdot \mathbf{V}) + G_A \frac{\partial (\mathbf{N} \cdot \mathbf{V})}{\partial \mathbf{n}} + \kappa G_A \mathbf{N} \cdot \mathbf{V} \right\} \mathbf{n} \cdot \mathbf{W} \, d\sigma. \quad (33)$$

By Corollary 1, we know that $G_A = 0$ on Σ^*. Hence, noting that $\mathbf{N}|_\Sigma = \mathbf{n}$, we obtain

$$d^2 J_A(\Sigma^*)[\mathbf{V}, \mathbf{W}] = \int_{\Sigma^*} \left\{ G'_A \mathbf{n} \cdot \mathbf{V} + \frac{\partial G_A}{\partial \mathbf{n}} (\mathbf{n} \cdot \mathbf{V}) \mathbf{n} \cdot \mathbf{W} \right\} d\sigma. \quad (34)$$

Here, because $p_N \equiv 0$, and $u_N = 0$ and $\partial_{\mathbf{n}} u_N = \lambda$ on Σ^*, $G'|_{\Sigma^*}$ is given by

$$G'_A|_{\Sigma^*} = \left\{ (\lambda p'_N + u_N u'_N)\kappa + \left(\lambda p_N + \frac{1}{2} u_N^2 \right)\kappa' \right.$$
$$\left. - \langle \nabla u'_N, \nabla p_N \rangle - \langle \nabla u_N, \nabla p'_N \rangle + \lambda(\nabla p'_N \cdot \mathbf{n} + \nabla p_N \cdot \mathbf{n}') \right\} \Big|_{\Sigma^*}$$
$$= \lambda \kappa p'_N.$$

On the other hand, we note that, for $\varphi, \psi \in H^3(\Omega)$, $\nabla(\nabla \varphi \cdot \nabla \psi) \cdot \mathbf{n} = (\nabla^2 \varphi \nabla \psi + \nabla^2 \psi \nabla \varphi) \cdot \mathbf{n}$. This identity holds true because the Hessian $\nabla^2 \varphi$ of φ is symmetric. Hence, the term $\partial_{\mathbf{n}} G_A$ vanishes on Σ^* because

$$\partial_{\mathbf{n}} G_A|_{\Sigma^*} = \left\{ (\lambda \partial_{\mathbf{n}} p_N + u_N \partial_{\mathbf{n}} u_N)\kappa + \left(\lambda p_N + \frac{1}{2} u_N^2 \right) \partial_{\mathbf{n}} \kappa \right.$$
$$\left. - (\nabla^2 u_N \nabla p_N + \nabla^2 p_N \nabla u_N) \cdot \mathbf{n} + \lambda \nabla^2 p_N \mathbf{n} \cdot \mathbf{n} \right\} \Big|_{\Sigma^*}$$
$$= 0.$$

Thus, we have

$$d^2 J_A(\Sigma^*)[\mathbf{V}, \mathbf{W}] = \int_{\Sigma^*} \lambda \kappa p'_{NW} \mathbf{n} \cdot \mathbf{V} \, d\sigma,$$

where p'_{NW} satisfies the PDE system (32), proving the proposition. $\square$

In view of the previous proposition, we see that in order to evaluate the shape Hessian of J, we first need to compute the solution p'_{NW} of (32) (although the derivation of this set of equations follows standard techniques issued, for example, in [71], we provide it in the appendix for the sake of completeness; see Proposition

A.1) which depends on u'_{NW} and hence to the perturbation field $\mathbf{W}$. In terms of numerical aspect, this step is quite problematic to implement in an iterative procedure because it would require the solution of (32) for each deformation field $\mathbf{W}$ at every iteration. To resolve the issue, we can again apply the adjoint method (see Remark 4 in Sect. 3.4) as done in the proof of Proposition 1. Before we do this, let us first examine the symmetry of the shape Hessian $\mathrm{d}^2 J(\Sigma^*)$ of J with respect to the velocity fields $\mathbf{V}$ and $\mathbf{W}$.

3.4 Symmetricity of the shape Hessian at a critical shape

Here, let us derive the shape Hessian $\mathrm{d}^2 J(\Sigma^*)[\mathbf{V}, \mathbf{W}]$, but in a slightly different fashion, of J without imposing assumption (A) in expressing its shape gradient (see expression (26)). We will show that, in this case, the corresponding expression for the shape Hessian is symmetric with respect to $\mathbf{V}$ and $\mathbf{W}$. Again, we denote $w = u_{\mathrm{N}} - u_{\mathrm{R}}$ and let $\mathbf{N}_s = \mathbf{N}_s(\mathbf{W})$ again be a smooth extension of $\mathbf{n}_s$. Then, $J(\Sigma) = \frac{1}{2} \int_\Sigma |w|^2 \, \mathrm{d}\sigma$ and from (17), we obtain

$$\mathrm{d}J(\Sigma)[\mathbf{V}] = \int_\Sigma \{ww'_V + g\mathbf{V} \cdot \mathbf{n}\} \, \mathrm{d}\sigma,$$

where $g = w\nabla w \cdot \mathbf{n} + \frac{1}{2}\kappa w^2$. Furthermore, we get

$$\begin{aligned}
\mathrm{d}^2 & J(\Sigma)[\mathbf{V}, \mathbf{W}] \\
&= \int_\Sigma \{w'_W w'_V + w w''_{VW} + [\partial_{\mathbf{n}} w w'_V + w\partial_{\mathbf{n}} w'_V + \kappa w w'_V]\mathbf{W} \cdot \mathbf{n}\} \, \mathrm{d}\sigma \\
&\quad + \int_\Sigma \{g'_W \mathbf{V} \cdot \mathbf{N} + g\mathbf{V} \cdot \mathbf{N}'_W + [\partial_{\mathbf{n}} g\mathbf{V} \cdot \mathbf{N} + g\partial_{\mathbf{n}}(\mathbf{V} \cdot \mathbf{N}) + \kappa g\mathbf{V} \cdot \mathbf{N}]\mathbf{W} \cdot \mathbf{n}\} \, \mathrm{d}\sigma,
\end{aligned}$$

(35)

where w''_{VW} denotes the shape derivative of w along the directions of $\mathbf{V}$ and $\mathbf{W}$ (applied consecutively) and $g'_W = w'_W \nabla w \cdot \mathbf{N} + w\nabla w'_W \cdot \mathbf{N} + w\nabla w \cdot \mathbf{N}'_W + \frac{1}{2}\kappa'_W w^2 + \kappa w w'_W$. Now, according to Corollary 1, we have $w \equiv 0$ and $g \equiv 0$ at $\Sigma = \Sigma^*$ which also gives us $g'_W \equiv 0$ on Σ^*. Therefore, $\mathrm{d}^2 J(\Sigma^*)[\mathbf{V}, \mathbf{W}] = \int_{\Sigma^*} w'_V w'_W \, \mathrm{d}\sigma$. Meanwhile, for $\beta = \kappa$, we know that $u'_R \equiv 0$ on $\bar{\Omega}^*$ by Lemma 2. Thus, we obtain

$$\mathrm{d}^2 J(\Sigma^*)[\mathbf{V}, \mathbf{W}] = \int_{\Sigma^*} u'_{\mathrm{NV}} u'_{\mathrm{NW}} \, \mathrm{d}\sigma,$$

(36)

which clearly shows the symmetry (with respect to the deformation fields $\mathbf{V}$ and $\mathbf{W}$) of the shape Hessian at a critical shape.

Let us now write (36) in its equivalent form using the adjoint method. For this purpose, we will denote the corresponding adjoint of u'_{NV} and u'_{NW} by Φ_W and Φ_V, respectively. (The choice of subscripts for these adjoints will be made clear below.)

Clearly, both Φ_W and Φ_V are harmonic functions and both vanishes on Γ. Meanwhile, on Σ^*, we take $\partial_{\mathbf{n}}\Phi_W = u'_{\mathrm{NW}}$ and $\partial_{\mathbf{n}}\Phi_V = u'_{\mathrm{NV}}$, so that (via Green's second identity) we obtain the following equalities

$$\int_{\Sigma^*} u'_{NV} u'_{NW} \, d\sigma = \int_{\Sigma^*} u'_{NV} \partial_{\mathbf{n}} \Phi_W \, d\sigma = \int_{\Sigma^*} \Phi_W \partial_{\mathbf{n}} u'_{NV} \, d\sigma = \int_{\Sigma^*} \Phi_W (\lambda \kappa \mathbf{V} \cdot \mathbf{n}) \, d\sigma$$
$$= \int_{\Sigma^*} u'_{NW} \partial_{\mathbf{n}} \Phi_V \, d\sigma = \int_{\Sigma^*} \Phi_V \partial_{\mathbf{n}} u'_{NW} \, d\sigma = \int_{\Sigma^*} \Phi_V (\lambda \kappa \mathbf{W} \cdot \mathbf{n}) \, d\sigma.$$

Consequently, the adjoint states Φ_W and Φ_V satisfy the PDE systems

$$-\Delta \Phi_W = 0 \text{ in } \Omega^*, \quad \Phi_W = 0 \text{ on } \Gamma, \quad \partial_{\mathbf{n}} \Phi_W = u'_{NW} \text{ on } \Sigma^*; \qquad (37)$$

$$-\Delta \Phi_V = 0 \text{ in } \Omega^*, \quad \Phi_V = 0 \text{ on } \Gamma, \quad \partial_{\mathbf{n}} \Phi_V = u'_{NV} \text{ on } \Sigma^*, \qquad (38)$$

respectively. Hence, we conclude that (36) can also be expressed as

$$d^2 J(\Sigma^*)[\mathbf{V}, \mathbf{W}] = \int_{\Sigma^*} \lambda \kappa \Phi_W \mathbf{V} \cdot \mathbf{n} \, d\sigma = \int_{\Sigma^*} \lambda \kappa \Phi_V \mathbf{W} \cdot \mathbf{n} \, d\sigma, \qquad (39)$$

where Φ_W and Φ_V satisfy (37) and (38), respectively. Evidently, this shows that, at the optimal shape solution Ω^* of J, only the normal components of $\mathbf{V}$ and $\mathbf{W}$ contributes to the shape Hessian.

Remark 4 We emphasize that the shape Hessian $d^2 J_A(\Sigma^*)[\mathbf{V}, \mathbf{W}] = \int_{\Sigma^*} \lambda \kappa p'_{NW} \mathbf{n} \cdot \mathbf{V} \, d\sigma$ given in Proposition 3 is also impractical to use in numerical calculation because an appropriate choice for the deformation field $\mathbf{W}$ is difficult to determine directly from the given boundary integral (*see* Sect. 5). To circumvent this difficulty, we again apply the adjoint method. First, we let Ψ be harmonic on Ω such that it vanishes on Γ. Letting $\partial_{\mathbf{n}} \Psi = \lambda \kappa \mathbf{V} \cdot \mathbf{n}$ on Σ, we get (via Green's second identity and Eq. (32)) the following equalities $\int_{\Sigma} \lambda \kappa p'_{NW} \mathbf{n} \cdot \mathbf{V} \, d\sigma = \int_{\Sigma} p'_{NW} \partial_{\mathbf{n}} \Psi \, d\sigma = \int_{\Sigma} \Psi \partial_{\mathbf{n}} p'_{NW} \, d\sigma = \int_{\Sigma} (\Psi u'_{NW} + \lambda \Psi) \mathbf{n} \cdot \mathbf{W} \, d\sigma$. Next, we let another function Π to be harmonic on Ω such that $\Pi = 0$ on Γ. Also, we let $\partial_{\mathbf{n}} \Pi = \Psi$, so that (via Green's second identity) we have $\int_{\Sigma} \Psi u'_{NW} \, d\sigma = \int_{\Sigma} \partial_{\mathbf{n}} \Pi u'_{NW} \, d\sigma = \int_{\Sigma} \Pi \partial_{\mathbf{n}} u'_{NW} \, d\sigma = \int_{\Sigma} \lambda \kappa \Pi \mathbf{n} \cdot \mathbf{W} \, d\sigma$. Summarizing these results we can therefore write the shape Hessian $d^2 J_A(\Sigma^*)[\mathbf{V}, \mathbf{W}]$ as

$$d^2 J_A(\Sigma^*)[\mathbf{V}, \mathbf{W}] = \int_{\Sigma^*} \lambda \kappa p'_{NW} \mathbf{n} \cdot \mathbf{V} \, d\sigma = \int_{\Sigma^*} \lambda(\Psi + \lambda \kappa \Pi) \mathbf{n} \cdot \mathbf{W} \, d\sigma, \qquad (40)$$

where Ψ and Π satisfy the following PDE systems

$$-\Delta \Psi = 0 \text{ in } \Omega^*, \quad \Psi = 0 \text{ on } \Gamma, \quad \partial_{\mathbf{n}} \Psi = \lambda \kappa \mathbf{V} \cdot \mathbf{n} \text{ on } \Sigma^*; \qquad (41)$$

$$-\Delta \Pi = 0 \text{ in } \Omega^*, \quad \Pi = 0 \text{ on } \Gamma, \quad \partial_{\mathbf{n}} \Pi = \Psi \text{ on } \Sigma^*, \qquad (42)$$

respectively. Here, we notice that $\Psi \equiv u'_{NV}$ on $\bar{\Omega}^*$.

Hence, looking back to Eq. (38), we find that Φ_V is exactly equal to Π satisfying (42) which means that we may actually write the shape Hessian $d^2 J(\Sigma^*)[\mathbf{V}, \mathbf{W}]$ given in (39) as

$$\mathrm{d}^2 J(\Sigma^*)[\mathbf{V}, \mathbf{W}] = \int_{\Sigma^*} \lambda \kappa \Pi \mathbf{n} \cdot \mathbf{W} \, \mathrm{d}\sigma. \tag{43}$$

Remark 5 In (35), we notice the dependence of the shape Hessian $\mathrm{d}^2 J(\Sigma)[\mathbf{V}, \mathbf{W}]$ (for Ω different from the optimal domain Ω^*) to the shape derivative κ'_W of the mean curvature κ along $\mathbf{W} \in \Theta$ appearing on g'_W. The explicit form of κ'_W can be shown to be given by (see [22, 71])

$$\kappa'_W = \mathrm{trace}\left\{ D\left[(D\mathbf{W}\mathbf{n} \cdot \mathbf{n})\mathbf{n} - (D\mathbf{W})^\top \mathbf{n} \right] - D\mathbf{n}D\mathbf{W} \right\} - \nabla\kappa \cdot \mathbf{W}.$$

Clearly, this expression consists of a second-order tangential derivative of the perturbation field $\mathbf{W}$, and this derivative actually exists due to our assumption that Ω is of class $C^{2,1}$ [22, 71]. From this observation, we deduce that the shape Hessian defines a continuous bilinear form

$$\mathrm{d}^2 J(\Sigma) \,:\, \mathbf{H}^1(\Sigma) \times \mathbf{H}^1(\Sigma) \to \mathbb{R};$$

that is, $|\mathrm{d}^2 J(\Sigma)[\mathbf{V}, \mathbf{W}]| \lesssim \|\mathbf{V}\|_{\mathbf{H}^1(\Sigma)} \|\mathbf{W}\|_{\mathbf{H}^1(\Sigma)}$. Here, the notation $\mathbf{H}^1(\cdot)$ denotes the Sobolev space $\mathbf{H}^1(\cdot) := \{\mathbf{u} := (u_1, u_2) \,:\, u_1, u_2 \in H^1(\cdot)\}$ and is equipped with the norm $\|\mathbf{u}\|^2_{\mathbf{H}^1(\cdot)} = \|u_1\|^2_{H^1(\cdot)} + \|u_2\|^2_{H^1(\cdot)}$. Similar definition is also given to the $\mathbf{H}^1_{\Gamma,0}(\cdot)$-space.

In view of the previous remark, it is natural to ask whether it is true that $\mathrm{d}^2 J(\Sigma^*)[\mathbf{V}, \mathbf{V}] \gtrsim \|\mathbf{V}\|^2_{\mathbf{H}^1(\Sigma^*)}$. This question actually refers to the *stability* of a local minimizer Ω^* of J. In relation to this, we recall from [23, 24] (a result regarding *sufficient* second order conditions) that a local minimizer Ω^* is stable *if and only if* the shape Hessian $\mathrm{d}^2 J(\Sigma^*)$ is strictly coercive in its corresponding energy space $\mathbf{H}^1(\Sigma^*)$. Unfortunately, this kind of strict coercivity cannot be established for the shape Hessian $\mathrm{d}^2 J(\Sigma^*)$ of J. Nevertheless, we shall show in the next subsection that sufficient condition can be derived to obtain strict coercivity in a weaker space. We note that the derived coercivity criterion is exactly the same as in the case of the shape Hessian $\mathrm{d}^2 J_i$ of the cost functional J_i, $i = 1, 2, 3, 4$, as shown in [31–33, 68], respectively. It is worth remarking that, among these cost functions, only the shape Hessian $\mathrm{d}^2 J_2(\Sigma^*)$ of J_2 is $\mathbf{H}^1(\Sigma^*)$-coercive under the derived coercivity criterion (see [31, Proposition 2.12]). For the sake of comparison, let us also compute the shape Hessian of the cost functional $J_1(\Sigma)$ at $\Sigma = \Sigma^*$. From Remark 2, we know that the gradient of $J_1(\Sigma)$ only differs by the addition of the integral $\int_\Sigma (u_N \nabla u_N \cdot \mathbf{n})\mathbf{n} \cdot \mathbf{V} \, \mathrm{d}\sigma =: \int_\Sigma g_1 \mathbf{n} \cdot \mathbf{V} \, \mathrm{d}\sigma$ from the shape gradient of $J(\Sigma)$. Computing the shape derivative of g_1 at $\Omega = \Omega^*$ along the deformation field $\mathbf{W}$, we get $g'_{1W}|_{\Sigma^*} = u'_{NW}(\nabla u_N \cdot \mathbf{N}) + u_N(\nabla u'_{NW} \cdot \mathbf{N} + \nabla u_N \cdot \mathbf{N}'_W)|_{\Sigma^*} = \lambda u'_{NW}$. Meanwhile, we have $\nabla(u_N \nabla u_N \cdot \mathbf{n}) \cdot \mathbf{n} = (\nabla u_N \cdot \mathbf{n})^2 + u_N[(\nabla^2 u_N)\mathbf{n}] \cdot \mathbf{n} = \lambda^2$ on Σ^*. Hence, from (34) with G replaced by g_1, together with Eq. (31) in Proposition 3, we get the final expression for the shape Hessian of J_1 at $\Omega = \Omega^*$ (cf. [32, Equation (21)]):

Proposition 4 *Let Ω be of class $C^{2,1}$ and $\mathbf{V}, \mathbf{W} \in \Theta$. Then, the shape Hessian of J_1 at Ω^* is given by*

$$\mathrm{d}^2 J_1(\Sigma^*)[\mathbf{V}, \mathbf{W}] = \int_{\Sigma^*} \left\{ \lambda(\kappa p'_{NW} + u'_{NW})\mathbf{n} \cdot \mathbf{V} + \lambda^2(\mathbf{n} \cdot \mathbf{V})\mathbf{n} \cdot \mathbf{W} \right\} \mathrm{d}\sigma.$$

Here, we mention that the above expression was also computed in [32] but through shape calculus for star shape domains, hence, we refer the readers to the aforementioned reference for comparison.

Meanwhile, following Remark 4, we can also write $\mathrm{d}^2 J_1(\Sigma^*)[\mathbf{V}, \mathbf{W}]$ in terms of appropriate adjoint states. To do this, we let Υ be harmonic in Ω and be zero on Γ. Moreover, we let $\partial_{\mathbf{n}} \Upsilon = \lambda \mathbf{V} \cdot \mathbf{n}$ on Σ, so that by Green's second identity we have, $\int_\Sigma u'_{NW}(\lambda \mathbf{n} \cdot \mathbf{V}) \, \mathrm{d}\sigma = \int_\Sigma u'_{NW} \partial_{\mathbf{n}} \Upsilon \, \mathrm{d}\sigma = \int_\Sigma \Upsilon \partial_{\mathbf{n}} u'_{NW} \, \mathrm{d}\sigma = \int_\Sigma \lambda \kappa \Upsilon \mathbf{n} \cdot \mathbf{W} \, \mathrm{d}\sigma.$ Hence, using the results from Remark 4, we therefore have the following equivalent expression for $\mathrm{d}^2 J_1(\Sigma^*)[\mathbf{V}, \mathbf{W}]$:

$$\mathrm{d}^2 J_1(\Sigma^*)[\mathbf{V}, \mathbf{W}] = \int_{\Sigma^*} \{ \lambda^2 \kappa \Pi + \lambda \kappa \Upsilon + \lambda \Psi + \lambda^2(\mathbf{n} \cdot \mathbf{V}) \}\mathbf{n} \cdot \mathbf{W} \, \mathrm{d}\sigma,$$

where the adjoint states Ψ and Π satisfy the boundary value problems (41) and (42), respectively, while Υ is the unique solution to the PDE system

$$-\Delta \Upsilon = 0 \text{ in } \Omega^*, \quad \Upsilon = 0 \text{ on } \Gamma, \quad \partial_{\mathbf{n}} \Upsilon = \lambda \mathbf{V} \cdot \mathbf{n} \text{ on } \Sigma^*. \tag{44}$$

Here, it is worth to stress out that the shape Hessian $\mathrm{d}^2 J_1(\Sigma^*)[\mathbf{V}, \mathbf{W}]$ depends on the solutions of three boundary value problems as opposed to the case of $\mathrm{d}^2 J_A(\Sigma^*)[\mathbf{V}, \mathbf{W}]$ which depends only on the solutions of two PDE systems. In terms of numerical aspects, this means that we need to solve an additional variational problem in order to evaluate the descent direction for a gradient-based descent algorithm.

3.5 Coercivity of the shape Hessian at its optimal solution

Let us now determine which weaker space of $\mathbf{H}^1(\Sigma^*)$ does the shape Hessian $\mathrm{d}^2 J(\Sigma^*)$ is strictly coercive. To do this, we use the method already used in [28] (see also [31–33, 68]). We start by introducing the following operators which are linear continuous as a multiplier by a smooth function (see [68, Section 3.4]):

$$\mathcal{L} : \mathbf{H}^{1/2}(\Sigma^*) \to H^{1/2}(\Sigma^*), \quad \mathcal{L}\mathbf{V} := \lambda V_n;$$
$$\mathcal{M} : H^{1/2}(\Sigma^*) \to H^{1/2}(\Sigma^*), \quad \mathcal{M}v := \kappa v.$$

Here, $V_n := \mathbf{V} \cdot \mathbf{n}$ and κ is, of course, the mean curvature of Σ^*. The continuity of these operators follows from the following result.

Lemma 3 *Let $\Omega \subset \mathbb{R}^2$ be a bounded Lipschitz domain with boundary $\Gamma := \partial\Omega$. Then, the map $v \mapsto \phi v$ is continuous in $H^{1/2}(\Gamma)$ for any $v \in H^{1/2}(\Gamma)$ and $\phi \in C^{0,1}(\Gamma)$.*

Proof Recall that the fractional Sobolev space $H^{1/2}(\Gamma)$ (the trace space for $H^1(\Omega)$) is equipped with the norm

$$\|v\|_{1/2,2} = \|v\|_{L^2(\Gamma)} + |v|_{1/2,2,\Gamma}, \quad |v|_{1/2,2,\Gamma} = \left(\int_\Gamma \int_\Gamma \frac{|v(x) - v(y)|^2}{|x - y|^2} \, \mathrm{d}x \, \mathrm{d}y \right)^{1/2}.$$

Let ϕ be a Lipschitz function. Then, we have the inequality

$$|\phi(x)v(x) - \phi(y)v(y)| \lesssim \|\phi\|_\infty |v(x) - v(y)| + |v(y)||x - y|.$$

Hence, $|\phi v|_{1/2,2,\Gamma}$ can be estimated as follows

$$
\begin{aligned}
|\phi v|_{1/2,2,\Gamma} &= \left(\int_\Gamma \int_\Gamma \frac{|\phi(x)v(x) - \phi(y)v(y)|^2}{|x - y|^2} \, \mathrm{d}x \, \mathrm{d}y \right)^{1/2} \\
&\lesssim \|\phi\|_\infty |v|_{1/2,2,\Gamma} + \left(\int_\Gamma \int_\Gamma |v(y)|^2 \, dx \, dy \right)^{1/2} \\
&\lesssim \|\phi\|_\infty |v|_{1/2,2,\Gamma} + |\Gamma|^{1/2} \|v\|_{L^2(\Gamma)}.
\end{aligned}
$$

Because $\|\phi v\|_{L^2(\Gamma)} \lesssim \|\phi\|_\infty \|v\|_{L^2(\Gamma)}$, then the assertion is proved. $\qquad\square$

In addition to the operators introduced above, let us also define the map $\mathcal{S}$ as the *Steklov-Poincaré* operator on Σ^* which is defined by (see [72])

$$\mathcal{S} : H^{1/2}(\Sigma^*) \to H^{-1/2}(\Sigma^*), \quad \mathcal{S}(\Phi) := \left. \frac{\partial \Psi}{\partial \mathbf{n}} \right|_{\Sigma^*}, \tag{45}$$

where $\Psi \in H^1(\Omega^*)$ satisfies

$$-\Delta\Psi = 0 \quad \text{in } \Omega^*, \quad \Psi = 0 \quad \text{on } \Gamma, \quad \Psi = \Phi \quad \text{on } \Sigma^*.$$

The operator $\mathcal{S}$, also called the *Dirichlet-to-Neumann* map, is $H^{1/2}(\Sigma^*)$-coercive (cf. [33, Lemma 2]). Its inverse $\mathcal{R}$ called the *Neumann-to-Dirichlet* map is defined by

$$\mathcal{R} : H^{-1/2}(\Sigma^*) \to H^{1/2}(\Sigma^*), \quad \mathcal{R}\left(\frac{\partial \Psi}{\partial \mathbf{n}} \right) := \Phi|_{\Sigma^*},$$

where $\Phi \in H^1(\Omega^*)$ satisfies

$$-\Delta\Phi = 0 \quad \text{in } \Omega^*, \quad \Phi = 0 \quad \text{on } \Gamma, \quad \partial_\mathbf{n}\Phi = \partial_\mathbf{n}\Psi \quad \text{on } \Sigma^*.$$

Now, using the operators $\mathcal{L}$, $\mathcal{M}$, $\mathcal{R}$, and denoting the $L^2(\Sigma^*)$-inner product by $(\cdot, \cdot)_{L^2(\Sigma^*)}$, we can write (31) as

$$\mathrm{d}^2 J_\mathrm{A}(\Omega^*)[\mathbf{V}, \mathbf{W}] = (\mathcal{M}\mathcal{L}\mathbf{V}, \mathcal{R}(\mathcal{L}\mathbf{W} + \mathcal{R}(\mathcal{M}\mathcal{L}\mathbf{W})))_{L^2(\Sigma^*)}.$$

By the continuity of the maps $\mathcal{L}$ and $\mathcal{M}$, and the bijectivity of $\mathcal{R}$, we deduce that the shape Hessian $\mathrm{d}^2 J_\mathrm{A}$ at Ω^* is $\mathbf{L}^2(\Sigma^*)$-coercive (whenever κ is non-negative) and we state this result formally as follows.

Proposition 5 *For Σ^* with non-negative mean curvature κ, the shape Hessian $\mathrm{d}^2 J_\mathrm{A}$ at Ω^* is $\mathbf{L}^2(\Sigma^*)$-coercive; i.e.,*

$$\mathrm{d}^2 J_\mathrm{A}(\Sigma^*)[\mathbf{V}, \mathbf{V}] \gtrsim \|\mathbf{V}\|^2_{\mathbf{L}^2(\Sigma^*)}.$$

The above result also means that the minimization problem "$\min_\Omega J(\Sigma)$ subject to (3) and (6)" [with condition (A) imposed in computing the gradient] is (algebraically) *ill-posed*. We further discuss this notion of ill-posedness (in the case of the present shape optimization formulation) briefly as follows. As already mentioned in the previous subsection, the shape optimization problem is *well-posed* if its local minimum is stable; that is, if the shape Hessian $\mathrm{d}^2 J_\mathrm{A}(\Sigma^*)$ is strictly coercive in its energy space $\mathbf{H}^1(\Sigma^*)$ (i.e., $\mathrm{d}^2 J_\mathrm{A}(\Sigma^*)[\mathbf{V}, \mathbf{V}] \gtrsim \|\mathbf{V}\|^2_{\mathbf{H}^1(\Sigma^*)}$). If, on the other hand, the positivity of the shape Hessian at Σ^* only holds on a weaker (Sobolev) space, then the shape optimization problem is said to be (algebraically) ill-posed (cf. [30, 32]). This means, in particular, that tracking the Dirichlet data in the L^2-norm is not sufficient, and as strongly assumed by the authors in [34], they have to be tracked relative to H^1. This aforementioned *lack of coercivity* is known from other PDE-constrained optimal control problems as the so-called *two-norm discrepancy* (see, e.g., [30] and the references therein) and this concept of norm discrepancy under shape optimization framework was first observed in [23–25, 27], among others.

Remark 6 In case of the cost functional $J_4(\Omega) = \frac{1}{2}|u_\mathrm{N} - u_\mathrm{R}|^2_{H^1(\Omega)}$ examined in [68], the shape Hessian is likewise a continuous bilinear form, i.e., $\mathrm{d}^2 J_4(\Omega) : \mathbf{H}^1(\Sigma) \times \mathbf{H}^1(\Sigma) \to \mathbb{R}$. This result is primarily due to the fact that the computed expression for $\mathrm{d}^2 J_4(\Omega)$ also consists of the shape derivative κ' of the mean curvature κ. Also, using the operators introduced above, the shape Hessian $\mathrm{d}^2 J_4$ at Ω^* was shown to be expressible as

$$\mathrm{d}^2 J_4(\Omega^*)[\mathbf{V}, \mathbf{W}] = (\mathcal{M}\mathcal{L}\mathbf{V}, \mathcal{R}(\mathcal{M} + \mathcal{S})\mathcal{L}\mathbf{W})_{L^2(\Sigma^*)},$$

which is $\mathbf{H}^{1/2}(\Sigma^*)$-coercive provided that Σ^* has non-negative mean curvature κ.

Remark 7 Similarly, we have that $\mathrm{d}^2 J_1(\Omega) : \mathbf{H}^1(\Sigma) \times \mathbf{H}^1(\Sigma) \to \mathbb{R}$ and using the operators introduced above, we may write the shape Hessian of J_1 at $\Omega = \Omega^*$ given in Proposition 4 as follows:

$$\mathrm{d}^2 J_1(\Omega^*)[\mathbf{V}, \mathbf{W}] = (\mathcal{R}(\mathcal{M} + \mathcal{S})\mathcal{L}\mathbf{V}, \mathcal{R}(\mathcal{M} + \mathcal{S})\mathcal{L}\mathbf{W})_{L^2(\Sigma^*)},$$

This expression is also $\mathbf{H}^{1/2}(\Sigma^*)$-coercive (i.e., $\mathrm{d}^2 J_1(\Sigma^*)[\mathbf{V}, \mathbf{V}] \gtrsim \|\mathbf{V}\|^2_{\mathbf{H}^{1/2}(\Sigma^*)}$) provided that Σ^* has non-negative mean curvature κ.

On the other hand, in case of the shape Hessian $\mathrm{d}^2 J(\Sigma^*)[\mathbf{V}, \mathbf{W}]$, we deduce (via the continuity of the maps $\mathcal{L}$ and $\mathcal{M}$, and the bijectivity of $\mathcal{R}$) that

$$\mathrm{d}^2 J(\Sigma^*)[\mathbf{V}, \mathbf{V}] = \|\mathcal{R}(\mathcal{M}\mathcal{L}\mathbf{V})\|^2_{L^2(\Sigma^*)} \sim \|\mathcal{M}\mathcal{L}\mathbf{V}\|^2_{H^{-1}(\Sigma^*)},$$

whenever κ is non-negative. Here, the notation "$P \sim Q$" means that "$P \lesssim Q$ and $P \gtrsim Q$." Hence, the positivity of $\mathrm{d}^2 J(\Sigma^*)$ holds only in the weaker space $\mathbf{L}^2(\Sigma^*)$.

4 Existence of optimal domains of the shape optimization problem

Before going to the numerical treatment of the proposed shape optimization reformulation "$\min_\Omega J(\Sigma)$ subject to (3) and (6)" [or equivalently, "$\min_\Omega J(\Sigma)$ subject to (7) and (8)"] of (1) and for completeness, let us first address the question of existence of optimal solution to the said problem. On the other hand, as regards to the existence of solution to the exterior Bernoulli FBP (1), we refer the readers to [1].

To carry out our present task, we use the results established in [68] regarding the continuity of the state problems with respect to domain. We begin by rewriting the weak formulations (7) and (8) of (3) and (6), respectively, as follows:

Find $z_{\mathrm{N}} = u_{\mathrm{N}} - u_{\mathrm{N}0} \in H^1_{\Gamma,0}(\Omega)$ such that

$$\int_\Omega \nabla z_{\mathrm{N}} \cdot \nabla \varphi \, \mathrm{d}x + \int_\Omega \nabla u_{\mathrm{N}0} \cdot \nabla \varphi \, \mathrm{d}x - \int_\Sigma \lambda \varphi \, \mathrm{d}\sigma = 0, \quad \forall \varphi \in H^1_{\Gamma,0}(\Omega); \quad (46)$$

find $z_{\mathrm{R}} = u_{\mathrm{R}} - u_{\mathrm{R}0} \in H^1_{\Gamma,0}(\Omega)$ such that

$$\int_\Omega \nabla z_{\mathrm{R}} \cdot \nabla \varphi \, \mathrm{d}x + \int_\Omega \nabla u_{\mathrm{R}0} \cdot \nabla \varphi \, \mathrm{d}x + \int_\Sigma \beta z_{\mathrm{R}} \varphi \, \mathrm{d}\sigma - \int_\Sigma \lambda \varphi \, \mathrm{d}\sigma = 0, \quad \forall \varphi \in H^1_{\Gamma,0}(\Omega). \tag{47}$$

In above equations, $u_{\mathrm{N}0}$ and $u_{\mathrm{R}0}$ are two fixed functions in $H^1(U)$ such that $u_{\mathrm{N}0} = u_{\mathrm{R}0} = 1$ on Γ. Given the unique solvability of (46) and (47) in $H^1(\Omega)$, we define the map $\Omega \mapsto (z_{\mathrm{N}}, z_{\mathrm{R}}) = (z_{\mathrm{N}}(\Omega), z_{\mathrm{R}}(\Omega))$ and denote its graph by

$$\mathscr{F} = \{(\Omega, z_{\mathrm{N}}(\Omega), z_{\mathrm{R}}(\Omega)) : \Omega \in \mathcal{O}_{\mathrm{ad}} \text{ and } z_{\mathrm{N}}(\Omega), z_{\mathrm{R}}(\Omega) \text{ satisfies } (46) - -(47) \text{ on } \Omega\}.$$

Hence, the problem "$\min_\Omega J(\Sigma)$ subject to (7) and (8)" is equivalent to the problem of finding a solution $(\Omega, z_{\mathrm{N}}(\Omega), z_{\mathrm{R}}(\Omega))$ that minimizes $J(\Omega) = J(\Omega, z_{\mathrm{N}}(\Omega), z_{\mathrm{R}}(\Omega))$ on $\mathscr{F}$. Such minimization problem is usually solved by endowing the set $\mathscr{F}$ with a topology for which $\mathscr{F}$ is compact and J is lower semi-continuous. For this purpose, we follow the ideas developed in [43] and the ones furnished in [13, 42].

Let us now characterize the set of admissible domains $\mathcal{O}_{\mathrm{ad}}$ and then give an appropriate topology on it. In the previous section, we assume a $C^{2,1}$ regularity for the domain Ω to guarantee the existence of the shape derivatives of the states and to establish the shape Hessian of J, for the existence proof of optimal solution to the problem

$$\begin{cases} \text{Find } (\Omega^*, z_{\mathrm{N}}(\Omega^*), z_{\mathrm{R}}(\Omega^*)) \in \mathscr{F} \text{ such that} \\ J(\Omega^*, z_{\mathrm{N}}(\Omega^*), z_{\mathrm{R}}(\Omega^*)) \leqslant J(\Omega, z_{\mathrm{N}}(\Omega), z_{\mathrm{R}}(\Omega)), \ \forall (\Omega, z_{\mathrm{N}}(\Omega), z_{\mathrm{R}}(\Omega)) \in \mathscr{F}, \end{cases} \tag{48}$$

it is enough to assume that Ω has a $C^{1,1}$ smooth free boundary Σ (cf. [68]). Hence, we let Σ be parametrized by a vector function $\phi \in C^{1,1}(\mathbb{R}, \mathbb{R}^2)$ (i.e., $\Sigma = \Sigma(\phi) = \{\phi = (\phi_1(t), \phi_2(t)) : t \in (0, 1]\}$) where, in addition, ϕ is assume to possess the following properties:

(P$_1$) ϕ is injective on (0, 1] and is 1-periodic;
(P$_2$)   there exist positive constants c_0, c_1, c_2 and c_3 such that

$$|\phi(t)| \leqslant c_0, \quad c_1 \leqslant |\phi'(t)| \leqslant c_2, \quad |\phi''(t)| \leqslant c_3, \text{ a.e. in } (0, 1);$$

(P$_3$) $\overline{\Omega} = \overline{\Omega}(\phi) \subset U$, U is a fixed, connected, bounded open subset of $\mathbb{R}^2$;
(P$_4$)   there is a positive constant γ such that dist$(\Gamma, \Sigma(\phi)) \geqslant \gamma$.

If ϕ satisfies the above conditions, then we say that ϕ is in $\mathcal{U}_{\text{ad}}$. The set of admissible domains $\mathcal{O}_{\text{ad}}$ we consider here is now given as follows

$$\mathcal{O}_{\text{ad}} = \{\Omega = \Omega(\phi) \subset U : \phi \in \mathcal{U}_{\text{ad}}\}. \tag{49}$$

The set U in assumption (P$_3$) and the one introduced in Sect. 3 are not necessarily the same set. However, we point out that in (P$_3$), we are assuming that all admissible domains $\Omega(\phi)$ are contained in the *hold-all* domain U in the same manner that the universal set U in Eq. (9) holds all the possible deformations of the reference domain Ω. Also, we assume that U is large enough that it contains the optimal domain Ω^* that solves the exterior Bernoulli FBP (1). Here, we are in fact requiring that dist$(\Sigma(\phi), \partial U) > 0$ for all $\phi \in \mathcal{U}_{\text{ad}}$ and dist$(\Sigma^*, \partial U) > 0$. In this way, we can say that the shape optimization problem "$\min_{\Omega} J(\Sigma)$ subject to (7) and (8)" is indeed equivalent to the free boundary problem (1). Meanwhile, in view of (49), we see that every admissible domain $\Omega(\phi)$ is a uniformly open set in $\mathbb{R}^2$ and therefore satisfy the well-known *uniform cone property* (cf. [46]). Moreover, as a consequence, these admissible domains satisfy a very important extension property. More precisely, for every $k \geqslant 1$, $p > 1$ and domain $\Omega \in \mathcal{O}_{\text{ad}}$, there exists an extension operator

$$E_{\Omega} : W^{k,p}(\Omega) \to W^{k,p}(U) \tag{50}$$

such that $\|E_{\Omega} u\|_{W^{k,p}(U)} \leqslant C\|u\|_{W^{k,p}(\Omega)}$, where C is a positive constant independent of the domain Ω (see [18]). Using these properties, we can ensure a uniform extension $\tilde{u} \in H^1(U)$ from Ω to U of every function $u \in H^1(\Omega)$. In the discussion that follows, we will use this result to finally define the topology we shall work with.

Let us first define the convergence of a sequence $\{\phi_n\} \subset \mathcal{U}_{\text{ad}}$ by

$$\phi_n \to \phi \iff \phi_n \to \phi \text{ and } \phi_n' \to \phi' \text{ uniformly on } [0, 1], \tag{51}$$

i.e., if and only if $\phi_n \to \phi$ in the C^1-topology. We can then define the convergence of a sequence of domains $\{\Omega_n\} := \{\Omega(\phi_n)\} \subset \mathcal{O}_{\text{ad}}$ by

$$\Omega_n \to \Omega \iff \phi_n \to \phi. \tag{52}$$

Meanwhile, we define the convergence of a sequence $\{z_{Nn}\}$ of solutions of (46) on Ω_n to the solution of (46) on Ω as follows

$$z_{\text{N}n} \to z_{\text{N}} \iff \tilde{z}_{\text{N}n} \to \tilde{z}_{\text{N}} \text{ weakly in } H^1(U). \tag{53}$$

Similarly, the convergence of a sequence $\{z_{\text{R}n}\}$ of solutions of (47) on Ω_n to the solution of (47) on Ω is define

$$z_{\text{R}n} \to z_{\text{R}} \iff \tilde{z}_{\text{R}n} \to \tilde{z}_{\text{R}} \text{ weakly in } H^1(U). \tag{54}$$

In (53) and (54), the extensions $\tilde{z}_i, \tilde{z}_{in}$, $i = \text{N,R}$, are defined as $E_\Omega z_{\text{i}}, E_\Omega z_{in}$, $i = \text{N,R}$, respectively, where E_Ω is of course the extension operator (50).

Finally, the topology we introduce on $\mathscr{F}$ is the one induced by the convergence defined by

$$(\Omega_n, z_{\text{N}n}, z_{\text{R}n}) \to (\Omega, z_{\text{N}}, z_{\text{R}}) \iff \begin{cases} \phi_n \to \phi, \\ z_{\text{N}n} \to z_{\text{N}}, \\ z_{\text{R}n} \to z_{\text{R}}. \end{cases} \tag{55}$$

We now state the main result of this section.

Theorem 1 *The minimization problem* (48) *admits a solution in* $\mathscr{F}$.

As stated before, the existence proof is reduced to proving the compactness of $\mathscr{F}$ and the lower semi-continuity of J. Regarding the former problem, we note that the convergence $\phi_n \to \phi$ follows immediately from the compactness of $\mathcal{U}_{\text{ad}}$ and the Arzelà-Ascoli theorem, hence, the compactness of $\mathscr{F}$ with respect to the convergence (55) is already guaranteed. This means that we only need to show the continuity of the state problems (3) and (6) with respect to the domain in order to complete the proof of compactness of $\mathscr{F}$. The proof of this continuity is not straightforward but has already been done in [68] using the tools established in [14, 15], so we simply state the result as follows.

Proposition 6 [68] *With the convergence of a sequence of domains given in* (52), *we let* $\{(\phi_n, z_{\text{N}n}, z_{\text{R}n})\}$ *be a sequence in* $\mathscr{F}$ *where* $z_{\text{N}n} := z_{\text{N}}(\phi_n)$ *and* $z_{\text{R}n} := z_{\text{R}}(\phi_n)$ *are the weak solutions of* (46) *and* (47) *on* $\Omega_n := \Omega(\phi_n)$, *respectively. Then, there exists a subsequence* $\{(\phi_k, z_{\text{N}k}, z_{\text{R}k})\}$ *and elements* $\phi \in \mathcal{U}_{\text{ad}}$ *and* $z_{\text{N}}, z_{\text{R}} \in H^1(U)$ *such that*

$$\phi_k \to \phi, \quad \tilde{z}_{\text{N}k} \rightharpoonup z_{\text{N}} \text{ in } H^1(U), \quad \tilde{z}_{\text{R}k} \rightharpoonup z_{\text{R}} \text{ in } H^1(U),$$

where $z_{\text{N}} = z_{\text{N}}(\phi) = \tilde{z}_{\text{N}}|_{\Omega(\phi)}$ *and* $z_{\text{R}} = z_{\text{R}}(\phi) = \tilde{z}_{\text{R}}|_{\Omega(\phi)}$ *are the unique solutions of equations* (46) *and* (47) *on* $\Omega := \Omega(\phi)$, *respectively.*

In the proof of the above proposition, three essential estimates were utilized. The first one is a result regarding the uniform Poincaré inequality proved in [15] (see, particularly, Corollary 3(ii)]). The second one concerns about the uniform continuity of the trace operator with respect to the domain (see [13, Theorem 4]), and the last auxiliary result is about a uniform extension of the state variables from Ω_n to U such that their respective $H^1(U)$-norms are bounded above by a

constant positive number (see first part of the proof of Proposition 6 given in [68]). For completeness, we recall them as follows:

Lemma 4 *Let $\phi_n, \phi \in \mathcal{U}_{ad}$ and $\Omega(\phi_n), \Omega(\phi) \in \mathcal{O}_{ad}$. Then, the following results hold.*

  (i) *For every $u \in H^1_{\Gamma,0}(\Omega)$, we have the estimate $\|u\|_{L^2(\Omega)} \lesssim |u|_{H^1(\Omega)}$.*
  (ii) *For all real number q such that $\frac{1}{2} < q \leqslant 1$ and functions $u \in H^1(U)$, we have*

   $$\|u\|_{L^2(\Sigma(\phi))} \lesssim \|u\|_{H^q(U)},$$

   where $\| \cdot \|_{H^q(U)}$ denotes the $H^q(U)$-norm.
  (iii) *There exists a uniform extension $\tilde{z}_{Rn}$ (respectively $\tilde{z}_{Nn}$) of z_{Rn} (respectively z_{Nn}) from Ω_n to U and a constant $C_R > 0$ independent of n such that $\|\tilde{z}_{Rn}\|_{H^1(U)} \leqslant C_R$ (respectively $\|\tilde{z}_{Nn}\|_{H^1(U)} \leqslant C_N$, where $C_N > 0$ is constant).*

In relation to the second statement of the above lemma, we note that due to assumption (P$_3$) and the uniform cone property of the domain $\Omega(\phi) \in \mathcal{O}_{ad}$, the norm of the trace map tr : $H^1_0(U) \to L^2(\Sigma(\phi))$ can actually be bounded uniformly with respect to $\Omega(\phi) \in \mathcal{O}_{ad}$; see [59]. On the other hand, we mention that the proof of Lemma 4(iii) given in [68] uses the first two estimates (i) and (ii). Note that the third part of the lemma already guarantees the existence of a subsequence of $\{\tilde{z}_{Rn}\}$ (respectively $\{\tilde{z}_{Nn}\}$) which weakly converges in $H^1(U)$ to a limit denoted by $\tilde{z}_R$ (respectively $\tilde{z}_N$). Hence, the proof of Proposition 6 is completed by showing that the restriction of $\{\tilde{z}_R\}$ (respectively $\{\tilde{z}_N\}$) in $\Omega(\phi)$ coincides with the unique solution of (47) (respectively (46)). Because of the basic role Lemma 4(iii) plays in the proof of the lower-semicontinuity of J, we provide its proof below.

Proof of Lemma 4(iii) Throughout the proof we use the notation $(\cdot)_n := (\cdot)(\phi_n)$. From a famous paper of Chenais [18], we know that the solution z_{Rn} of (47) on Ω_n admits an extension $\tilde{z}_{Rn}$ in $H^1(U)$ such that

$$\|\tilde{z}_{Rn}\|_{H^1(U)} \lesssim \|z_{Rn}\|_{H^1(\Omega_n)}.$$

So, to establish our desired result, we need to prove that $\|z_{Rn}\|_{H^1(\Omega_n)}$ is bounded with respect to n. In view of (8), taking $\varphi = z_{Rn} \in H^1_{\Gamma,0}(\Omega_n)$, we have

$$\int_{\Omega_n} |\nabla z_{Rn}|^2 \, dx + \int_{\Sigma_n} \beta |z_{Rn}|^2 \, d\sigma = -\int_{\Omega_n} \nabla u_{R0} \cdot \nabla z_{Rn} \, dx + \int_{\Sigma_n} \lambda z_{Rn} \, d\sigma.$$

This yields the estimate

$$|z_{Rn}|^2_{H^1(\Omega_n)} \leqslant |u_{R0}|_{H^1(U)} |z_{Rn}|_{H^1(\Omega_n)} + |\lambda| |U|^{1/2} \|z_{Rn}\|_{L^2(\Sigma_n)}. \tag{56}$$

Next, we show that $\|z_{Rn}\|_{L^2(\Sigma_n)}$ can be bounded by $|z_{Rn}|_{H^1(\Omega_n)}$. This is where we apply the first two parts of the lemma (i.e., Lemma 4(i) and (ii)) to obtain

$$\|z_{\mathrm{R}n}\|_{L^2(\Sigma_n)} \lesssim \|\tilde{z}_{\mathrm{R}n}\|_{H^1(U)} \lesssim \|z_{\mathrm{R}n}\|_{H^1(\Omega_n)}$$
$$\lesssim |z_{\mathrm{R}n}|_{H^1(\Omega_n)}.$$

Going back to (56), we get

$$|z_{\mathrm{R}n}|_{H^1(\Omega_n)} \lesssim \|u_{\mathrm{R}0}\|_{H^1(U)} + |\lambda||U|^{1/2}.$$

Applying Lemma 4(i) once more, we obtain

$$\|z_{\mathrm{R}n}\|_{H^1(\Omega_n)} \lesssim \|u_{\mathrm{R}0}\|_{H^1(U)} + |\lambda||U|^{1/2},$$

which establishes the boundedness of $\{\|\tilde{z}_{\mathrm{R}n}\|_{H^1(U)}\}$. The same line of argument can be used to prove that there exists a uniform extension $\tilde{z}_{\mathrm{N}n}$ of $z_{\mathrm{N}n}$ from Ω_n to U and a constant $C_{\mathrm{N}} > 0$ independent of n such that $\|\tilde{z}_{\mathrm{N}n}\|_{H^1(U)} \leqslant C_{\mathrm{N}}$. (In fact, taking $\beta = 0$ in above proof easily verifies this statement.) $\square$

Having recalled the above results, we now proceed on the second part of the proof of Theorem 1 by proving the next result.

Proposition 7 *The cost functional*

$$J(\Sigma) = J(\Omega, u_{\mathrm{N}}(\Omega), u_{\mathrm{R}}(\Omega)) = \frac{1}{2} \int_{\Sigma} |u_{\mathrm{N}}(\Omega) - u_{\mathrm{R}}(\Omega)|^2 \, \mathrm{d}\sigma$$

is lower semi-continuous on $\mathscr{F}$ in the topology induced by (55).

To prove the above proposition, we will exploit the parametrization ϕ of Σ. Also, its properties stated in assumption (P_3) will be used implicitly many times in the proof. The following result, which is a consequence of Lemma 4(ii) (see [13, Corollary 2], and also [14, Corollary 1]), will also be central to the proof Proposition 7 given below.

Lemma 5 [13, 14] *Let $\phi_n, \phi \in \mathcal{U}_{\mathrm{ad}}$ be a sequence such that $\phi_n \to \phi$ in the $C^1([0,1], \mathbb{R}^2)$-norm. Then, for any $u \in H^1(U)$, we have $\lim_{n\to\infty} u \circ \phi_n = u \circ \phi$ in $L^2([0,1])$*

Proof of Proposition 7 Let $\{(\Omega_n, u_{\mathrm{N}n}, u_{\mathrm{R}n})\}$ be a sequence in $\mathscr{F}$, $\Omega_n := \Omega(\phi_n)$, and assume that

$(\Omega_n, u_{\mathrm{N}n}, u_{\mathrm{R}n}) \to (\Omega, u_{\mathrm{N}}, u_{\mathrm{R}})$ as $n \to \infty$,

where $\Omega := \Omega(\phi)$ and the triple $(\Omega, u_{\mathrm{N}}, u_{\mathrm{R}})$ is in $\mathscr{F}$. For convenience, we let $w_n = u_{\mathrm{N}n} - u_{\mathrm{R}n}$ (recalling that $w = u_{\mathrm{N}} - u_{\mathrm{R}}$) and their extensions in $H^1(U)$ by $\tilde{w}_n$ and $\tilde{w}$, respectively. Here, we emphasize that $w = \tilde{w}|_{\Omega}$ is in $H^1_{\Gamma,0}(\Omega)$ which is essentially due to the boundedness of the trace operator. Moreover, for any $u \in H^1_{\Gamma,0}(U)$, the restriction $u|_{\Omega_n}$ is in $H^1_{\Gamma,0}(\Omega_n)$. We have

$$2|J(\Sigma(\phi_n)) - J(\Sigma(\phi))|$$

$$= \left| \int_{\Sigma(\phi_n)} |w_n|^2 \, d\sigma - \int_{\Sigma(\phi)} |w|^2 \, d\sigma \right|$$

$$\leqslant \left| \int_0^1 \left[|(w_n \circ \phi_n)(t)|^2 |\phi_n'(t)| - |(w \circ \phi)(t)|^2 |\phi'(t)| \right] dt \right|$$

$$\leqslant \left| \int_0^1 \left[(w_n \circ \phi_n)^2 - (w \circ \phi)^2 \right] |\phi_n'| \, dt \right| + \left| \int_0^1 (w \circ \phi)^2 (|\phi_n'| - |\phi'|) \, dt \right|$$

$$=: \mathbb{I}_1 + \mathbb{I}_2.$$

We first look for an estimate for the second integral $\mathbb{I}_2$. For this purpose, we apply the estimates in Lemma 4 and the compactness of the injection of $H^1(U)$ into $H^q(U)$ for $\frac{1}{2} < q < 1$, to obtain

$$\mathbb{I}_2 \lesssim \sup_{[0,1]} |\phi_n' - \phi'| \|w\|_{L^2(\Sigma(\phi))}^2 \lesssim \sup_{[0,1]} |\phi_n' - \phi'| \|\tilde{w}\|_{H^1(U)}^2 \lesssim \sup_{[0,1]} |\phi_n' - \phi'|.$$

Clearly, using the convergence $\phi_n' \to \phi'$ in the $C^1([0,1], \mathbb{R}^2)$-norm (see (51)), we get the limit $\lim_{n \to \infty} \mathbb{I}_2 = 0$.

On the other hand, to get an estimate for the first integral $\mathbb{I}_1$, we first apply the identity $a^2 - b^2 = (a-b)^2 + 2b(a-b)$ to obtain

$$\mathbb{I}_1 \leqslant \left| \int_0^1 \left(w_n \circ \phi_n - w \circ \phi \right)^2 |\phi_n'| \, dt \right| + 2 \left| \int_0^1 (w \circ \phi)(w_n \circ \phi_n - w \circ \phi)|\phi_n'| \, dt \right|$$

$$=: \mathbb{I}_{11} + 2\mathbb{I}_{12}.$$

For $\mathbb{I}_{12}$, we have the estimate

$$\mathbb{I}_{12} \leqslant \left| \int_0^1 (w \circ \phi)(w_n \circ \phi_n - w \circ \phi_n)|\phi_n'| \, dt \right| + \left| \int_0^1 (w \circ \phi)(w \circ \phi_n - w \circ \phi)|\phi_n'| \, dt \right|$$

$$\lesssim \|w\|_{L^2(\Sigma)} \left(\|w_n - w\|_{L^2(\Sigma_n)} + \|w \circ \phi_n - w \circ \phi\|_{L^2([0,1])} \right)$$

$$\lesssim \|\tilde{w}_n - \tilde{w}\|_{H^q(U)} + \|w \circ \phi_n - w \circ \phi\|_{L^2([0,1])}.$$

On the other hand, for $\mathbb{I}_{11}$, we have

$$\mathbb{I}_{11} \leqslant \left| \int_0^1 (w_n \circ \phi_n - w \circ \phi_n)^2 |\phi_n'| \, \mathrm{d}t \right|$$

$$+ 2 \left| \int_0^1 (w_n \circ \phi_n - w \circ \phi_n)(w \circ \phi_n - w \circ \phi) |\phi_n'| \, \mathrm{d}t \right|$$

$$+ \left| \int_0^1 (w \circ \phi_n - w \circ \phi)^2 |\phi_n'| \, \mathrm{d}t \right|$$

$$\lesssim \|w_n - w\|_{L^2(\Sigma_n)}^2 + \|w_n - w\|_{L^2(\Sigma_n)}^2 (\|w\|_{L^2(\Sigma_n)}$$

$$+ \|w\|_{L^2(\Sigma)}) + \|w \circ \phi_n - w \circ \phi\|_{L^2([0,1])}$$

$$\lesssim \|\tilde{w}_n - \tilde{w}\|_{H^q(U)} + \|w \circ \phi_n - w \circ \phi\|_{L^2([0,1])}.$$

The above estimates were obtained using the inequalities in Lemma 4. Combining them, we arrive at

$$\mathbb{I}_1 \lesssim \|\tilde{w}_n - \tilde{w}\|_{H^q(U)} + \|w \circ \phi_n - w \circ \phi\|_{L^2([0,1])}.$$

Applying Lemma 5, and again using the compactness of the injection of $H^1(U)$ into $H^q(U)$ for $\frac{1}{2} < q < 1$, the convergences $\tilde{w}_n \rightharpoonup \tilde{w}$ in $H^1(U)$-weak and $\phi_n' \to \phi'$ in the $C^1([0,1], \mathbb{R}^2)$-norm (see Proposition 6), we obtain $\lim_{n \to \infty} \mathbb{I}_1 = 0$. Thus, $\lim_{n \to \infty} |J(\Sigma(\phi_n)) - J(\Sigma(\phi))| = 0$. Consequently, we find that $\lim_{n \to \infty} J(\Omega_n, u_{Nn}, u_{Rn}) = J(\Omega, u_N, u_R)$; that is, J is continuous, and in particular, lower semi-continuous. $\qquad \square$

To conclude this section, let us formally provide the proof of Theorem 1 using Proposition 6 and Proposition 7.

Proof of Theorem 1 Let $(\Omega_n, z_{Nn}, z_{Rn})$, $\Omega_n = \Omega(\phi_n)$, be a minimizing sequence for the cost function J; that is, $(\Omega_n, z_{Nn}, z_{Rn})$ is such that

$$\lim_{n \to \infty} J(\Omega_n, z_{Nn}, z_{Rn}) = \inf\{J(\Omega, z_N, z_R) : (\Omega, z_N, z_R) \in \mathscr{F}\}.$$

From Proposition 6, there exists a subsequence $(\Omega_k, z_{Nk}, z_{Rk})$ and an element $\Omega = \Omega(\phi) \in \mathcal{O}_{ad}$ such that $\Omega_k \to \Omega$ (i.e., $\phi_k \to \phi$ uniformly in the C^1 topology), $\tilde{z}_{Nk} \rightharpoonup \tilde{z}_N$, $\tilde{z}_{Rk} \rightharpoonup \tilde{z}_R$ in $H^1(U)$, and the functions $\tilde{z}_N|_\Omega$ and $\tilde{z}_R|_\Omega$ are the unique weak solutions to (46) and (47) in Ω, respectively. Using these, together with the continuity of J proved in Proposition 7, we conclude that (by virtue of [43, Theorem 2.10])

$$J(\Omega, \tilde{z}_N|_\Omega, \tilde{z}_R|_\Omega) = \lim_{k \to \infty} J(\Omega_k, z_{Nk}, z_{Rk}) = \inf\{J(\Omega, z_N, z_R) : (\Omega, z_N, z_R) \in \mathscr{F}\}.$$

$$\square$$

Remark 8 It is worth remarking that in [32], the authors did not tackle the question of existence of optimal solution of the shape optimization problem examined in their paper which is the Poisson case of (1) with a regular Dirichlet and Neumann data on the fixed boundary and free boundary, respectively. Nevertheless, the authors tacitly

supposed the existence of optimal domains and assumed that it is sufficiently regular to accomplish their objectives. We mention that, with the appropriate modification on the proof of Theorem 1, the existence analysis for the shape optimization problem studied in [32] can be carried out in a similar fashion (see [13]).

5 Numerical algorithm and examples

Here, using the gradient and Hessian informations, we will formulate a boundary variation algorithm to numerically solve the minimization problem (5). We shall use a Lagrangian-like method to carry out the numerical realization of the problem in contrast to the one applied in [12, 44, 50] which is an Eulerian-like type method known as *level-set method* (see [64]). Of course, our approach is also different from [31–33] which employs the concept of *boundary integral equations* and were then solved by boundary element methods. Furthermore, there is another numerical method which was recently proposed in [40] that employs the notion of *conformal mapping* method to solve the FBP (1). This solution method was recently developed by Haddar and Kress in [40] and relates the Bernoulli problem in the context of inverse problems. Much more recently, another method was also introduced by Kress in [54] in an attempt to improve the use of boundary integral equations for numerically solving the Bernoulli problem. In terms of numerical performance, he demosntrated that his recently proposed method inspired by Trefftz' integral equation method [73] is more robust and wider applicable than that of [40]. We mention here that Trefftz' approach, in principle, can be considered as a so-called *trial method* (see, e.g., [72]) which is also a prominent numerical method for solving free boundary value problems such as the Bernoulli problem.

5.1 Numerical algorithm

In the following discussion, we give the details of the numerical algorithm we use to solve some concrete numerical examples of (5).

5.1.1 The Sobolev gradient method

Let us denote by Ω_k the shape of the domain at the kth iteration. Then, at the $(k+1)$th iteration, the shape Ω can be updated as $\Omega_{k+1} := \Omega_{t_{k+1}} = (\mathbf{I}_2 + t_k \mathbf{V})\Omega$, where $t_k \geqslant 0$ is some small step size parameter and $\mathbf{V}$ represents the descent deformation field $\mathbf{V}_k$ at the kth iterate. In perturbing the domain Ω, we may take $\mathbf{V}|_{\Sigma} = -G\mathbf{n}$ as the descent direction. However, this choice of the descent direction may cause undesirable oscillations on the free boundary of the shape solution Ω^*. To avoid such phenomena, we compute the descent direction via the so-called H^1 *gradient method* [6]; that is, we take $\mathbf{V}$ as the unique solution in $\mathbf{H}^1_{\Gamma,0}(\Omega)$ of the variational problem

$$\int_\Omega (\nabla \mathbf{V} : \nabla \boldsymbol{\varphi} + \mathbf{V} \cdot \boldsymbol{\varphi}) \, dx = - \int_\Sigma G\mathbf{n} \cdot \boldsymbol{\varphi} \, d\sigma, \quad \forall \boldsymbol{\varphi} \in \mathbf{H}^1_{\Gamma,0}(\Omega). \tag{57}$$

In this sense, the deformation field $\mathbf{V}$, also called in some literature as a *Sobolev gradient* (see, e.g., [60]), provides a smooth extension of $G\mathbf{n}$ over the entire domain Ω, which not only smoothes the boundary [5] but also provides a preconditioning of the descent direction. The method of regularizing the descent direction using (57) is similar to the idea behind the so-called *traction method* introduced and popularized in [2–5].

On the other hand, we note that the kernel G given in (15) depends on the mean curvature of Σ. This means that we first need to calculate κ in order to determine $\mathbf{V}$. In this investigation, we evaluate this expression by first creating a smooth extension of $\mathbf{n}$ using the idea of the H^1 gradient method and then calculate κ as the divergence of that smooth extension. This technique is possible because, by Proposition 5.4.8 of [46, p. 218] (see also [38, Lemma 16.1, p. 390]), we know that, for a domain Ω of class C^2, there exists a unitary C^1 extension $\tilde{\mathbf{n}}$ of $\mathbf{n}$ such that the mean curvature may be defined as

$$\kappa = \mathrm{div}_\Sigma \mathbf{n} = \mathrm{div}\, \tilde{\mathbf{n}}.$$

Hence, based on this idea, we may numerically compute κ via the equation $\kappa = \mathrm{div}\, \mathbf{N}$, where $\mathbf{N}$ is the smoothed extension of $\mathbf{n}$ satisfying the equation

$$\int_\Omega \nabla \mathbf{N} : \nabla \boldsymbol{\varphi} \, dx + \int_\Sigma \mathbf{N} \cdot \boldsymbol{\varphi} \, d\sigma = \int_\Sigma \mathbf{n} \cdot \boldsymbol{\varphi} \, d\sigma, \quad \forall \boldsymbol{\varphi} \in \mathbf{H}^1(\Omega). \tag{58}$$

5.1.2 Step size

Let us now turn our attention to the computation of the step size to be used in our algorithm. It is worth mentioning that the choice for t_k can be decided in many ways. Here, we shall update $t_k \in (0, \varepsilon]$ (where $\varepsilon > 0$ is some sufficiently small real number) by following a heuristic approach inspired by the Armijo–Goldstein line search strategy similar to the one offered in [50], but for level-set methods. Given the choice of descent direction $\mathbf{V}|_\Sigma = -G\mathbf{n}$ (this means, basically, that $a(\cdot, \cdot)$ in equation (60) below is the usual inner product in $L^2(\Sigma)$) and the definition of the domain Ω_ε, we know that

$$J(\Sigma_\varepsilon) \simeq J(\Sigma_0) + \varepsilon dJ(\Sigma_0)[\mathbf{V}] = J(\Sigma_0) - \varepsilon \|G\|^2_{L^2(\Sigma_0)} (< J(\Sigma_0)).$$

The requirement $J(\Sigma_\varepsilon) = (1 - \alpha)J(\Sigma_0)$ for some $\alpha \in (0, 1)$ then suggests the choice $\varepsilon = \alpha J(\Sigma_0)/\|G\|^2_{L^2(\Sigma_0)}$. However, since we are regularizing $\mathbf{V}$ via (57), we need to replace the L^2-norm of G appearing in the denominator of the previous formula with the $\mathbf{H}^1(\Omega)$-norm of $\mathbf{V}$, and then finally define the step size t_k as

$$t_k = \alpha J(\Sigma_k)/\|\mathbf{V}\|^2_{\mathbf{H}^1(\Omega)}. \tag{59}$$

We further explain the above formula as follows. In general, we may in fact consider the variational equation

$$a(\mathbf{V}, \boldsymbol{\varphi}) = -\langle G\mathbf{n}, \boldsymbol{\varphi}\rangle_{L^2(\Sigma)}, \quad \forall \boldsymbol{\varphi} \in \mathcal{X}, \tag{60}$$

where $a(\cdot, \cdot)$ is some bounded coercive bilinear form on an appropriate space $\mathcal{X}$, to obtain a regularization of the descent direction $-G\mathbf{n}$ (see, e.g., [5, Section 6.3]). Then, using (60) and the requirement that the relation $J(\Sigma_\varepsilon) = (1 - \alpha)J(\Sigma_0) = J(\Sigma_0) + \varepsilon\langle G\mathbf{n}, \mathbf{V}\rangle_{L^2(\Sigma)}$ holds for some $\alpha \in (0, 1)$, we end up with the equation

$$\varepsilon = -\alpha\frac{J(\Sigma_0)}{\langle G\mathbf{n}, \mathbf{V}\rangle_{L^2(\Sigma)}} = \alpha\frac{J(\Sigma_0)}{a(\mathbf{V}, \mathbf{V})},$$

for any $\mathbf{V} \in \mathbf{H}^1_{\Gamma,0}(\Omega)$. Hence, at each iteration, we may choose, for a fixed α, the step size parameter t_k as $t_k = \alpha J(\Sigma_k)/a(\mathbf{V}, \mathbf{V})$. This formula for t_k clearly provides a natural choice for the magnitude of the step size when the descent direction $\mathbf{V}$ is regularized using equation (60). Nevertheless, as investigated in [67] through various numerical experiments, it is possible to change the denominator $a(\mathbf{V}, \mathbf{V})$ in the formula for t_k to get a better step size. In fact, by changing the $\mathbf{H}^1(\Omega)$-norm in (59) by either the $\mathbf{H}^1_{\Gamma,0}(\Omega)$- or the $\mathbf{L}^2(\Sigma)$-norm, for instance, we can speed up the convergence of the algorithm given below, as exhibited in [67]. Indeed, this claim can easily be supported by the fact that the sequence of inequalities $\|\mathbf{V}\|^{-2}_{\mathbf{H}^1(\Omega)} \lesssim \|\mathbf{V}\|^{-2}_{\mathbf{H}^1_{\Gamma,0}(\Omega)} \lesssim \|\mathbf{V}\|^{-2}_{\mathbf{L}^2(\Omega)}$ obviously holds.

Now, with $\alpha \in (0, 1)$ fixed, the step size will be decided according to the following rule: we take t_k as in (59) whenever there is a decrease in the computed cost value from the previous to the next iteration loop (i.e., if $J(\Sigma_{k+1}) \leqslant J(\Sigma_k)$). Otherwise, if the cost value increases, we reduce the step size and go backward: the next iteration is initialized with the previous shape Ω_k. We also reduce the step size t_k if reversed triangles are detected within the mesh update.

5.1.3 The boundary variation algorithm (first-order method)

The main steps required for the computation of the kth domain is summarized as follows:

Step 1 Fix the step size parameter and choose an initial shape Ω_0.
Step 2 Solve the state equations and their corresponding adjoint state systems on Ω_k. Also, solve the variational problem (58) on Ω_k.
Step 3 Using the shape gradient, compute the descent direction $\mathbf{V}_k$ via (57) and the step size t_k by (59).
Step 4 Using $\mathbf{V}_k$ and t_k, perturb the current domain by $\Omega_{k+1} = (\mathbf{I}_2 + t_k\mathbf{V}_k)\Omega_k$.

Finally, to complete the above steps, we need to specify the stopping condition. Here, we terminate the algorithm as soon as the inequality condition

$$J(\Sigma_{k+1})/J(\Sigma_0) < \eta, \tag{61}$$

is satisfied for some sufficiently small real number $\eta > 0$ or if the algorithm already completed a specified (maximum) computing time. It worth mentioning that a typical stopping criterion is to find that whether the shape gradients in some suitable norm are small enough. However, since we use the continuous shape gradients, it is hopeless for us to expect very small gradient norm because of numerical discretization errors. In addition, because we will be comparing our proposed method with that of the classical Dirichlet-data-tracking approach and since this method uses a different cost function, a normalization of the cost histories with the initial cost value that corresponds to each method seems more appropriate to our case.

We shall refer to the above sequence of procedures with $\mathrm{d}J_A$ given by (15) as the gradient as Algorithm A.1. On the other hand, when using the full shape gradient $\mathrm{d}J$ given in Proposition 2 in Step 3, the above steps will be referred to as Algorithm B.1.

5.1.4 Incorporating the shape Hessian information in the numerical procedure

We remark that, with the help of the shape Hessian information, we can obviously improve the convergence of the numerical method given in the previous section in terms of the number of iterations required to complete the iteration scheme (see, e.g., [28, 68, 72]). However, the drawback of a second-order method is that, in most cases, it demands additional computational burden and time to carry out the task. In this section, we will formulate a second-order optimization algorithm to solve the minimization problem (5) following an idea first proposed by the second-author in [7] (see also [8, Problem 4.2, Eq. (29)]). Particularly, we use a variant of the so-called H^1 *Newton* (or *Sobolev Newton*) method which utilizes the Hessian information to compute the descent direction. The basic idea of this method is that it incorporates the shape Hessian in obtaining a regularized descent direction for the algorithm similar to equation (60) (*see* Remark 9 below). In our case, however, we propose to use only the shape Hessian information at the solution of the FBP (1) (i.e., we use (40)).

To do the task, we define the descent direction $\mathbf{W} \in \mathbf{H}_{\Gamma,0}^1(\Omega)$ as the unique solution of the variational equation

$$\int_\Omega (\nabla \mathbf{W} : \nabla \boldsymbol{\varphi} + \mathbf{W} \cdot \boldsymbol{\varphi}) \, \mathrm{d}x = -\int_\Sigma (G + H^*[\mathbf{V}]) \mathbf{n} \cdot \boldsymbol{\varphi} \, \mathrm{d}\sigma, \quad \forall \boldsymbol{\varphi} \in \mathbf{H}_{\Gamma,0}^1(\Omega), \tag{62}$$

where G, as before, is the kernel of the shape gradient while $H^*[\mathbf{V}]$, in this case, denotes only the kernel of the shape Hessian at the solution of the FBP (1), i.e., $\int_{\Sigma^*} H^*[\mathbf{V}] \mathbf{n} \cdot \mathbf{W} \, \mathrm{d}\sigma := \mathrm{d}^2 J(\Sigma^*)[\mathbf{V}, \mathbf{W}]$ (cf. (43)). In case of the shape gradient computed with assumption (**A**), the corresponding notation is $H_A^*[\mathbf{V}]$. In terms of the adjoint states, these kernels of the shape Hessians are exactly given by

$$H^*[\mathbf{V}] = \lambda \kappa \Pi[\mathbf{V}] \quad \text{and} \quad H_A^*[\mathbf{V}] = \lambda(\Psi[\mathbf{V}] + \lambda \kappa \Pi[\mathbf{V}]), \tag{63}$$

respectively. Here, of course, Ψ and Π satisfy Eqs. (41) and (42), respectively. In above expressions, we added the notation $(\cdot)[\mathbf{V}]$ to emphasize that the expression it is attached to is dependent to the deformation field $\mathbf{V}$.

Now, the main steps to compute the kth domain Ω_k are essentially the same as that given in Sect. 5.1.3. However, in order to take into account the procedure in computing $\mathbf{W}$, we divide the third step of the original algorithm as follows:

Step 3.1   Using the shape gradient, compute the descent direction $\mathbf{V}_k$ via (57).
Step 3.2   Compute Ψ and Π by solving the PDE systems (41) and (42) at $\Omega = \Omega_k$.
Step 3.3   Using the shape gradient and the shape Hessian, compute the descent direction $\mathbf{W}_k$ using (62).

Moreover, in Step 4 of the original algorithm, we replace $\mathbf{V}_k$ with the new deformation field $\mathbf{W}_k$; that is, we perturb the kth domain by $\Omega_{k+1} = (\mathbf{I}_2 + t_k \mathbf{W}_k)\Omega_k$. Here, the step size t_k can still chosen on the basis of the formula given in (59). However, in our experience, this formula for the step size does not give much improvement in terms of convergence speed for the second-order shape optimization algorithm. To exploit the advantage of utilizing the shape Hessian information, an appropriate step size formula has to be used to achieve at least a superlinear (or even quadratic) convergence rate for the algorithm (*see* Remark 10 below).

Remark 9 We also remark that the computed boundary integral expression (33) with G_A replaced by G in the proof of Proposition 3, in general, can be further written into the following form

$$\mathrm{d}^2 J(\Sigma)[\mathbf{V},\mathbf{W}] = \int_\Sigma \left[G_W' V_\mathrm{n} + \left(\partial_\mathbf{n} G + \kappa G \right) V_\mathrm{n} W_\mathrm{n} - GK + G(D\mathbf{V})W_\mathrm{n} \right] \mathrm{d}\sigma,$$

where $K = \mathbf{v}_\Sigma \cdot (D_\Sigma \mathbf{n})\mathbf{w}_\Sigma + \mathbf{n} \cdot (D_\Sigma \mathbf{v})\mathbf{w}_\Sigma + \mathbf{n} \cdot (D_\Sigma \mathbf{w})\mathbf{v}_\Sigma$, $V_\mathrm{n} := \mathbf{V} \cdot \mathbf{n}$ for $\mathbf{V} \in \Theta$, $\mathbf{v} = \mathbf{V}|_\Sigma$, $\mathbf{v} = \mathbf{v}_\Sigma + v_\mathrm{n}\mathbf{n} := (\mathbf{v} \cdot \tau)\tau + (\mathbf{v} \cdot \mathbf{n})\mathbf{n}$ and D_Σ denotes the tangential differential operator called the *tangential Jacobian matrix* given as $D_\Sigma \mathbf{v} = D\mathbf{V}|_\Sigma - (D\mathbf{V}\mathbf{n})\mathbf{n}^\top$ (see, e.g., [22, Eq. (5.2), p. 495]). Evidently, the above expression for the shape Hessian is composed of symmetric and non-symmetric terms with respect to the deformation fields $\mathbf{V}$ and $\mathbf{W}$ (cf. [63]). This lack of symmetry and complexity in form of the shape Hessian provides much difficulty for its utilization and numerical implementation [62, 70]. Nevertheless, as proposed by Simon in [70], one can still utilize the shape Hessian in an optimization procedure in a much simpler way by dropping the non-symmetrical part of the Hessian (see, e.g., [49]), allowing one to obtain a second order expansion of the form $J(\Sigma) + \mathrm{d}J(\Sigma)[\mathbf{V}] + \mathrm{d}^2 J(\Sigma)[\mathbf{V},\mathbf{V}]$ of $J(\Sigma)$ with respect to the descent direction $\mathbf{V}$. Note that, at the optimal shape solution $\Omega = \Omega^*$, the necessary optimality condition give rise to the variational formulation of the Newton equation

$$\mathrm{d}^2 J(\Sigma)[\mathbf{V},\mathbf{W}] = -\mathrm{d}J(\Sigma)[\mathbf{V}], \quad \forall \mathbf{V} \in \mathbf{H}^1_{\Gamma,0}(\Omega),$$

whose solution $\mathbf{W}$ may be used as a descent direction in a gradient-based descent algorithm (cf. equation in Step 3 of [43, Section 4.1.1, Algorithm 4.1, p. 131]). Following this idea, and employing a smoothing technique such as (60), we arrive at Eq. (62) which gives us a new regularized descent direction $\mathbf{W}$.

Remark 10 In addition to the previous remark, and as also noted by Simon in [70] (*see* his remark in Section 2.1), we mention that the velocity of gradient methods (such as Algorithm A.1) can be improved by choosing the step size as the negative ratio between the shape gradient over the shape Hessian. For example, the kth approximation of Ω_0 can be computed as $\Omega_{k+1} = (\mathbf{I}_2 + t_k^f \mathbf{V}_k)\Omega_k$ where $t_k^f = -\mathrm{d}J(\Sigma_k)[\mathbf{V}_k]/\mathrm{d}^2 J(\Sigma_k)[\mathbf{V}_k, \mathbf{V}_k]$. Here, the step generated by the formula for t^f is commonly called as the *(full) Newton step* (see, e.g., [61, Section 3.3]).

In our case, since we are using regularized descent directions, the above idea is, in a sense, equivalent to taking t_k as a scalar multiple of the ratio of the square of the $\mathbf{H}^1(\Omega)$-norm of $\mathbf{V}$ over the squared $\mathbf{H}^1(\Omega)$-norm of $\mathbf{W}$. Indeed, from a similar proposition issued in Sect. 5.1.2, we can naturally take

$$t_k = \tilde{\alpha}\|\mathbf{V}\|^2_{\mathbf{H}^1(\Omega_k)}/\|\mathbf{W}\|^2_{\mathbf{H}^1(\Omega_k)}, \tag{64}$$

for a fixed $\tilde{\alpha} \in (0, 1]$, as the kth step size of the second-order optimization algorithm proposed in Sect. 5.1.4.

In (64), we introduced the step size parameter $\tilde{\alpha}$ simply to control the magnitude of the descent step during each iteration. We recall that, in most optimization problems, the introduction of a step size parameter to Newton's method is primarily due to the fact that the method is quite sensitive if the initial guess is too bad. Common strategies to globalize the method is to introduce a *line search strategy* or to work with the so-called *trust region methods* (see, e.g., Section 3.4 and Chapter 4 of [61]). In practice, the former strategy is accomplished by scaling the Newton's step by some coefficient $0 < \tilde{\alpha} \leqslant 1$ in every iteration [as we have done in (64)]. Taking $\tilde{\alpha} = 1$ obviously amounts to a full Newton step and choosing $\tilde{\alpha} < 1$ yields the so-called *damped Newton method* (see, e.g., [16, Section 9.5.2, p. 487]) which has an increased convergence radius (this, however, does not work well in general), and also has a reduced convergence order (not quadratically anymore). Nevertheless, when the approximant is judged to be near to a solution, $\tilde{\alpha} = 1$ is taken and the convergence would be as good as for the standard (or *pure*) Newton's method.

Here, we opted to apply a line search method in our proposed second-order (shape optimization) algorithm to address two main issues when taking the full Newton step. Firstly, we notice that, in some situations, choosing a full Newton step is not necessarily the best strategy to start the approximation procedure, especially if the initial guess is far from the (optimal shape) solution. Secondly, we observe that the full Newton step is sometimes too large that the cost functions become insensitive with respect to geometric perturbations, occasionally causing the algorithm to overshoot or converge prematurely to a less optimal solution (*see* Example 5.2.4). On the other hand, although the step size parameter $\tilde{\alpha}$ can be made at most equal to the unit value when the approximant is estimated to be close to the optimal solution, we only fixed $\tilde{\alpha}$ to be of constant

value ($\leqslant 1$) throughout the iteration process. Nevertheless, a backtracking procedure as in Sect. 5.1.2 will still be employed in the algorithm, meaning that the maximum step size at each iteration of the algorithm is only bounded above by a fraction (determined by the value of $\tilde{\alpha}$) of the full Newton step.

Despite the fact that the idea is already known in the literature, we emphasize that the formula for the step size given by (64) is, to the best of our knowledge, novel to this work. We shall refer to the modifications of Algorithm A.1 and Algorithm B.1, exploiting the shape Hessian informations given in (63) and the new step size formula for t_k, as *Algorithm A.2* and *Algorithm B.2*, respectively. Also, for the sake of comparison, we will also run our propose iterative procedures using the classical Dirichlet-data-tracking approach in solving the numerical examples in the next section. We will refer to these procedures as *Algorithm C.1* for the first-order method (with shape gradient dJ_1 in Remark 2) and *Algorithm C.2* for the second-order method (with shape Hessian d^2J_1 given in Proposition 4). Regarding the latter method, it is worth to mention that a second-order shape optimization method that utilizes the Dirichlet-data-tracking cost functional J_1 in Lagrangian-like method has not been done yet in previous numerical investigations. Hence, this paper is the first to investigate the feasibility and efficiency of employing the said formulation in a second-order shape optimization (finite element based solution) procedure for solving the exterior Bernoulli FBP (1).

5.2 Numerical examples

The test cases we give below are all performed in two-dimension using the programming software FREEFEM++ (see [45]). All weak formulations described in previous sections are solved using P2 finite element discretization where the number of discretization points on the free and fixed boundaries are initially set to $N_{ext} \times N_{int} = 120 \times 100$ discretization points. Meanwhile, we use the built-in function *movemesh* of FREEFEM++ in perturbing the reference domain Ω during the optimization process. In addition, we use the function *adaptmesh* with minimum edge size h_{min} and maximum edge size h_{max} during mesh adaption to refine and avoid the degeneracy of the triangles in the meshes. In all examples, we set $h_{min} = 1/80$ and $h_{max} = 1/40$ except for the third problem where we take $h_{min} = 1/10$ and $h_{max} = 1/5$. Moreover, we terminate the iterations as soon as $J(\Sigma_{k+1})/J(\Sigma_0) < 10^{-8}$ or if the algorithm already runs for 60 seconds of computing time. Furthermore, in all examples we give below, the Robin coefficient β is, of course, chosen to be equal to κ (the mean curvature of the free boundary) in Algorithm A.1 and Algorithm A.2, while for Algorithm B.1 and Algorithm B.2 we take $\beta = 100$. All computations are carried out on a 1.6 GHz Intel Core i5 Macintosh computer with 4GB RAM processors.

5.2.1 Example 1: axisymmetric case

We first consider a simple axisymmetric case. Given that $C(\mathbf{0}, r)$ and $C(\mathbf{0}, R)$ are the circles centered at the origin with radius $r > 0$ and $R > r$, respectively, the pure Dirichlet problem (problem (4))

$$-\frac{\partial^2 u}{\partial \rho^2} - \frac{1}{\rho}\frac{\partial u}{\partial \rho} = 0 \quad \text{for } r < \rho < R, \quad u(r) = 1, \quad \text{and} \quad u(R) = 0,$$

has the exact solution $u(\rho) = \log(\rho/R)/\log(r/R)$. In this case, $\partial_{\mathbf{n}}u(R) = 1/[R\log(r/R)]$. Hence, the exterior Bernoulli FBP (1) with

$$\Gamma = \{x \in \mathbb{R}^2 : |x| = r\} \quad \text{and} \quad \lambda = \frac{1}{R\log\left(\frac{r}{R}\right)}, \quad 0 < r < R, \tag{65}$$

has the unique exact free boundary solution $\Sigma^* = C(\mathbf{0}, R)$. Moreover, the explicit expression u_{D} satisfying (4) on Ω_ρ (the annular domain with inner radius r and outer radius ρ centered at the origin) is given by

$$u_{\mathrm{D}}(\Omega_\rho) = \frac{\log|x| - \log\rho}{\log r - \log\rho}.$$

Similarly, for the mixed Dirichlet–Neumann problem (3) with assumptions given by (65), the explicit expression for its solution u_{N} is given by

$$u_{\mathrm{N}}(\Omega_\rho) = \lambda\rho\log\left(\frac{|x|}{r}\right) + 1.$$

Meanwhile, for the mixed Dirichlet–Robin problem (6) with fixed $\beta > 0$ and λ in (65), the PDE system

$$-\frac{\partial^2 u}{\partial \rho^2} - \frac{1}{\rho}\frac{\partial u}{\partial \rho} = 0 \ \text{ for } r < \rho < R, \quad u(r) = 1, \quad \text{and} \quad \partial_{\mathbf{n}}u(R) + \beta u(R) = \lambda,$$

has the solution $u = u_{\mathrm{R}}(\Omega_\rho)$ explicitly given by

$$u_{\mathrm{R}}(\Omega_\rho) = \frac{1 + \lambda\rho\log\left(\frac{|x|}{r}\right) - \beta\rho\log\left(\frac{|x|}{\rho}\right)}{1 - \beta\rho\log\left(\frac{r}{\rho}\right)}.$$

Thus, when the free boundary is given by $\Sigma_\rho = \{x : |x| = \rho\}$, the exact values of the functionals J_1, J_2, J_3, J_4 and J are given by the following expressions:

$$J_1(\Sigma_\rho) = \frac{1}{2} \int_{\Sigma_\rho} u_{\mathrm{N}}^2 \, \mathrm{d}\sigma = \pi\rho \left(1 - \lambda\rho \log\left(\frac{r}{\rho}\right) \right)^2,$$

$$J_2(\Sigma_\rho) = \frac{1}{2} \int_{\Sigma_\rho} \left(\frac{\partial u_{\mathrm{D}}}{\partial \mathbf{n}} - \lambda \right)^2 \, \mathrm{d}\sigma = \frac{\pi}{\rho \left(\log\left(\frac{r}{\rho}\right) \right)^2} \left(1 - \lambda\rho \log\left(\frac{r}{\rho}\right) \right)^2,$$

$$J_3(\Omega_\rho) = \frac{1}{2} \int_{\Omega_\rho} \left| \nabla(u_{\mathrm{N}} - u_{\mathrm{D}}) \right|^2 \, \mathrm{d}x = \frac{\pi}{\log\left(\frac{\rho}{r}\right)} \left(1 - \lambda\rho \log\left(\frac{r}{\rho}\right) \right)^2,$$

$$J_4(\Omega_\rho) = \frac{1}{2} \int_{\Omega_\rho} \left| \nabla(u_{\mathrm{N}} - u_{\mathrm{R}}) \right|^2 \, \mathrm{d}x$$

$$= \frac{\pi}{\log\left(\frac{\rho}{r}\right)} \left[\frac{\beta\rho \log\left(\frac{r}{\rho}\right)}{1 - \beta\rho \log\left(\frac{r}{\rho}\right)} \right]^2 \left(1 - \lambda\rho \log\left(\frac{r}{\rho}\right) \right)^2,$$

$$J(\Sigma_\rho) = \frac{1}{2} \int_{\Sigma_\rho} |u_{\mathrm{N}} - u_{\mathrm{R}}|^2 \, \mathrm{d}\sigma = \pi\rho \left[\frac{\beta\rho \log\left(\frac{r}{\rho}\right)}{1 - \beta\rho \log\left(\frac{r}{\rho}\right)} \right]^2 \left(1 - \lambda\rho \log\left(\frac{r}{\rho}\right) \right)^2.$$

Figure 1 shows that the algorithms using J_1, J_2, J_3, J_4 and J are not equivalent.

Next, we evaluate the efficiency of the first-order shape optimization methods presented in the previous sections (i.e., Algorithm A.1, Algorithm B.1 and Algorithm C.1) in solving a concrete example of the present test problem. For this purpose, we let $r = 0.3$ and $R = 0.5$ (hence, $R^* = 0.5$), giving us $\lambda = -3.9152$. We choose the circle centered at the origin with radius 0.6 as our initial guess (i.e., we take $\Sigma_0 = C(\mathbf{0}, 0.6)$). The results of the convergence tests using Algorithm A.1, Algorithm B.1 and Algorithm C.1 for values of $\alpha = 0.1, 0.3, 0.5$ are depicted in Figure 2. This includes the histories of mean radii shown in Fig. 2a,

Fig. 1 Variation of the cost functionals J_1, J_2, J_3, J_4 and J with respect to ρ
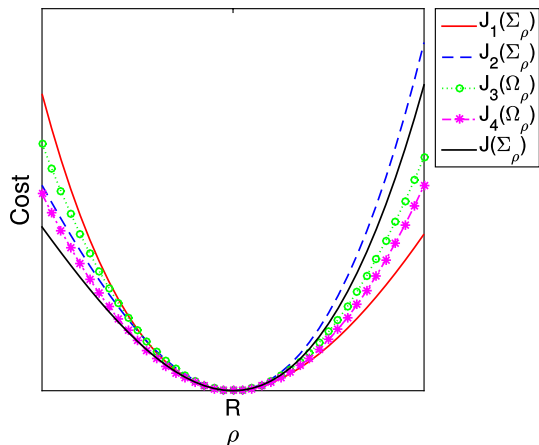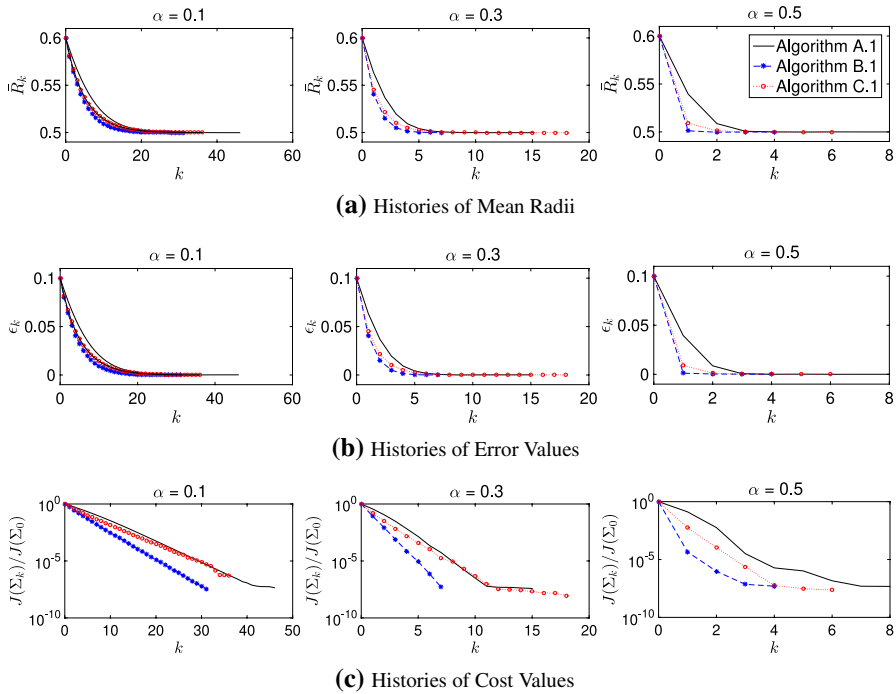
Fig. 2 Histories of **a** mean radii, **b** error values and **c** cost values of Example 5.2.1 for values of $\alpha = 0.1, 0.3, 0.5$ (left, middle and right plots, respectively) using the gradient based algorithms A.1, B.1 and C.1

the histories of relative errors $\epsilon_k = |\bar{R}_k - R^*|$ shown in Fig. 2b, and the histories of cost values (normalized with its initial value) plotted on logarithmic scale in Fig. 2c. In these figures, the 'kth mean radii,' denoted by $\bar{R}_k$, means the average distance from the origin of the nodes on the exterior boundary of the kth domain Ω_k, and Σ_k denotes the kth approximation of the optimal free boundary Σ^*. In all cases, the computed values of the cost functions at Σ_K that correspond to each algorithm, where K denotes the *optimal termination index* (i.e., $K := \min\{k \in \mathbb{N}_0 : \text{stopping condition is satisfied}\}$), are all found to be of magnitude less than 10^{-6}. Furthermore, the computed relative errors ϵ_k in all cases are of magnitude of order 10^{-4}. Meanwhile, we notice from Fig. 2a that our proposed formulation coupled with our present numerical scheme with $\alpha = 0.3$ solves the solution of the test problem as fast as the Kohn–Vogelius formulation (combined with the level-set method) used in [12] in terms of the number of iterations required to complete its corresponding iteration process. In fact, our proposed method with the step size parameter α set to 0.5 is even faster than the said approach used by Ben Abda et al. in [12]. On the other hand, it is evident from the shown figures that Algorithm B.1 possesses faster convergence rate than Algorithm C.1. Hence, our proposed method (without, of course, imposing condition (A)) is more efficient than the classical Dirichlet-data-tracking approach, at

least in solving the present case problem. In contrary, however, Algorithm A.1 (in which condition (A) is assumed) converges to the solution of the test problem slower than Algorithm C.1.

Now, we resolve the test problem using Algorithm A.2, Algorithm B.2 and Algorithm C.2. The computational results obtained from these second-order shape optimization methods are shown in Figure 3. Looking at the graphs depicted in the said figure, it seems that our proposed method, with or without condition (A) (respectively, Algorithm A.2, and Algorithm B.2) is faster than the second-order Dirichlet-data-tracking approach (i.e., Algorithm C.2). In this case, however, Algorithm B.2 and Algorithm C.2 were ran with $\tilde{\alpha} = 0.3$ while we used the full Newton step (i.e., $\tilde{\alpha} = 1$) for Algorithm A.2. Again, the computed final cost values, in all cases, are of magnitude less than 10^{-6} and the absolute errors at the final iterate ϵ_K are all found to be of magnitude of order 10^{-4}. Notice from the left most plot in Fig. 3 that the first iterate of Algorithm A.2 already overshoots the solution. Even so, the second iterate is already close enough to the optimal solution as evident in the said plot.

In the next two examples, we further examine the effect of imposing condition (A) in the shape optimization process. This time we consider two concrete problems that have non-trivial fixed boundaries. Also, due to the limitation of the proposed shape optimization method coupled with condition (A) (see Remark 1), we only consider cases wherein the optimal shape solution are *nearly* convex. More precisely, for the first problem, we consider the case when the fixed boundary has a shape like an inverted letter T. On the other hand, for the second case problem, we consider a fixed boundary that has two disjoint components similar to the one examined in [54]. In these cases, since the exact optimal free boundaries are difficult to solve analytically, we simply assume Σ^* as the final free boundary computed using finer meshes and at longer computing times.

5.2.2 Example 2: an inverted T-shaped fixed boundary

Next, we consider $\Gamma = \partial S$ as the boundary of the T-shape

$$S := ((-3/8, 3/8) \times (-1/4, 0)) \cup ((-1/8, 1/8) \times [0, 1/4)),$$

and let $\lambda = -10$. We solve the present problem using algorithms A.1, B.1, A.2, and B.2. For the first-order methods, we take $\alpha = 0.1$ while for the second-order algorithms, we choose $\tilde{\alpha} = 0.9$. The results of the computations are shown in Fig. 4. Here, the evolution of the free boundaries with initial profile $\Sigma_0 = C(\mathbf{0}, 0.6)$ are illustrated in Fig. 4a. Observe from these figures that the evolution of the free boundaries
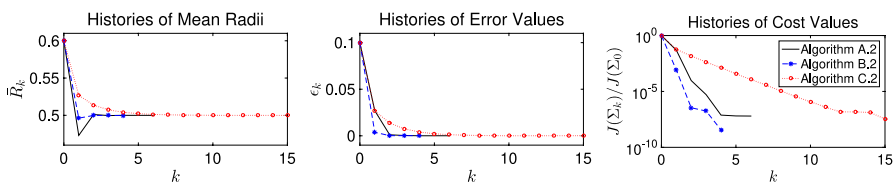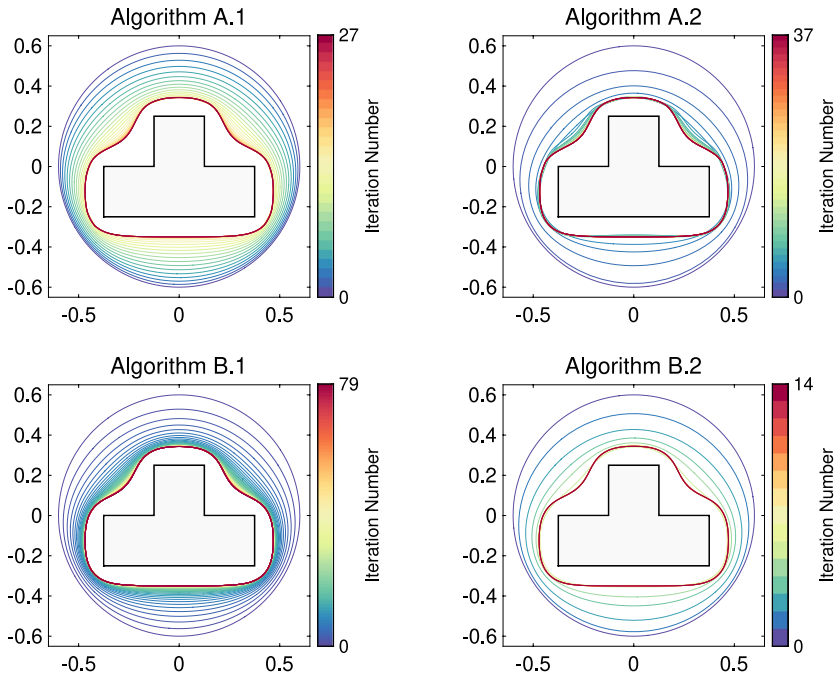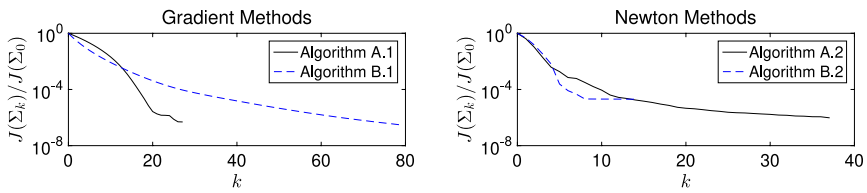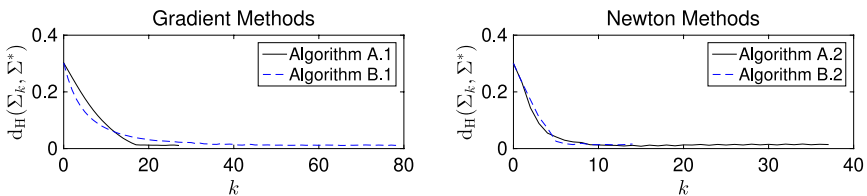

Fig. 3 Histories of mean radii (left plot), error values (mid plot) and cost values (right plot) for Example 5.2.1 using the second-order shape optimization algorithms A.2, B.2 and C.2

(a) Evolution of the free boundaries generated by gradient methods (*left*) and by Newton methods (*right*)

(b) Histories of cost values

(c) Histories of Hausdorff distances

Fig. 4 Computational results of Example 5.2.2 using algorithms A.1, B.1, A.2 and B.2

are clearly different from each other (as expected), especially when the approximant is closing to the optimal free boundary. Meanwhile, a comparison between the histories of cost values and histories of Hausdorff distances between the kth approximation and the (approximate) optimal free boundaries (here, we denote by $d_H(\Sigma_k, \Sigma^*)$) obtained from the four algorithms are shown in Fig. 4b, c, respectively. Looking at

these figures, it seems that Algorithm B.1 is converging faster than Algorithm A.1 at first few iterations, but then the condition is reversed after 12 iterations. Meanwhile, comparing their corresponding second-order methods, it appears that Algorithm A.2 and Algorithm B.2 are comparable in terms of convergence speed. On the other hand, the second-order methods are obviously much faster than the first-order methods as expected. In these numerical tests, the computed cost values are all found to be of magnitude of order 10^{-4}. Furthermore, the calculated Hausdorff distances between the final free boundaries obtained from the four algorithms (including the approximate optimal free boundary) are found to be of order 10^{-3}. This means that the computed final free boundaries are almost identical.

5.2.3 Example 3: a domain with fixed boundary having two disjoint components

For the third example, we look at one of the test problems studied in [54]. Particularly, we let $\lambda = -1.5$ and define the fixed boundary Γ as the union of two disjoint kite-shaped figures which are parametrically defined as follows:

$$\Gamma^1 = \{(1 + 0.7\cos\theta - 0.4\cos 2\theta, \sin\theta)^\top, 0 \leqslant \theta \leqslant 2\pi\},$$
$$\Gamma^2 = \{(-2 + \cos\theta + 0.4\cos 2\theta, 0.5 + 0.7\sin\theta)^\top, 0 \leqslant \theta \leqslant 2\pi\}.$$

Here, the initial guess Σ_0 for the free boundary is taken to be the circle $C(\mathbf{0}, 5.0)$. In addition, we again choose $\alpha = 0.1$ and $\tilde{\alpha} = 0.9$ in the first- and second-order methods. The results of the computations using algorithms A.1, B.1, A.2, and B.2 are shown in Fig. 5. In particular, Fig. 5a shows the evolutions of the free boundaries obtained using the four algorithms while the remaining plots, Fig. 5b, c, illustrate the histories of cost values and Hausdorff distances $d_H(\Sigma_k, \Sigma^*)$, respectively. In this problem, it appears that Algorithm B.1 is completely much faster than Algorithm A.1 as oppose to the previous problem. However, we notice a similar convergence behavior on the second-order methods as in the previous example. More precisely, it seems that Algorithm B.2 converges faster that Algorithm A.2 as the approximant gets closer to the optimal free boundary. Meanwhile, as in the previous example, the computed cost values are all found to be of magnitude of order 10^{-4}, and the computed final free boundaries are almost identical with each other (i.e., their Hausdorff distances are computed to be of order 10^{-3}).

In the last two examples presented above, the computed final free boundaries are found to be *nearly* convex. To complete our numerical investigation, we need to consider another example wherein the optimal free boundary is clearly non-convex. For this purpose, however, we focus on comparing our proposed method with that of the classical Dirichlet-tracking approach (noting, of course, that condition (A) is not appropriate to take into account in solving this new last and final case problem).

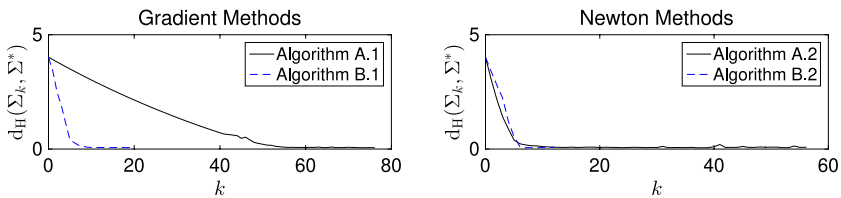### 5.2.4 Example 4: a dumb-bell like shape fixed boundary

We consider $\Gamma = \partial D$ as the boundary of a dumbbell-like domain D similar to the one examined by Eppler and Harbrecht in [29] which has the following parametrization
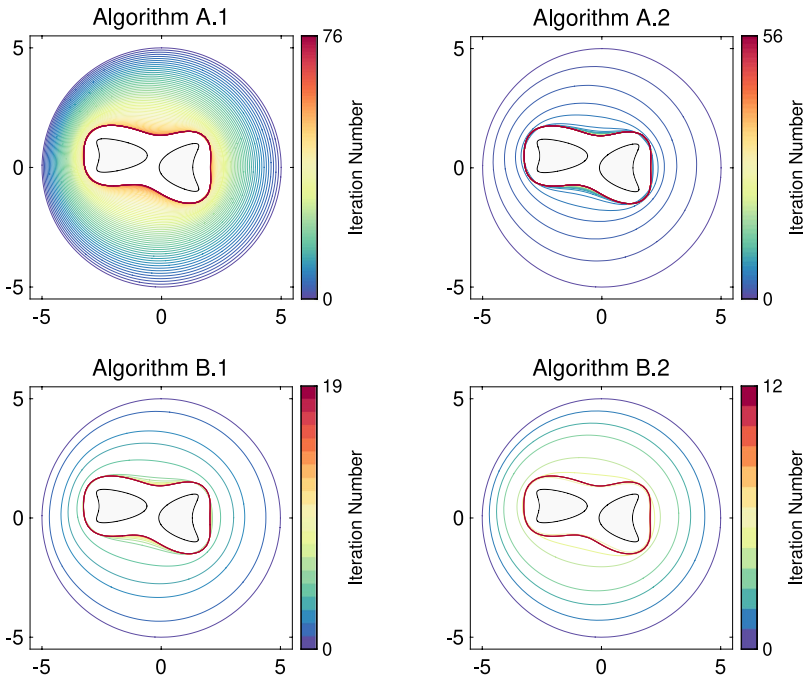
(a) Evolution of the free boundaries generated by gradient methods (*left*) and by Newton methods (*right*)
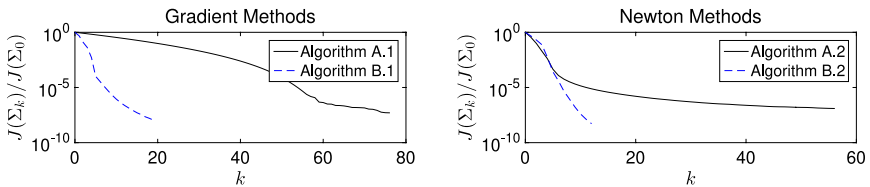
(b) Histories of cost values

(c) Histories of Hausdorff distances

Fig. 5 Computational results of Example 5.2.3 using algorithms A.1, B.1, A.2 and B.2

$$D := \{(0.45 \cos \theta, 0.3 \sin \theta(1.25 + \cos 2\theta))^\top, 0 \leqslant \theta \leqslant 2\pi\}.$$

For this problem, we again choose the circle $C(\mathbf{0}, 0.6)$ as the geometric profile of the
initial free boundary Σ_0. Moreover, we let $\alpha = 0.3$ as the step-size parameter for the

first-order methods and take $\tilde{\alpha} = 0.8$ for the second-order algorithms. The computational results using algorithms B.1, C.1, B.2, and C.2 are summarized in Fig. 6. Looking at Fig. 6a, it is evident that the free boundaries evolve differently from each algorithm. In particular, referring to the results of the first-order methods shown in the other plots (Fig. 6b, c), it seems that our proposed method is somewhat faster than the classical Dirichlet-data-tracking approach. Regarding second-order methods, however, it looks like that the classical approach is converging faster than the Dirichlet-data-gap tracking formulation. In fact, as early as the second iterate, the classical Dirichlet-data-tracking approach was already able to detect the non-convexity of the optimal free boundary. Nevertheless, as the approximants get closer to the optimal free boundary, we observe that the proposed method then converge faster than the classical approach (at least based on the right plot depicted in Fig. 6c). Even so, the computed optimal free boundary obtained from the two formulations are almost identical as evident in Fig. 6d (in fact, the computed Hausdorff distance between the computed final free boundaries obtained from the two formulations has magnitude of order 10^{-3}). Lastly, in all cases, the computed cost values are all found to be of magnitude of order 10^{-5} or lower. However, as we see in the right plot in Fig. 6b, it seems that the cost functional J is less sensitive than the Dirichlet-data-tracking cost functional J_1 in this example. We further explain this property of the cost function below, giving emphasis on the notion of ill-posedness of the proposed formulation "$\min_\Omega J(\Sigma)$ subject to (7) and (8)" discussed in Sect. 3.5.

Sensitivity of the cost functionals J and J_1. We conclude our numerical example by discussing the effect of the step size parameter $\tilde{\alpha}$ in the 'sensitivity property' of the cost functionals J and J_1. As pointed out at the end of Sect. 5.1.4, the main purpose of introducing a step size parameter in our second-order methods is to control the magnitude of the step size (i.e., to limit the maximum step) at every iteration. Recall that, at the kth iterate, we only accept the step size t_k only if it provides a decrease in the cost value (i.e., if $J(\Sigma_{k+1}) \leqslant J(\Sigma_k)$); otherwise, we do a backtracking procedure. In our numerical experiments, we observe that taking a full Newton step at every iterate is not a good strategy at all because the cost functional J (as well as J_1) seems to be insensitive with respect to large geometric perturbations. For illustration, we refer to Fig. 7a where we logarithmically plot the histories of cost values obtained from resolving the present case problem using Algorithm B.2 and Algorithm C.2 with the full Newton step $t_k = \|\mathbf{V}\|^2_{\mathbf{H}^1(\Omega_k)} / \|\mathbf{W}\|^2_{\mathbf{H}^1(\Omega_k)}$ (i.e., $\tilde{\alpha} = 1.0$). Noticeably, several adjacent iterations differ only with very small values (and almost insignificant). Hence, the non-uniform sensitivity of the cost with respect to the descent directions. This observation can actually be viewed as a validation to our findings that the present formulation is algebraically ill-posed (*see* Proposition 5 and Remark 7). That is, in this case, the ill-posedness of the present optimization formulation could also mean that larger deformations in the domains may have little effect on the cost functional. On the other hand, the evolution of the free boundaries with the full Newton step are shown in Fig. 7b while a comparison between the computed free boundaries using the two second-order algorithms is depicted in Fig. 7c. In the latter figure, the difference between the two computed geometries is clearly discernible and, in this case, the final free boundary computed through the classical
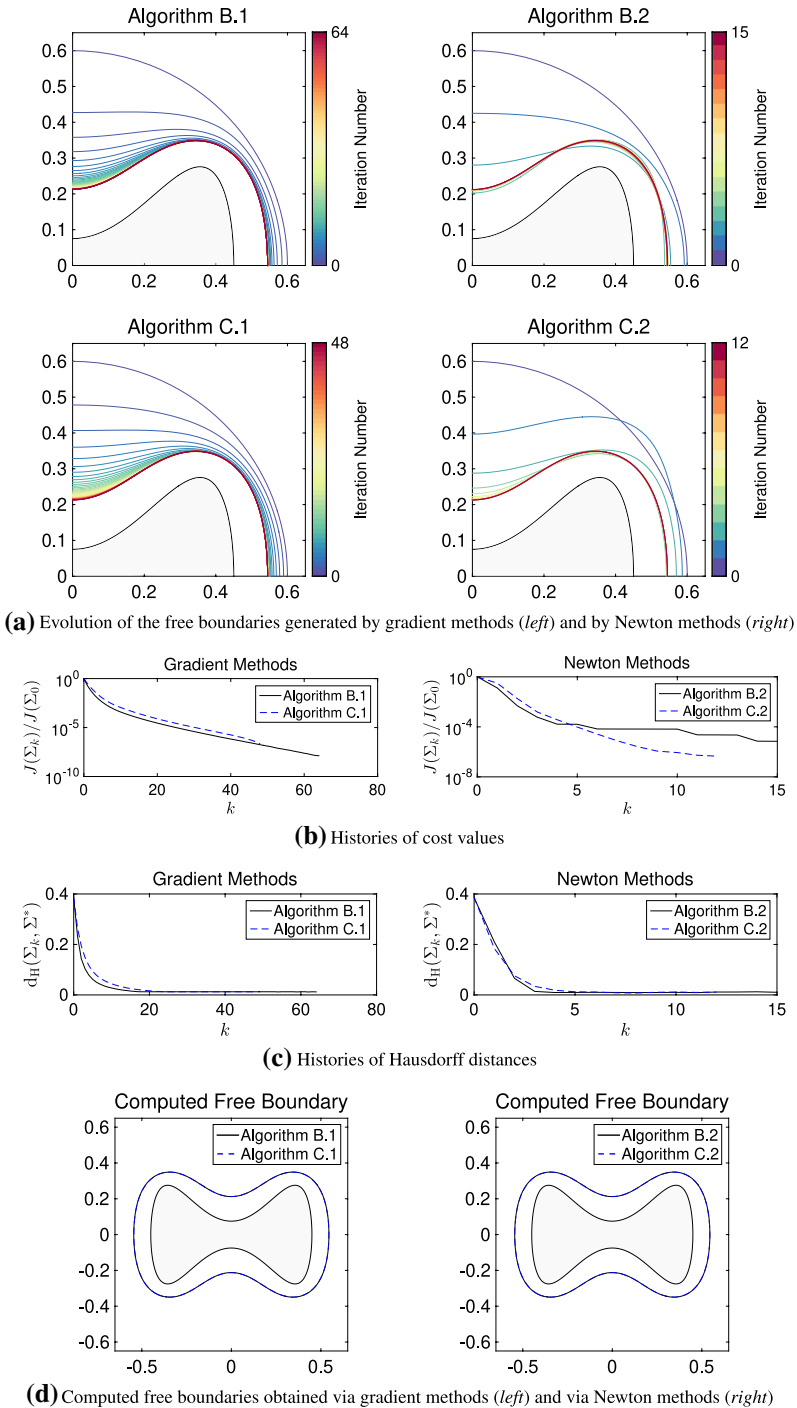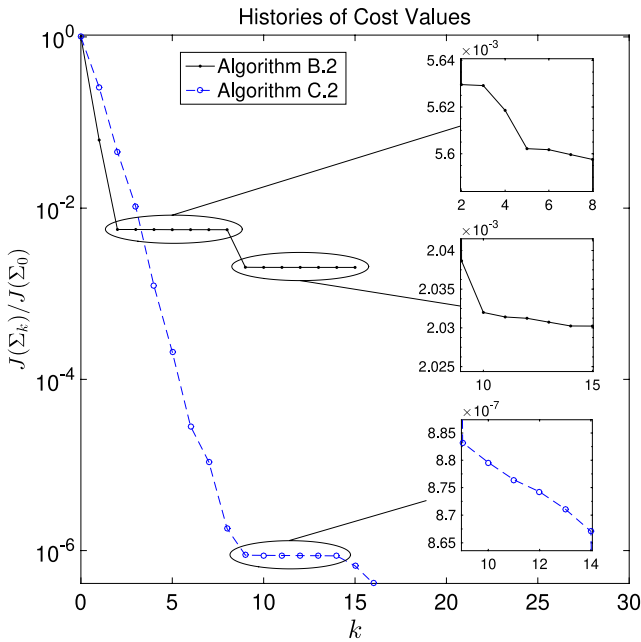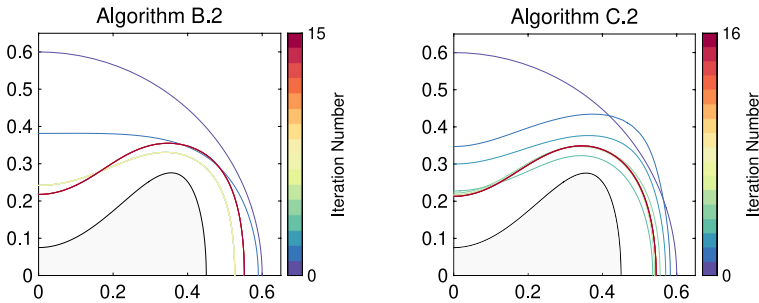
(a) Evolution of the free boundaries generated by gradient methods (*left*) and by Newton methods (*right*)

(b) Histories of cost values

(c) Histories of Hausdorff distances

(d) Computed free boundaries obtained via gradient methods (*left*) and via Newton methods (*right*)

Fig. 6 Computational results of Example 5.2.4 using algorithms B.1, C.1, B.2 and C.2

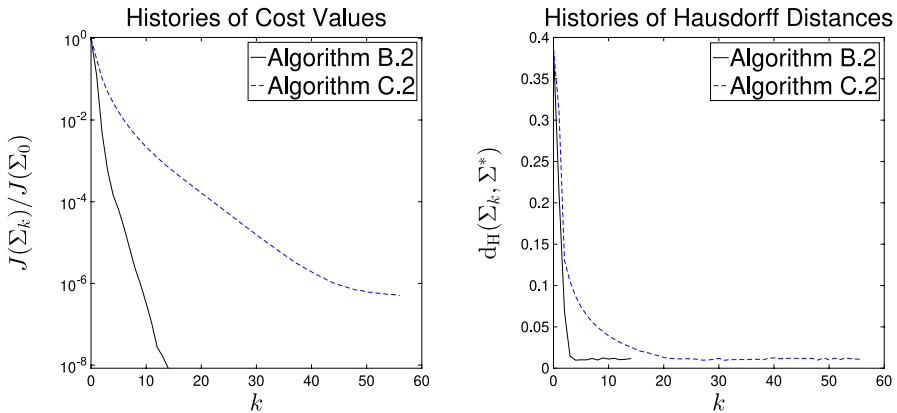**(a)** Histories of cost values

(b) Evolution of the free boundaries using Algorithm B.2 (*left*) and Algorithm C.2 (*right*)
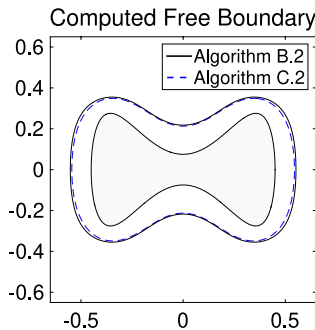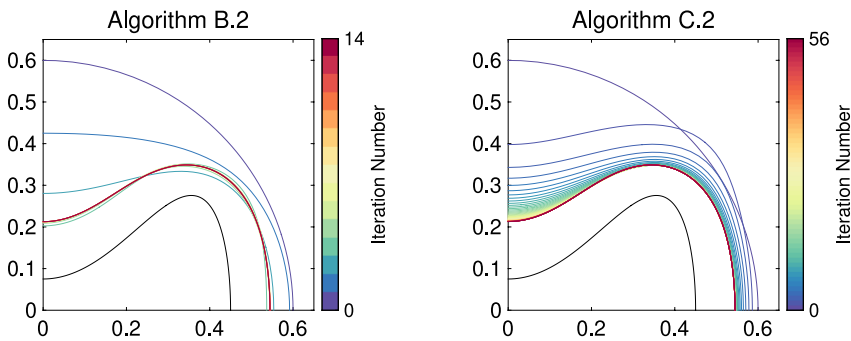

(c) Computed free boundaries

Fig. 7 Computational results of Example 5.2.4 using Algorithms B.2 and C.2 with the full Newton step (i.e., $\tilde{\alpha} = 1$.)

approach (i.e., Algorithm C.2) is more accurate than the one obtained via the pro-
posed method (i.e., Algorithm B.2). Meanwhile, scaling the (full) Newton steps by a
factor of $\tilde{\alpha} = 0.2$ at every iteration (in both Algorithms B.2 and C.2) lead to the
computational results shown in Fig. 8. The figure shows, in particular, the histories
of cost values and Hausdorff distances both plotted in Fig. 8a (left and right plot,
respectively). Referring, in particular, to the left plot shown in Fig. 8a, it is clear that
the costs J and J_1 are decreasing almost uniformly from the initial to their respective
final values. However, it is apparent from the figure that the cost J is more sensitive
(and therefore has higher convergence behavior) than J_1. In fact, because the number
of iterations required by Algorithm B.2 to reach the optimal free boundary is less
than that of Algorithm C.2 (as evident in the right graph plotted in Fig. 8a), we can
conclude that the proposed method is indeed much faster than the classical Dir-
ichlet-data-tracking approach. This observation is, of course, also evident from the
evolution of the free boundaries shown in Fig. 8b wherein we recognized a big dif-
ference on how the two algorithms actually develop the initial free boundary into an

(a) Histories of cost values (*left*) and Hausdorff distances (*right*)

(b) Evolution of the free boundaries

Fig. 8 Computational results of Example 5.2.4 using Algorithms B.2 and C.2 with the scaled full New-
ton step (i.e., $\tilde{\alpha} = 0.2$)

optimal one. We mention here that we also ran the two algorithms using several other values for $\tilde{\alpha}$ between zero and the unit value (to solve the present case problem), and, as in the previous cases, we found that the proposed method is, in general, faster that the classical approach of minimizing the Dirichlet-data-tracking cost functional. Nevertheless, the cost function J becomes more insensitive than J_1 as the step size parameter $\tilde{\alpha}$ increases in value.

6 Conclusion

We presented a second-order shape optimization algorithm for solving the exterior Bernoulli free boundary problem using a new boundary cost functional which measures the L^2-gap at the free boundary of two auxiliary states, one of which is a solution of a mixed Dirichlet–Neumann problem and the other of which satisfies a mixed Dirichlet–Robin problem. The novelty of the present investigation is the utilization of the shape Hessian information at the solution of the free boundary problem in the iterative scheme formulated to numerically solve the minimization problem. Numerical results revealed that the first- and second-order shape optimization methods put forward in this study is, in general, faster than the classical approach of tracking the Dirichlet data in L^2 sense. Thus, in this investigation, the robustness of the proposed method was shown not only theoretically but also numerically.

Appendix 1: Shape derivative of the adjoint state p_N

Let us first introduce some notations and present some properties of the operator T_t (see Sect. 3) that will be useful to our analysis. For $t \in (0, \varepsilon)$ ($\varepsilon > 0$ sufficiently small), the transformation T_t is invertible and $T_t, T_t^{-1} \in \mathscr{D}^1(\mathbb{R}^2, \mathbb{R}^2)$ (see, e.g., [10, Lemma 11]). In addition, the Jacobian matrix of the transformation $T_t = T_t(\mathbf{V})$ associated with the velocity field $\mathbf{V}$ denoted by $\det DT_t(X)$ is strictly positive. Here, we shall use the notations $(DT_t)^{-1}$ and $(DT_t)^{-\top}$ to denote the inverse and inverse transpose of the Jacobian matrix DT_t, respectively. Also, for convenience, we write $A_t = \det DT_t(X)(DT_t^{-1})(DT_t)^{-\top}$ and $w_t = \det DT_t(X)|(DT_t)^{-\top}\mathbf{n}|$ which represent the Jacobian matrix of T_t with respect to the boundary $\partial\Omega$.

The following lemma, whose proof can be found in [22, 71], will also be essential to our analysis.

Lemma A.1 *Let* $\mathbf{V}$ *be a fixed vector field in* Θ *(see* (9)*) and* $I = (-t_0, t_0)$, *with* $t_0 > 0$ *sufficiently small. Then, the following regularity properties of* T_t *hold*

(i) $t \mapsto \det DT_t(X) \in C^1(I, C(\bar{\Omega}))$

(ii) $t \mapsto A_t \in C^1(I, C^1(\bar{\Omega}))$

(iii) $t \mapsto w_t \in C^1(I, C(\Sigma))$

(iv) $\lim_{t \searrow 0} w_t = 1$

(v) $\dfrac{\mathrm{d}}{\mathrm{d}t} w_t|_{t=0} = w'(0) = \mathrm{div}_\Sigma \mathbf{V}$

(vi) $\dfrac{\mathrm{d}}{\mathrm{d}t} A_t|_{t=0} = A'(0),$

where $A'(0) = (\mathrm{div}\,\mathbf{V})\mathbf{I}_2 - (D\mathbf{V} + (D\mathbf{V})^\top)$ and the limits defining the derivatives at $t = 0$ exist uniformly in $x \in \bar{\Omega}$.

Before we derive the shape derivative of p_{N}, and for completeness, let us first prove the unique solvability of the adjoint problem on the perturbed domain Ω_t.

Lemma A.2 *For any $t > 0$ sufficiently small, the variational problem: find $p_{\mathrm{N}}^t \in H^1(\Omega)$ such that $p_{\mathrm{N}}^t = 0$ on Γ and*

$$\int_\Omega A_t \nabla p_{\mathrm{N}}^t \cdot \nabla \varphi \, \mathrm{d}x - \int_\Sigma w_t u_{\mathrm{N}}^t \varphi \, \mathrm{d}\sigma = 0, \quad \forall \varphi \in H^1_{\Gamma,0}(\Omega). \tag{66}$$

admits a unique solution p_{N}^t in $H^1(\Omega)$.

Proof We first note that the variational problem being examined is obtained from the problem: find $p_{\mathrm{N}t} \in H^1(\Omega_t)$ such that $p_{\mathrm{N}t} = 0$ on Γ and

$$\int_{\Omega_t} \nabla p_{\mathrm{N}t} \cdot \nabla \varphi \, \mathrm{d}x_t - \int_{\Sigma_t} u_{\mathrm{N}t} \varphi \, \mathrm{d}\sigma_t = 0, \quad \forall \varphi \in H^1_{\Gamma,0}(\Omega_t), \tag{67}$$

via the application of domain and boundary transformation formulas (see, e.g., [71, Proposition 2.46–2.47]). In fact, the functions $\phi_t : \Omega_t \to \mathbb{R}$ and $\phi^t : \Omega \to \mathbb{R}$ are related through the equation $\phi^t = \phi_t \circ T_t$. Hence, if $p_{\mathrm{N}t}$ solves the variational equation (67), then $p_{\mathrm{N}}^t = p_{\mathrm{N}t} \circ T_t$ satisfies (66). In addition, the boundary condition $p_{\mathrm{N}}^t = p_{\mathrm{N}t} \circ T_t = 0$ on Γ implies that p_{N}^t is actually in $H^1_{\Gamma,0}(\Omega)$.

Now, consider the bilinear form $b_t(\cdot, \cdot) : \mathbf{H}^1_{\Gamma,0}(\Omega) \to \mathbb{R}$ defined by

$$b_t(\phi^t, \varphi) = \int_\Omega A_t \nabla \phi^t \cdot \nabla \varphi \, \mathrm{d}x, \quad \forall \phi^t, \varphi \in H^1_{\Gamma,0}(\Omega). \tag{68}$$

Note that, as a consequence of Lemma A.1, A_t is bounded. Hence, it is clear that $b_t(\cdot, \cdot)$ is continuous because $|b_t(\phi^t, \varphi)| = \left| \int_\Omega A_t \nabla \phi^t \cdot \nabla \varphi \, \mathrm{d}x \right| \lesssim \|A_t\|_{L^\infty(\Omega)} \|\phi^t\|_{H^1(\Omega)} |\varphi|_{H^1(\Omega)}$. Moreover, $b_t(\cdot, \cdot)$ is coercive. Indeed, from the fact that $A_t \to \mathbf{I}$ uniformly on $\bar{\Omega}$ as $t \to 0$, we know that there exist sufficiently small values for $t > 0$ such that $\|A_t - \mathbf{I}\|_{L^\infty(\Omega)} < 1$. So, we have

$$b_t(\phi^t, \phi^t) = \int_\Omega A_t \nabla \phi^t \cdot \nabla \phi^t \, dx = \left| \int_\Omega (A_t - \mathbf{I}) \nabla \phi^t \cdot \nabla \phi^t + |\nabla \phi^t|^2 \, dx \right|$$

$$\geqslant \|\nabla \phi^t\|_{L^2(\Omega)}^2 - \|A_t - \mathbf{I}\|_{L^\infty(\Omega)} \|\nabla \phi^t\|_{L^2(\Omega)}^2$$

$$\gtrsim |\nabla \phi^t|_{H^1(\Omega)}^2.$$

Next, we consider the functional $\omega : H^1_{\Gamma,0}(\Omega) \to \mathbb{R}$ defined by $\langle \omega, \varphi \rangle = \int_\Sigma w_t u_N^t \varphi \, d\sigma$. Evidently, this functional is continuous because of the boundedness of $|w_t|_\infty$ and due to the sequence of inequalities

$$\left| \int_\Sigma w_t u_N^t \varphi \, d\sigma \right| \lesssim |w_t|_\infty \|u_N^t\|_{L^2(\Sigma)} \|\varphi\|_{L^2(\Sigma)} \lesssim |w_t|_\infty \|u_N^t\|_{H^1(\Omega)} |\varphi|_{H^1(\Omega)}.$$

Thus, by Lax–Milgram theorem, the function p_N^t, vanishing on Γ, is the unique solution to the variational equation (66) in $H^1(\Omega)$. This proves the lemma. □

Proposition A.1 *Let Ω be a bounded $C^{2,1}$ domain. The shape derivative of the adjoint state variable $p_N \in H^3(\Omega)$ at $\Omega = \Omega^*$ satisfying the mixed Dirichlet–Neumann problem (16) is a solution to the following mixed boundary value problem:*

$$-\Delta p_{NW}' = 0 \text{ in } \Omega^*, \quad p_{NW}' = 0 \text{ on } \Gamma, \quad \partial_{\mathbf{n}} p_{NW}' = u_{NW}' + \lambda \mathbf{W} \cdot \mathbf{n} \quad \text{on } \Sigma^*.$$

Proof The proof mainly contains two parts; we first prove the existence of the material derivative of p_N, then we formally proceed on the derivation of its shape derivative.

Step 1. Existence of the material derivative of p_N. The variational formulation of (16) on the reference domain Ω is given as follows: find $p_N \in H^1_{\Gamma,0}(\Omega)$ such that

$$\int_\Omega \nabla p_N \cdot \nabla \varphi \, dx - \int_\Sigma u_N \varphi \, d\sigma = 0, \quad \forall \varphi \in H^1_{\Gamma,0}(\Omega). \tag{69}$$

Subtracting (66) with $t = 0$ from the case where $t > 0$, for all $\varphi \in H^1_{\Gamma,0}(\Omega)$, we obtain

$$\int_\Omega \{A_t \nabla p_N^t - \nabla p_N^t + \nabla p_N^t - \nabla p_N\} \cdot \nabla \varphi \, dx - \int_\Sigma \{w_t u_N^t - u_N^t + u_N^t - u_N\} \varphi \, d\sigma = 0.$$

Hence, we have a unique solution $p_N^t - p_N \in H^1_{\Gamma,0}(\Omega)$ to the variational equation

$$\int_\Omega \nabla (p_N^t - p_N) \cdot \nabla \varphi \, dx = -\int_\Omega (A_t - \mathbf{I}) \nabla p_N^t \cdot \nabla \varphi \, dx$$
$$+ \int_\Sigma (w_t - 1) u_N^t \varphi \, d\sigma + \int_\Sigma (u_N^t - u_N) \varphi \, d\sigma, \tag{70}$$

for all $\varphi \in H^1_{\Gamma,0}(\Omega)$. We note that ∇p_N^t is uniformly bounded in $L^2(\Omega; \mathbb{R}^2)$ and we have the convergence $\nabla p_N^t \to \nabla p_N$ also in that space. Indeed, using the boundedness of $\|A_t\|_{L^\infty(\Omega)}$ from below, we get the estimate

$$\|\nabla p_{\mathrm{N}}^{t}\|_{L^{2}(\Omega)}^{2} \lesssim \int_{\Omega} A_{t} \nabla p_{\mathrm{N}}^{t} \cdot \nabla p_{\mathrm{N}}^{t} \, \mathrm{d}x = \int_{\Sigma} w_{t} u_{\mathrm{N}}^{t} p_{\mathrm{N}}^{t} \, \mathrm{d}\sigma \lesssim |w_{t}|_{\infty} \|u_{\mathrm{N}}^{t}\|_{H^{1}(\Omega)} \|p_{\mathrm{N}}^{t}\|_{L^{2}(\Omega)}.$$

Because u_{N}^{t} is uniformly bounded in $H^{1}(\Omega)$ (cf. [10, Theorem 23], see also [50, Proposition 3.1]), the uniform boundedness of $\nabla p_{\mathrm{N}}^{t}$ in $L^{2}(\Omega;\mathbb{R}^{2})$ immediately follows, and so the convergence $\nabla p_{\mathrm{N}}^{t} \to \nabla p_{\mathrm{N}}$ in $L^{2}(\Omega;\mathbb{R}^{2})$. Next, we divide both sides of (70) by t and denote $\phi^{t} := \frac{1}{t}(p_{\mathrm{N}}^{t} - p_{\mathrm{N}})$ to obtain

$$\int_{\Omega} \nabla \phi^{t} \cdot \nabla \varphi \, \mathrm{d}x = -\int_{\Omega} \left(\frac{A_{t} - \mathbf{I}}{t} \right) \nabla p_{\mathrm{N}}^{t} \cdot \nabla \varphi \, \mathrm{d}x + \int_{\Sigma} \left(\frac{w_{t} - 1}{t} \right) u_{\mathrm{N}}^{t} \varphi \, \mathrm{d}\sigma$$

$$+ \int_{\Sigma} \left(\frac{u_{\mathrm{N}}^{t} - u_{\mathrm{N}}}{t} \right) \varphi \, \mathrm{d}\sigma,$$

for all $\varphi \in H_{\Gamma,0}^{1}(\Omega)$. We choose a sequence $\{t_{n}\}$ such that $t_{n} \to 0$ as $n \to \infty$. Our goal is to show that the limit $\lim_{n \to \infty} \phi^{t}$ exists. Using the boundedness of $\frac{1}{t_{n}}(A_{t} - \mathbf{I})$ and $\frac{1}{t_{n}}(w_{t} - 1)$ in L^{∞}, we deduce that $\nabla p_{\mathrm{N}}^{t_{n}}$ is bounded in $L^{2}(\Omega;\mathbb{R}^{2})$, and thus the boundedness of $\phi^{t_{n}}$ in $H_{\Gamma,0}^{1}(\Omega)$. Hence, we can extract a subsequence, which we still denote by $\{t_{n}\}$, such that $\lim_{n \to \infty} t_{n} = 0$. Moreover, there exists an element ϕ of $H_{\Gamma,0}^{1}(\Omega)$ such that $\phi^{t_{n}} \rightharpoonup \phi$ weakly in $H_{\Gamma,0}^{1}(\Omega)$. From the convergences $\nabla p_{\mathrm{N}}^{t_{n}} \to \nabla p_{\mathrm{N}}$ in $L^{2}(\Omega;\mathbb{R}^{2})$ and $u_{\mathrm{N}}^{t_{n}} \to u_{\mathrm{N}}$ in $L^{2}(\Sigma)$, together with Lemma A.1(v)–(vi), we get

$$\int_{\Omega} \nabla \phi \cdot \nabla \varphi \, \mathrm{d}x = -\int_{\Omega} A \nabla p_{\mathrm{N}} \cdot \nabla \varphi \, \mathrm{d}x + \int_{\Sigma} u_{\mathrm{N}} \varphi \mathrm{div}_{\Sigma} \mathbf{W} \, \mathrm{d}\sigma + \int_{\Sigma} \dot{u}_{\mathrm{N}} \varphi \, \mathrm{d}\sigma,$$

for all $\varphi \in H_{\Gamma,0}^{1}(\Omega)$, where $\dot{u}_{\mathrm{N}} = \lim_{t \searrow 0} \frac{1}{t}(u_{\mathrm{N}}^{t} - u_{\mathrm{N}})$ which is exactly the material derivative of u_{N} at $t = 0$ in the direction $\mathbf{W}$. This function exists and is actually an element of $H_{\Gamma,0}^{1}(\Omega)$ as shown, for example, in [9]. Hence, the above equation admits a unique solution in $H^{1}(\Omega)$ and we deduce that $\phi^{t_{n}} \rightharpoonup \phi$ for any sequence $\{t_{n}\}$. This implies the strong convergence of $\phi^{t_{n}}$ to ϕ in $L^{2}(\Sigma)$. Now, taking $\varphi = \phi^{t_{n}} \in H_{\Gamma,0}^{1}(\Omega)$, we obtain

$$\lim_{t_{n} \to 0} |\phi^{t_{n}}|_{H^{1}(\Omega)}^{2} = -\lim_{t_{n} \to 0} \left\{ \int_{\Omega} \left(\frac{A(t_{n}) - \mathbf{I}}{t_{n}} \right) \nabla p_{\mathrm{N}}^{t_{n}} \cdot \nabla \phi^{t_{n}} \, \mathrm{d}x \right\}$$

$$+ \lim_{t_{n} \to 0} \left\{ \int_{\Sigma} \left(\frac{w(t_{n}) - 1}{t_{n}} \right) u_{\mathrm{N}}^{t_{n}} \phi^{t_{n}} \, \mathrm{d}\sigma \right\}$$

$$+ \lim_{t_{n} \to 0} \left\{ \int_{\Sigma} \left(\frac{u_{\mathrm{N}}^{t_{n}} - u_{\mathrm{N}}}{t_{n}} \right) \phi^{t_{n}} \, \mathrm{d}\sigma \right\}$$

$$= -\int_{\Omega} A \nabla p_{\mathrm{N}} \cdot \nabla \phi \, \mathrm{d}x + \int_{\Sigma} u_{\mathrm{N}} \phi \mathrm{div}_{\Sigma} \mathbf{W} \, \mathrm{d}\sigma + \int_{\Sigma} \dot{u}_{\mathrm{N}} \phi \, \mathrm{d}\sigma = |\phi|_{H^{1}(\Omega)}.$$

The norm convergence and the weak convergence of $\phi^{t_{n}}$ in $H_{\Gamma,0}^{1}(\Omega)$ implies the strong convergence of $\phi^{t_{n}}$ to $\phi \in H_{\Gamma,0}^{1}(\Omega)$. This guarantees the existence of the material derivative of p_{N}.

Step 2. Computing the shape derivative of p_{N} *at* $\Omega = \Omega^{*}$ *along the deformation field* $\mathbf{W}$. From the previous step, we showed the existence of the material derivative

of p_N in $H_{\Gamma,0}^1(\Omega)$. Denoting this derivative by $\dot{p}_N$, we know that it satisfies the variational equation

$$
\begin{aligned}
\int_\Omega \nabla \dot{p}_N \cdot \nabla \varphi \, dx = &- \int_\Omega A \nabla p_N \cdot \nabla \varphi \, dx + \int_\Sigma u_N \varphi \operatorname{div}_\Sigma \mathbf{W} \, d\sigma \\
&+ \int_\Sigma \dot{u}_N \varphi \, d\sigma, \quad \forall \varphi \in H_{\Gamma,0}^1(\Omega).
\end{aligned}
\tag{71}
$$

In addition, it is clear that $\dot{p}_N = 0$ on Γ. Applying Green's formula to the above variational form, we get

$$
\begin{aligned}
-\int_\Omega \varphi \Delta \dot{p}_N \, dx + \int_\Sigma \varphi \partial_{\mathbf{n}} \dot{p}_N \, d\sigma = &\int_\Omega \varphi \operatorname{div}(A \nabla p_N) \, dx - \int_\Sigma \varphi A \partial_{\mathbf{n}} p_N \, d\sigma \\
&+ \int_\Sigma u_N \varphi \operatorname{div}_\Sigma \mathbf{W} \, d\sigma + \int_\Sigma \dot{u}_N \varphi \, d\sigma, \quad \forall \varphi \in H_{\Gamma,0}^1(\Omega).
\end{aligned}
$$

First, let us choose $\varphi \in H_0^1(\Omega)$. Then, we have $-\int_\Omega \varphi \Delta \dot{p}_N \, dx = \int_\Omega \varphi \operatorname{div}(A \nabla p_N) \, dx$. Since, $H_0^1(\Omega)$ is dense in $L^2(\Omega)$, we obtain $-\Delta \dot{p}_N = \operatorname{div}(A \nabla p_N)$ in Ω. Next, we choose $\varphi \in H_{\Gamma,0}^1(\Omega)$ such that φ is arbitrary in Σ. This gives us

$$
\int_\Sigma \varphi \partial_{\mathbf{n}} \dot{p}_N \, d\sigma = - \int_\Sigma \varphi A \partial_{\mathbf{n}} p_N \, d\sigma + \int_\Sigma u_N \varphi \operatorname{div}_\Sigma \mathbf{W} \, d\sigma + \int_\Sigma \dot{u}_N \varphi \, d\sigma.
$$

Because the traces of functions in $H_{\Gamma,0}^1(\Omega)$ are dense in $L^2(\Sigma)$, we arrive at $\partial_{\mathbf{n}} \dot{p}_N = -A \partial_{\mathbf{n}} p_N + u_N \operatorname{div}_\Sigma \mathbf{W} + \dot{u}_N$ on Σ. Summarizing these results, we see that $\dot{p}_N$ satisfies the following boundary value problem:

$$
-\Delta \dot{p}_N = \operatorname{div}(A \nabla p_N) \text{ in } \Omega, \quad \dot{p}_N = 0 \text{ on } \Gamma, \quad \partial_{\mathbf{n}} \dot{p}_N = -A \partial_{\mathbf{n}} p_N + u_N \operatorname{div}_\Sigma \mathbf{W} + \dot{u}_N \quad \text{on } \Sigma.
$$

From above equations, and due to the fact that $\mathbf{W}$ vanishes on Γ, we immediately obtain [in view of the identity (12)] $p_N' = \dot{p}_N - \mathbf{W} \cdot \nabla p_N = 0$ on Γ. Now, we consider $\varphi \in H^2(\Omega)$. Note that for $C^{1,1}$ domain, we have that $u_N \in H^2(\Omega)$ (see [10, Theorem 29] and also [50]). Hence, $u_N \in H^{3/2}(\Sigma)$ which, in turn, means that $p_N \in H^2(\Omega)$ by standard elliptic regularity theory. Given this regularity of p_N and since $-\Delta p_N = 0$ in Ω, we can therefore write $- \int_\Omega A \nabla p_N \cdot \nabla \varphi \, dx$ as follows (see [50, Lemma 4.1])

$$
\begin{aligned}
-\int_\Omega A \nabla p_N \cdot \nabla \varphi \, dx = &\int_\Omega \nabla(\mathbf{W} \cdot \nabla p_N) \cdot \nabla \varphi \, dx + \int_\Sigma \partial_{\mathbf{n}} p_N (\mathbf{W} \cdot \nabla \varphi) \, d\sigma \\
&- \int_\Sigma (\nabla p_N \cdot \nabla \varphi) \mathbf{W} \cdot \mathbf{n} \, d\sigma,
\end{aligned}
\tag{72}
$$

for all $\varphi \in H^2(\Omega)$. Hence, using the identity (12), we have the equation

$$
\int_\Omega \nabla \dot{p}_N \cdot \nabla \varphi \, dx = \int_\Omega \nabla p_N' \cdot \nabla \varphi \, dx + \int_\Omega \nabla(\mathbf{W} \cdot \nabla p_N) \cdot \nabla \varphi \, dx, \quad \forall \varphi \in H_{\Gamma,0}^1(\Omega).
$$

Combining this equation with (71) and (72) yields

$$\int_\Omega \nabla(\mathbf{W} \cdot \nabla p_\mathrm{N}) \cdot \nabla\varphi\, dx + \int_\Sigma \partial_\mathbf{n} p_\mathrm{N}(\mathbf{W} \cdot \nabla\varphi)\, d\sigma - \int_\Sigma (\nabla p_\mathrm{N} \cdot \nabla\varphi)\mathbf{W} \cdot \mathbf{n}\, d\sigma$$

$$+ \int_\Sigma u_\mathrm{N}\varphi\mathrm{div}_\Sigma \mathbf{W}\, d\sigma + \int_\Sigma \dot{u}_\mathrm{N}\varphi\, d\sigma$$

$$= \int_\Omega \nabla p_\mathrm{N}' \cdot \nabla\varphi\, dx + \int_\Omega \nabla(\mathbf{W} \cdot \nabla p_\mathrm{N}) \cdot \nabla\varphi\, dx, \quad \forall \varphi \in H^2 \cap H^1_{\Gamma,0}(\Omega).$$

Applying Green's formula on the right side of the above equation we arrive at

$$-\int_\Omega \varphi\Delta p_\mathrm{N}'\, dx + \int_\Sigma \varphi\partial_\mathbf{n} p_\mathrm{N}'\, d\sigma = \int_\Sigma \partial_\mathbf{n} p_\mathrm{N}(\mathbf{W} \cdot \nabla\varphi)\, d\sigma - \int_\Sigma (\nabla p_\mathrm{N} \cdot \nabla\varphi)\mathbf{W} \cdot \mathbf{n}\, d\sigma$$

$$+ \int_\Sigma u_\mathrm{N}\varphi\mathrm{div}_\Sigma \mathbf{W}\, d\sigma + \int_\Sigma \dot{u}_\mathrm{N}\varphi\, d\sigma, \quad \forall \varphi \in H^2 \cap H^1_{\Gamma,0}(\Omega).$$

Now, we choose $\varphi \in C_0^\infty(\Omega)$. This leads us to $-\Delta p_\mathrm{N}' = 0$ in Ω. Moreover, we get

$$\int_\Sigma \varphi\partial_\mathbf{n} p_\mathrm{N}'\, d\sigma = \int_\Sigma (u_\mathrm{N}\mathbf{W} - \nabla p_\mathrm{N}\mathbf{W} \cdot \mathbf{n}) \cdot \nabla\varphi\, d\sigma + \int_\Sigma u_\mathrm{N}\varphi\mathrm{div}_\Sigma \mathbf{W}\, d\sigma + \int_\Sigma \dot{u}_\mathrm{N}\varphi\, d\sigma.$$

Observe that $(u_\mathrm{N}\mathbf{W} - \nabla p_\mathrm{N}\mathbf{W} \cdot \mathbf{n}) \cdot \mathbf{n} = 0$. Hence, we can replace $\nabla\varphi|_\Sigma$ by the tangential gradient $\nabla_\Sigma\varphi$. Using the tangential Green's formula (see equation 21) thrice, noting that $\mathbf{W} \cdot \mathbf{n}\nabla_\Sigma p_\mathrm{N} \cdot \mathbf{n} = 0$, and then using the relation $\dot{u}_\mathrm{N} = u_\mathrm{N}' + \mathbf{W} \cdot \nabla u_\mathrm{N}$, we obtain

$$\int_\Sigma \varphi\partial_\mathbf{n} p_\mathrm{N}'\, d\sigma = \int_\Sigma \varphi\mathrm{div}_\Sigma(\nabla p_\mathrm{N}\mathbf{W} \cdot \mathbf{n})\, d\sigma + \int_\Sigma \dot{u}_\mathrm{N}\varphi\, d\sigma$$

$$= \int_\Sigma \varphi\kappa(\nabla p_\mathrm{N}\mathbf{W} \cdot \mathbf{n}) \cdot \mathbf{n}\, d\sigma - \int_\Sigma (\nabla_\Sigma\varphi \cdot \nabla p_\mathrm{N})\mathbf{W} \cdot \mathbf{n}\, d\sigma + \int_\Sigma \dot{u}_\mathrm{N}\varphi\, d\sigma$$

$$= \int_\Sigma \varphi\kappa u_\mathrm{N}\mathbf{W} \cdot \mathbf{n}\, d\sigma - \int_\Sigma (\nabla_\Sigma\varphi \cdot \nabla_\Sigma p_\mathrm{N})\mathbf{W} \cdot \mathbf{n}\, d\sigma + \int_\Sigma \dot{u}_\mathrm{N}\varphi\, d\sigma$$

$$= \int_\Sigma \varphi\kappa u_\mathrm{N}\mathbf{W} \cdot \mathbf{n}\, d\sigma + \int_\Sigma \varphi\mathrm{div}_\Sigma(\nabla_\Sigma p_\mathrm{N}\mathbf{W} \cdot \mathbf{n})\, d\sigma + \int_\Sigma (u_\mathrm{N}' + \mathbf{W} \cdot \nabla u_\mathrm{N})\varphi\, d\sigma,$$

for all $\varphi \in H^2 \cap H^1_{\Gamma,0}(\Omega)$. Since the trace of functions from $H^2(\Omega)$ is dense in $L^2(\Sigma)$, we deduce the boundary condition on for p_N' given by $\partial_\mathbf{n} p_\mathrm{N}' = \mathrm{div}_\Sigma(\nabla_\Sigma p_\mathrm{N}\mathbf{W} \cdot \mathbf{n}) + \kappa u_\mathrm{N}\mathbf{W} \cdot \mathbf{n} + u_\mathrm{N}' + \mathbf{W} \cdot \nabla u_\mathrm{N}$. Summarizing these results, and letting $\Omega = \Omega^*$, we get

$$-\Delta p_\mathrm{N}' = 0 \text{ in } \Omega^*, \quad p_\mathrm{N}' = 0 \text{ on } \Gamma, \quad \partial_\mathbf{n} p_\mathrm{N}' = u_\mathrm{N}' + \lambda\mathbf{W} \cdot \mathbf{n} \quad \text{on } \Sigma^*,$$

as desired.   □

It is worth remarking that the existence of the shape derivative p_N' of p_N can only be justified if u_N is H^3-regular. Hence, we require that Ω be at least of class $C^{2,1}$ so that u_N (as well as u_R) is in $H^3(\Omega)$ (see, e.g., [10, Theorem 29]).

References

1. Alt, A., Caffarelli, L.A.: Existence and regularity for a minimum problem with free boundary. J. Reine. Angew. Math. **325**, 105–144 (1981)
2. Azegami, H.: A solution to domain optimization problems. Trans. Jpn. Soc. Mech. Eng. Ser. A **60**, 1479–1486 (1994). (in Japanese)
3. Azegami, H., Shimoda, M., Katamine, E., Wu, Z.C.: A domain optimization technique for elliptic boundary value problems. In: Hernandez, S., El-Sayed, M., Brebbia, C.A. (eds.) Computer Aided Optimization Design of Structures IV, Structural Optimization, pp. 51–58. Computational Mechanics Publications, Southampton (1995)
4. Azegami, H., Wu, Z.Q.: Domain optimization analysis in linear elastic problems: approach using traction method. SME Int. J. Ser. A **39**, 272–278 (1996)
5. Azegami, H., Kaizu, S., Shimoda, M., Katamine, E.: Irregularity of shape optimization problems and an improvement technique. In: Hernandez, S., Brebbia, C.A. (eds.) Computer Aided Optimization Design of Structures IV, Structural Optimization, pp. 309–326. Computational Mechanics Publications, Southampton (1997)
6. Azegami, H.: Solution of shape optimization problem and its application to product design, mathematical analysis of continuum mechanics and industrial applications. In: Itou, H., Kimura, M., Chalupecký, V., Ohtsuka, K., Tagami, D., Takada, A. (eds.) Computer Aided Optimization Design of Structures IV, Structural Optimization, vol. 26, pp. 83–98. Mathematics for Industry, Springer, Singapore (2016)
7. Azegami, H.: Shape Optimization Problems. Morikita Publishing Co. Ltd, Tokyo (2016). (in Japanese)
8. Azegami, H.: Second derivatives of cost functions and H^1 Newton method in shape optimization problems, mathematical analysis of continuum mechanics and industrial applications II. In: van Meurs, P., Kimura, M., Notsu, H. (eds.) Proceedings of the International Conference CoMFoS16, vol. 30, pp. 61–72. Mathematics for Industry, Springer, Singapore (2017)
9. Bacani, J.B.: Methods of shape optimization in free boundary problems. Ph.D. thesis, Karl-Franzens-Universität-Graz (2013)
10. Bacani, J.B., Peichl, G.: On the first-order shape derivative of the Kohn–Vogelius cost functional of the Bernoulli problem. Abstr. Appl. Anal. **2013**, 19 (2013). Article ID 384320
11. Bacani, J.B., Peichl, G.: Solving the exterior Bernoulli problem using the shape derivative approach. In: Mathematics and Computing 2013. International Conference in Haldia, India, vol. 91, pp. 251–269 . Springer Proceedings in Mathematics and Statistics, vol. XXII, Springer(2014)
12. Ben Abda, A., Bouchon, F., Peichl, G., Sayeh, M., Touzani, R.: A Dirichlet-Neumann cost functional approach for the Bernoulli problem. J. Eng. Math. **81**, 157–176 (2013)
13. Boulkhemair, A., Nachaoui, A., Chakib, A.: A shape optimization approach for a class of free boundary problems of Bernoulli type. Appl. Math. **58**, 205–221 (2013)
14. Boulkhemair, A., Chakib, A., Nachaoui, A.: Uniform trace theorem and application to shape optimization. Appl. Comput. Math. **7**, 192–205 (2008)
15. Boulkhemair, A., Chakib, A.: On the uniform Poincaré inequality. Commun. Partial Differ. Equ. **32**, 1439–1447 (2007)
16. Boyd, S., Vandenberghe, L.: Convex Optimization. Cambridge University Press, Cambridge (2004)
17. Bühler, T., Salamon, D.A.: Functional Analysis. Graduate studies in mathematics, vol. 191. AMS, Providence (2018)
18. Chenais, D.: On the existence of a solution in a domain identification problem. J. Math. Anal. Appl. **52**, 189–219 (1975)
19. Clarke, F.: Functional Analysis, Calculus of Variations and Optimal Control. Graduate Texts in Mathematics, vol. 264. Springer, London (2013)
20. Delfour, M.C., Zolésio, J.-P.: Shape sensitivity analysis by min max differentiability. SIAM J. Control Optim. **26**(4), 834–862 (1988)
21. Delfour, M.C., Zolésio, J.-P.: Structure of shape derivatives for nonsmooth domains. J. Funct. Anal. **104**(1), 1–33 (1992)
22. Delfour, M.C., Zolésio, J.-P.: Shapes and Geometries: Metrics, Analysis, Differential Calculus, and Optimization. Advanced Design Control, vol. 22, 2nd edn. SIAM, Philadelphia (2011)
23. Dambrine, M., Pierre, M.: About stability of equilibrium shapes. Model. Math. Anal. Numer. **34**, 811–834 (2000)

24. Dambrine, M.: On variations of the shape Hessian and sufficient conditions for the stability of critical shapes. Rev. R. Acad. Cienc. Exactas Fis. Nat. Ser. A. Mat. **96**, 95–121 (2002)
25. Eppler, K.: Boundary integral representations of second derivatives in shape optimization. Discuss. Math. Differ. Incl. Control. Optim. **20**, 487–516 (2000)
26. Eppler, K.: Optimal shape design for elliptic equations via BIE-methods. J. Appl. Math. Comput. Sci. **10**, 69–85 (2000)
27. Eppler, K.: Second derivatives and sufficient optimality conditions for shape functionals. Control Cybern. **29**, 485–512 (2000)
28. Eppler, K., Harbrecht, H.: A regularized Newton method in electrical impedance tomography using shape Hessian information. Control Cybern. **34**, 203–225 (2005)
29. Eppler, K., Harbrecht, H.: Efficient treatment of stationary free boundary problems. Appl. Numer. Math. **56**, 1326–1339 (2006)
30. Eppler, K., Harbrecht, H., Schneider, R.: On convergence in elliptic shape optimization. SIAM J. Control Optim. **46**(1), 61–83 (2007)
31. Eppler, K., Harbrecht, H.: Tracking Neumann data for stationary free boundary problems. SIAM J. Control Optim. **48**, 2901–2916 (2009)
32. Eppler, K., Harbrecht, H.: Tracking the Dirichlet data in L^2 is an ill-posed problem. J. Optim. Theory Appl. **145**, 17–35 (2010)
33. Eppler, K., Harbrecht, H.: On a Kohn–Vogelius like formulation of free boundary problems. Comput. Optim. Appl. **52**, 69–85 (2012)
34. Eppler, K., Harbrecht, H.: Shape optimization for free boundary problems—analysis and numerics. Constrained Optim. Optim. Control Partial Differ. Equ. **160**, 277–288 (2012)
35. Fasano, A.: Some free boundary problems with industrial applications. In: Delfour, M. (ed.) Shape Optimization and Free Boundaries. Kluwer, Dordrecht (1992)
36. Flucher, M., Rumpf, M.: Bernoulli's free-boundary problem, qualitative theory and numerical approximation. J. Reine Angew. Math. **486**, 165–204 (1997)
37. Friedrichs, K.O.: Über ein Minimumproblem für Potentialströmungen mit freiem Rand. Math. Ann. **109**, 60–82 (1934)
38. Gilbarg, D., Trudinger, N.S.: Elliptic Partial Differential Equations of Second Order. Springer, Berlin (1998)
39. Grisvard, P.: Elliptic Problems in Nonsmooth Domains. Pitman Publishing, Marshfield (1985)
40. Haddar, H., Kress, R.: A conformal mapping algorithm for the Bernoulli free boundary value problem. Math. Methods Appl. Sci. **39**, 2477–2487 (2016)
41. Haslinger, J., Kozubek, T., Kunish, K., Peichl, G.H.: Shape optimization and fictitious domain approach for solving free-boundary value problems of Bernoulli type. Comput. Optim. Appl. **26**, 231–251 (2003)
42. Haslinger, J., Kozubek, T., Kunisch, K., Peichl, G.: An embedding domain approach for a class of 2-d shape optimization problems: mathematical analysis. J. Math. Anal. Appl. **209**, 665–685 (2004)
43. Haslinger, J., Mäkinen, R.A.E.: Introduction to Shape Optimization: Theory, Approximation, and Computation. SIAM, Philadelphia (2003)
44. Haslinger, J., Ito, K., Kozubek, T., Kunish, K., Peichl, G.H.: On the shape derivative for problems of Bernoulli type. Interfaces Free Bound. **11**, 317–330 (2009)
45. Hecht, F.: New development in FreeFem++. J. Numer. Math. **20**, 251–265 (2012)
46. Henrot, A., Pierre, M.: Shape Variation and Optimization: A Geometrical Analysis, Tracts in Mathematics 28. European Mathematical Society, Zürich (2018)
47. Henrot, A., Shahgholian, H.: Existence of classical solutions to a free boundary problem for the p-Laplace operator, I: the exterior convex case. J. Reine Angew. Math. **521**, 85–97 (2000)
48. Henrot, A., Shahgholian, H.: Convexity of free boundaries with Bernoulli type boundary condition. Nonlinear Anal. Theory Methods Appl. **28**(5), 815–823 (1997)
49. Hettlich, F., Rundell, W.: A second degree method for nonlinear inverse problems. SIAM J. Numer. Anal. **37**(2), 587–620 (2000)
50. Ito, K., Kunisch, K., Peichl, G.: Variational approach to shape derivative for a class of Bernoulli problem. J. Math. Anal. Appl. **314**, 126–149 (2006)
51. Ito, K., Kunisch, K., Peichl, G.: Variational approach to shape derivatives. ESAIM Control Optim. Calc. Var. **14**, 517–539 (2008)
52. Kashiwabara, T., Colciago, C.M., Dedè, L., Quarteroni, A.: Well-posedness, regularity, and convergence analysis of the finite element approximation of a generalized Robin boundary value problem. SIAM J. Numer. Anal. **53**, 105–126 (2015)

53. Kohn, R., Vogelius, M.: Determining conductivity by boundary measurements. Commun. Pure Appl. Math. **37**, 289–298 (1984)
54. Kress, R.: On Trefftz' integral equation for the Bernoulli free boundary value problem. Numer. Math. **136**, 503–522 (2017)
55. Laurain, A., Privat, Y.: On a Bernoulli problem with geometric constraints. ESAIM Control Optim. Calc. Var. **18**, 157–180 (2012)
56. Málek, J., Nečas, J., Rokyta, M., Røužička, M.: Weak and Measure-valued Solutions to Evolutionary PDEs. Chapman & Hall, London (1996)
57. McLean, W.: Strongly Elliptic Systems and Boundary Integral Equations. Cambridge University Press, Cambridge (2000)
58. Medková, D.: The Laplace Equation: Boundary Value Problems on Bounded and Unbounded Lipschitz Domains. Springer, Berlin (2018)
59. Nečas, J.: Direct Methods in the Theory of Elliptic Equations, Springer Monographs in Mathematics. Springer, Heidelberg (2012) (translated from the 1967 French original by Gerard Tronel and Alois Kufner; Editorial coordination and preface by Šárka Nečasová and a contribution by Christian G. Simader)
60. Neuberger, J.W.: Sobolev Gradients and Differential Equations. Springer, Berlin (1997)
61. Nocedal, J., Wright, S.J.: Numerical Optimization. Springer, New York (2006)
62. Novruzi, A., Roche, J.-R.: Newton's method in shape optimisation: a three-dimensional case. BIT Numer. Math. **40**, 102–120 (2000)
63. Novruzi, A., Pierre, M.: Structure of shape derivatives. J. Evol. Equ. **2**, 365–382 (2002)
64. Osher, S., Sethian, J.: Fronts propagating with curvature dependent speed: algorithms based on Hamilton–Jacobi formulations. J. Comput. Phys. **56**, 12–49 (1998)
65. Rabago, J.F.T., Bacani, J.B.: Shape optimization approach to the Bernoulli problem: a Lagrangian formulation. IAENG Int. J. Appl. Math. **47**, 417–424 (2017)
66. Rabago, J.F.T., Bacani, J.B.: Shape optimization approach for solving the Bernoulli problem by tracking the Neumann data: a Lagrangian formulation. Commun. Pure Appl. Anal. **17**, 2683–2702 (2018)
67. Rabago, J.F.T., Azegami, H.: An improved shape optimization formulation of the Bernoulli problem by tracking the Neumann data. J. Eng. Math. **117**, 1–29 (2019)
68. Rabago, J.F.T., Azegami, H.: A new energy-gap cost functional cost functional approach for the exterior Bernoulli free boundary problem. Evol. Equ. Control Theory **8**(4), 785–824 (2019)
69. Sauter, S.A., Schwab, C.: Boundary Element Methods. Springer, Berlin (2011)
70. Simon, J.: Second variation for domain optimization problems. In: Kappel, F., Kunisch, K., Schappacher, W. (eds.) Control and Estimation of Distributed Parameter Systems. International Series of Numerical Mathematics, vol. 91, pp. 361–378. Birkhäuser, Boston (1989)
71. Sokołowski, J., Zolésio, J.-P.: Introduction to Shape Optimization. In: Introduction to Shape Optimization. Springer Series in Computational Mathematics, vol. 16. Springer, Berlin (1992)
72. Tiihonen, T.: Shape optimization and trial methods for free boundary problems. RAIRO Modél. Math. Anal. Numér. **31**, 805–825 (1997)
73. Trefftz, E.: Über die Kontraktion kreisförmiger Flüssigkeitsstrahlen. Z. Math. Phys. **64**, 34–61 (1916)